https://ntrs.nasa.gov/search.jsp?R=19700030196 2020-03-11T22:51:02+00:00Z

OPTIMAL THREE DIMENSIONAL REENTRY TRAJECTORIES FOR APOLLO-TYPE VEHICLES

by

Walton E. Williamson Jr., B. S., M. S.

DISSERTATION

Presented to the Faculty of the Graduate School of
The University of Texas at Austin
in Partial Fulfillment
of the Requirements
for the Degree of

DOCTOR OF PHILOSOPHY

THE UNIVERSITY OF TEXAS AT AUSTIN

January 1970

OPTIMAL THREE DIMENSIONAL REENTRY TRAJECTORIES FOR APOLLO-TYPE VEHICLES

APPROVED BY SUPERVISORY COMMITTEE:

____

____

____

____

PREFACE

The development of necessary conditions for optimal trajectories and of numerical techniques to obtain numerical optimal solutions has been the subject of a considerable amount of research during recent years. From the engineering view point, the goal of all this theory is the application of these results to the problem of optimizing large complex, realistic systems. In the past, the numerical technique which has been used most often for optimizing complex systems is the gradient method. Solutions obtained by the gradient method, however, do not satisfy all of the necessary conditions for a true optimal trajectory. The classical optimality condition, $H_u = 0$, is not satisfied by gradient solutions. On large computers, second variation methods may be used to obtain true optimal solutions, i.e. solutions which satisfy all of the necessary conditions required for an optimal trajectory. The longer word length and increased computation speed allow sufficient accuracy for second variation methods to converge to true optimal solutions within a reasonable computing time.

In this study, a second variation method, the perturbation method, is used to study optimal three dimensional atmospheric reentry trajectories for Apollo-type vehicles. Because of the large variations in the aerodynamic forces, reentry trajectory optimization is an extremely complex problem requiring a very accurate numerical integration routine. It is shown, however, that the perturbation method can be used to obtain true optimal reentry trajectories. The computing time is not excessive.

The author would like to express his appreciation to Dr. B. D. Tapley for serving as his supervising professor and for guiding the research presented in this dissertation. He would also like to express his appreciation to Dr. W. T. Fowler, Dr. P. E. Russell, and Dr. V. Szebehely for serving on his supervising committee. Especially the author would like to thank his wife for her patience and encouragement during the preparation of this dissertation.

W. E. W.

January 1970

ABSTRACT

A numerical optimization method, the perturbation method, is used to calculate optimal three dimensional reentry trajectories for Apollo-type vehicles. A linear combination of the convective heating and the integral of the acceleration are minimized. The only control of the vehicle is the roll angle which specifies the orientation of the lift vector. The initial conditions for reentry are chosen to correspond to those encountered by an Apollo vehicle returning to the earth from a lunar mission. Specified terminal conditions are consistent with those required just prior to the opening of a drogue parachute.

Optimal trajectories obtained for the conditions described above are skip trajectories with high acceleration peaks. State variable inequality constraints are required in order to produce trajectories without these characteristics. The perturbation method is modified so that it may be used to calculate optimal trajectories with state variable inequality constraints. The modified perturbation method is used to calculate optimal reentry trajectories with an altitude inequality constraint over the skip segment of the trajectory. These trajectories have acceleration and heating histories which are acceptable for Apollo-type reentry vehicles.

TABLE OF CONTENTS

Page

PREFACE iii

ABSTRACT. v

LIST OF FIGURES viii

LIST OF TABLES. x

LIST OF SYMBOLS xi

NOTATIONAL CONVENTIONS. xv

CHAPTER 1 - INTRODUCTION 1

CHAPTER 2 - NUMERICAL OPTIMIZATION USING THE PERTURBATION METHOD. . 5

2.1 Optimization Problem 5
2.2 Perturbation Method. 7
2.3 Numerical Integration and Inversion Routines 10
2.4 Stability of the Perturbation Method 12

CHAPTER 3 - UNCONSTRAINED REENTRY OPTIMIZATION. 27

3.1 Reentry Problem. 27
3.2 Numerical Accuracy Studies 34
3.3 Numerical Results. 42

CHAPTER 4 - STATE VARIABLE INEQUALITY CONSTRAINTS 59

4.1 Summary of Theory and Numerical Methods for SVIC 59
4.2 Necessary Conditions for SVIC. 62
4.3 Application of Perturbation Method to SVIC 68
4.4 Example Problem (Constrained Brachistochrone). 74

CHAPTER 5 - ALTITUDE CONSTRAINED REENTRY. 82

5.1 Theoretical Development. 82
5.2 Numerical Results. 88

CHAPTER 6 - CONCLUSIONS AND RECOMMENDATIONS 104

6.1 Summary. 104

TABLE OF CONTENTS
(CONT'D)

Page

6.2 Results and Conclusions 104
6.3 Recommendations for Future Study. 106

APPENDICES 108

APPENDIX A 109

APPENDIX B 110

APPENDIX C 116

APPENDIX D 120

APPENDIX E 123

APPENDIX F 126

BIBLIOGRAPHY 128

VITA

LIST OF FIGURES

Figure Page

1 Spherical Earth Centered Coordinate System 28

2 Body Centered Coordinate System for Reentry Vehicle. . . . 28

3 State Variables r, θ, and V for Optimal Reentry Trajectory. 45

4 State Variables ϕ, γ, and ψ for Optimal Reentry Trajectory. 46

5 Control, Acceleration, and Heating Rate for Optimal Reentry Trajectory. 47

6 Terminal Norm vs. Number of Iterations for Regularized and Standard Variables. 49

7 Altitude Histories for Two Types of Reentry Trajectories . 54

8 Control Histories for Two Types of Reentry Trajectories. . 55

9 Acceleration Histories for Two Types of Reentry Trajectories 56

10 State Variables for Optimal Constrained Brachistochrone. . 81

11 Terminal Norm vs. Number of Iterations for Constrained Reentry 91

12 State Variables r, θ, and V for Optimal, Constrained Reentry Trajectory. 93

13 State Variables ϕ, γ, and ψ for Optimal, Constrained Reentry Trajectory. 94

LIST OF FIGURES

(CONT'D)

14 Control, Acceleration, and Heating Rate for Optimal, Constrained Reentry Trajectory 95

15 Comparison of Altitude Histories for Constrained Optimal Trajectory and Apollo 10 Trajectory. 100

16 Comparison of Control Programs for Constrained Optimal Trajectory and Apollo 10 Trajectory. 101

17 Comparison of Acceleration Histories for Constrained Optimal Trajectory and Apollo 10 trajectory. 102

LIST OF TABLES

TABLE Page

1 Comparison of Accuracy Obtained Using the MPF and the Riccati Transformation for the Linear Example 20

2 Eigenvalues of the A Matrix for a Reentry Trajectory 41

3 Eigenvalues of the Linear System for a Reentry Trajectory. . 41

4 Nominal and Converged Multipliers for Optimal Reentry Trajectory. 44

5 Nominal and Converged Multipliers for Constrained Brachistochrone 80

6 Nominal and Converged Multipliers for Constrained Reentry. . 90

7 Terminal Norm for Last Ten Iterations of Constrained Reentry 92

LIST OF SYMBOLS

The following is a list of all symbols used in this report. Vectors are indicated by brackets with the dimension of the variable in the brackets. Matrices are denoted by brackets with both dimensions inside the brackets.

I	Performance Index
Q	Integrand of the performance index
$\overline{G}$	Part of performance index expressed as a function of terminal states and time
x[n]	State variables
u[m]	Control variable
M[q]	Terminal constraints
f[n]	The derivatives with respect to time of the state variables
H	Variational Hamiltonian
λ[n]	Multipliers associated with state vector
t	Independent variable, time
ν[q]	Multipliers associated with terminal constraints
z[2n]	Variables consisting of states and multipliers
F[2n]	Derivatives of states and multipliers evaluated using the optimal control
h[n+1]	Boundary conditions for optimization problem
A[2n x 2n]	Partial derivatives of F with respect to z's (i.e. $\frac{\partial F}{\partial z}$)
Φ[2n x 2n]	Fundamental matrix

LIST OF SYMBOLS

(CONT'D)

n	Number of state variables
m	Number of control variables
q	Number of terminal constraints
$\Phi_1[2n \times n]$	First n columns of the fundamental matrix
$\Phi_2[2n \times n]$	Last n columns of the fundamental matrix
W	Riccati transformation variable
r	Riccati transformation variable
τ	Independent variable
R	Smoothing transformation function
$\overline{H}$	Variational Hamiltonian times the smoothing function
r	Radial distance from the center of the earth to the reentry vehicle
θ	Longitude
ϕ	Latitude
V	Magnitude of velocity
γ	Flight path angle
ψ	Heading angle
μ	Gravitational constant
L	Lift per unit mass
D	Drag per unit mass
β	Control angle for reentry vehicle
C_L	Lift coefficient
C_D	Drag coefficient

LIST OF SYMBOLS

(CONT'T)

ρ	Density of air
ρ_o	Density of air at sea level
k	Density constant
r_e	Radius of earth
S^*	Vehicle reference area per unit mass
λ_o	Scaling constant for heating term
$\dot{Q}_c$	Convective heating rate
$Y[2n]$	Variables adjoint to δz
$\Theta[2n \times 2n]$	Variables adjoint to Φ
S	Inequality constraint function
$y[p]$	Constants along a pth order constraint
$Z[n-p]$	Dependent variables along the constraint boundary
$g[n-p]$	Derivatives of the Z equations on a SVIC boundary
G	Hamiltonian along a boundary segment
$\mu[n-p]$	Multipliers associated with Z's
M	Inverse transformation at constraint boundary
N	Inverse transformation at constraint boundary
P	Augmented function of final time and state
v	Combination of states and multipliers on a boundary
r_d	Specified value of the altitude constraint
p	Order of the state variable inequality constraint

LIST OF SYMBOLS

(CONT'D)

Special Symbols

$\delta(\ )$	Variation of ( )
$\Delta(\ )$	Total change in ( )
$(\dot{\ })$	Derivative with respect to t
$(\acute{\ })$	Derivative with respect to τ
$(\ )^T$	Transpose
$(\ )^{-1}$	Inverse
$\frac{d}{dt}(\ )$	Derivative of ( ) with respect to t
$\frac{\partial}{\partial t}(\ )$	Partial derivative of ( ) with respect to t
$(\ )_x$	Partial derivative of ( ) with respect to x

Abbreviations

MPF	Method of Perturbation Functions
VSI	Variable Step Integrator
FSI	Fixed Step Integrator
TPBVP	Two Point Boundary Value Problem
SVIC	State Variable Inequality Constraint

NOTATIONAL CONVENTIONS

1. The derivative of a vector with respect to a scalar does not change the direction of the vector, i.e.,

$$\frac{d}{dt}\begin{bmatrix} x_1 \\ \vdots \\ x_n \end{bmatrix} = \begin{bmatrix} \dot{x}_1 \\ \vdots \\ \dot{x}_n \end{bmatrix} \quad ; \quad \frac{d}{dt}[x_1 \ \dots \ x_n] = [\dot{x}_1 \ \dots \ \dot{x}_n]$$

2. The derivative of a scalar with respect to a vector becomes a row vector, i.e.,

$$\frac{\partial}{\partial x}[Q] = [\frac{\partial Q}{\partial x_1} \ \dots \ \frac{\partial Q}{\partial x_n}]$$

3. The derivative of a column vector, f, with respect to a column vector, x, is

$$\frac{\partial}{\partial x}[f] = \begin{bmatrix} \frac{\partial f_1}{\partial x_1} & \dots & \frac{\partial f_1}{\partial x_n} \\ \vdots & & \vdots \\ \frac{\partial f_n}{\partial x_1} & \dots & \frac{\partial f_n}{\partial x_n} \end{bmatrix}$$

4. The derivative of a row vector, f, with respect to a column vector, x, is

$$\frac{\partial}{\partial x}[f] = \begin{bmatrix} \frac{\partial f_1}{\partial x_1} & \dots & \frac{\partial f_1}{\partial x_n} \\ \vdots & & \vdots \\ \frac{\partial f_n}{\partial x_1} & \dots & \frac{\partial f_n}{\partial x_n} \end{bmatrix}$$

CHAPTER I

INTRODUCTION

Until recently manned space flight has been confined to earth orbital missions. When the reentry phase of the trajectory is initiated from an earth orbit, the velocity is fairly small. Apollo reentry velocities for earth orbital missions are approximately 25,800 ft./sec. As manned space flight extends beyond earth orbital missions, however, the reentry maneuver becomes more complex. These trajectories involve substantially higher reentry velocities at the initiation of the reentry phase. The initial reentry velocity for an Apollo vehicle returning from a lunar mission is approximately 36,000 ft./sec. Consequently the acceleration and heating experienced by the reentry vehicle and crew are much higher. Careful design of nominal reentry trajectories is required to ensure that the acceleration and heating experienced by the astronauts and reentry vehicle are below certain tolerance limits.

The Apollo reentry vehicle uses the lifting capabilities of the body to fly trajectories which have these desired characteristics. The high initial reentry velocity is reduced through the conversion of kinetic energy to heat. As the initial velocity increases so does the heat generated. This requires elaborate insulating and ablating devices to protect the crew and vehicle from the extremely high temperatures produced during reentry.

Minimal heat producing trajectories thus become very important for crew safety. They also require less elaborate heat dissipative systems. From previous numerical experience[18], however, minimal heating trajectories produce unacceptable acceleration histories. Two quantities associated with the acceleration are important for a reentry trajectory.[52] The acceleration peaks must be below some prescribed maximum level. For manned reentry this maximum level is approximately 10 g's. The criteria for determining an acceptable acceleration history, however, is not just the maximum acceleration peak. Fairly high accelerations can be tolerated by the astronauts if they are applied over fairly short time intervals. Hence the integral of the acceleration or the acceleration dosage gives a reasonable measure of crew comfort as long as the acceleration peaks do not exceed some acceptable value. Thus it is desirable to have a minimal value of the acceleration dosage for a reentry trajectory.

Acceptable reentry trajectories will require a trade off between minimal heating trajectories and trajectories with acceptable acceleration histories. A possible approach to the trade off problem consists of setting up the reentry trajectory as an optimal control problem, and using numerical techniques to generate minimizing trajectories. Reentry trajectories are calculated which minimize a linear combination of the total heat and the integral of the deceleration experienced by the reentry vehicle. A weighting factor is chosen for the heating term such that the total heating and the integral of the deceleration are given a relative weighting. For this study the weighting factor is chosen such that the integral of the acceleration and the total heating are approximately equal. If the peak accelerations produced by this method are sufficiently low then the solution should represent a compromise between minimal heating and minimal acceleration trajectories. If the peak accelerations are too high, then methods for reducing the accelerations peaks such as state variable inequality constraints (SVIC) must be considered.

Since trajectory optimization is a difficult problem, a relatively simple model which represents the important factors governing reentry is desired. For the vehicle this consists of neglecting motion about the center of mass. Constant lift and drag coefficients are assumed. The control of the vehicle is the roll angle or out of plane orientation of the lift vector. Ref. 48 indicates that this gives a fairly accurate representation of the Apollo reentry vehicle.

The model for the earth's gravitational field and atmosphere are approximated by an inverse square force field and an exponential atmosphere. Constants for the atmosphere are selected to represent the actual atmosphere over the interval of interest. This model represents the dominant characteristics of Apollo-type reentry trajectories.

Reentry trajectory optimization has been considered by several authors. Methods used include the gradient[2,3,6,18,20,23,24,45] conjugate gradient[42], quasilinearization[14], sweep method[22,42], and perturbation method (MPF).[1,2,13,15,26] The gradient method which generates only approximately optimal solutions has been used more extensively than any other method. This is probably because the gradient method has the ability to produce reasonable trajectories and insight is gained in the types of trajectories desired even if optimal trajectories are not produced. If true optimal trajectories are desired, however, a second order method must be used. Since the purpose of the investigation is to obtain accurate optimal solutions for the reentry problem the perturbation method is chosen for the study. This method is discussed by Goodman and Lance[27], and Jurovics and McIntyre.[32] It has the disadvantage that initial values of the Lagrange multipliers must be guessed. Convergence depends on these guesses and if there is no appriori information available concerning the optimal trajectory, it is often difficult to guess multipliers which will allow convergence. After an optimal solution has been obtained, however, it is very easy to vary parameters and generate fields of extremals.

The MPF is considered in Chapter 2, and its relation to the optimal control problem is discussed. The numerical procedures involved in implementing MPF and the instability of the perturbation equations are also considered. The application of the MPF to the reentry problem is considered in Chapter 3. Optimal numerical solutions are presented. In Chapter 4, SVIC are discussed. A new method of solving these problems using a modified MPF is presented and a numerical example, a constrained Brachistochrone is solved. The method of solving SVIC problems developed in Chapter 4 is applied to the reentry problem in Chapter 5. An altitude constraint is applied to the skip segment of the reentry trajectory and numerical optimal reentry trajectories with the SVIC are shown. Chapter 6 summarizes the results of this study and presents recommendations for further study in this area.

CHAPTER 2

NUMERICAL OPTIMIZATION USING THE PERTURBATION METHOD

This chapter defines the notation and presents the equations which define admissible candidates for the optimal trajectory. The MPF is described also. Derivations of these relations are not given since they are presented in numerous places in the literature. It is felt, however, that a summary of the pertinent equations from these discussions would be helpful in understanding the remainder of this report. In the following section, the numerical integration and matrix inversion routines used in this report are described. In the last section, the stability problem associated with the perturbation equations is considered.

2.1 Optimization Problem

Necessary conditions for optimal control problems have been obtained through the use of Dynamic Programming[28], Pontryagin's Maximum Principle[16], and the Calculus of Variations.[29,30] Since the results are well known, they will be summarized only for the class of problems to be considered in this report.

The statement of the problem is as follows: Find u(t) in the interval $t_o \leq t \leq t_f$ to extremize

$$I = \int_{t_o}^{t_f} Q(x,t)dt + \overline{G}[x_f,t_f] \tag{2.1}$$

subject to

$$\dot{x} = f(x,u,t) \tag{2.2}$$

and

$$x_o = x_{os} \quad , \quad M(x_f, t_f) = 0 \tag{2.3}$$

where x is an n vector of state variables, u is a scalar control, f is an n vector containing the derivatives of x, M is a q vector of terminal constraints, x_{os} is a specified initial state, and Q and $\overline{G}$ are scalars associated with the performance index. The initial time, t_o, is fixed, and the final time, t_f, is free.

Necessary conditions for a minimal trajectory are

$$\dot{x} = H_\lambda^T \quad , \quad \dot{\lambda} = -H_x^T \tag{2.4}$$

and

$$H_u = 0 \quad , \quad H_{uu} \geq 0 \tag{2.5}$$

where H is the variational Hamiltonian, $H = \lambda^T f + Q$, and λ is an n vector of Lagrange multipliers associated with x. At t_o

$$x_o = x_{os} \quad , \quad t_o = 0 \tag{2.6}$$

and at t_f,

$$M(x_f, t_f) = 0 \quad , \qquad \lambda_f = P_{x_f}^T \quad , \quad P_{t_f} + H_f = 0 \tag{2.7}$$

where $P = \overline{G} + \nu^T M$ and ν is a q vector of multipliers associated with the M's.

If H_{uu} is positive definite, Eqs. (2.5) allow the optimal control to be determined explicitly as a function of x and λ. If the optimal value of the control is used to eliminate u from Eq. (2.4), the optimization problem is reduced to a two point boundary value problem (TPBVP). This is expressed as

$$\dot{z} = F(z,t) \tag{2.8}$$

where the 2n-vector z is defined as

$$z = \left[\frac{x}{\lambda}\right] \tag{2.9}$$

F is determined from Eq. (2.4) with the optimal control determined as a function of x and λ. Boundary conditions consist of n conditions, $x_o = x_{os}$, at $t_o = 0$ and $n+1$ conditions

$$h(z_f,t_f) = 0 \tag{2.10}$$

at t_f. The $n+1$ vector h consists of $n+1$ of the conditions from Eq. (2.7). The remainder of the conditions in Eq. (2.7) are used to eliminate the unknown vector, ν.

2.2 Perturbation Method

One method of attempting to solve the two point boundary value problem defined in the previous section is the method of perturbation functions (MPF). This method requires that values for the unknown initial Lagrange multipliers and the final time t_f be guessed. Then Eqs. (2.8) can be integrated numerically to generate a nominal trajectory. The terminal boundary conditions, Eqs. (2.10), will not generally be satisfied. Corrections to the guessed values for the unknown variables are calculated to drive the terminal constraints, h, to zero. This is accomplished by considering linear perturbations about the nominal trajectory. If the (i+1)-th trajectory is expanded about the i-th trajectory and only linear terms are considered then

$$\delta\dot{z} = \left(\frac{\partial F}{\partial z}\right)^i \delta z = A\delta z \tag{2.11}$$

and

$$\Delta h = -h^i = \left(\frac{\partial h}{\partial z_f}\right)^i \delta z_f + (\dot{h})^i \Delta t_f \tag{2.12}$$

where $\delta z = z^{i+1} - z^i$, $\frac{\partial F}{\partial z}$ or A is a $2n \times 2n$ matrix of partial derivatives evaluated along the i-th trajectory, $\dot{h} = \frac{\partial h}{\partial z_f}\dot{z}_f + \frac{\partial h}{\partial t_f}$, and h^i is the vector of terminal conditions evaluated on the i-th trajectory. The total change in h, $\Delta h = h^{i+1} - h^i$ becomes $\Delta h = -h^i$, if h^{i+1} is set equal to its desired value, zero. Eq. (2.11) can be integrated along a nominal trajectory to determine how changes in the n guessed multipliers at the initial time will produce changes in the values of the states and multipliers at the final time. This requires n integrations of Eq. (2.11). The $2n \times n$ matrix Φ_2 is defined such that

$$\dot{\Phi}_2(t,t_o) = A\Phi_2(t,t_o) \tag{2.13}$$

and

$$\Phi_2(t_o,t_o) = \left[\frac{0}{I}\right] \tag{2.14}$$

where I is the $n \times n$ identity matrix and 0 is the $n \times n$ null matrix. Changes in the final values of z are then related to changes in λ_o by

$$\delta z_f = \Phi_2(t_f,t_o)\delta\lambda_o \tag{2.15}$$

By using Eq. (2.15) in Eq. (2.12), the equation

$$-h^i = [\frac{\partial h}{\partial z_f}]^i \Phi_2(t_f,t_o)\delta\lambda_o + [\dot{h}]^i \Delta t_f \qquad (2.16)$$

is obtained. This linear system is solved for $\delta\lambda_o$ and Δt_f. These corrections are added to the i-th values of λ_o and t_f and the nonlinear equations, Eqs. (2.8), are reintegrated to obtain a new nominal. If Eqs. (2.8) and (2.10) were linear, the desired solution should be obtained after one correction. Since they are not for most problems of interest to the engineer, an iteration scheme must be used. Thus the nonlinear equations, Eqs. (2.8), and the perturbation equations, Eqs. (2.13), are integrated from t_o to a guessed final time using guessed values for the initial multipliers. Corrections are calculated to λ_o and t_f using the linearized boundary conditions and perturbation equations. The nonlinear equations and perturbation equations are reintegrated using the new values of λ_o and t_f. A new correction vector is calculated. This procedure is continued until $||h_i|| = h^T h$ (the norm of the terminal constraints) is below some prescribed small positive number. The procedure is then terminated.

For nonlinear problems, the corrections calculated from Eq. (2.16) are often so large that the linearized equations are not valid. In this case, if the correction vector calculated by Eq. (2.16) is used divergence often occurs. In order to avoid this, a decreasing terminal norm philosophy can be used. The correction calculated on the i-th iteration is added to the i-th unknown variables. The nonlinear equations are integrated with the new initial conditions. If the terminal norm for the (i + 1)-th integration is larger than the norm of the i-th integration, the magnitude of the i-th correction vector is decreased. The smaller correction vector is added to the i-th variables again. The nonlinear equations are reintegrated using the new (i + 1)-th variables. Scaling the correction vector and reintegrating the nonlinear equations continues until the terminal norm produced on the (i + 1)-th iteration is smaller than the norm on the i-th iteration. At this point the perturbation equations are integrated and a new correction vector is calculated. The procedure continues until the norm decreases below a small specified value.

From computational experience, the decreasing norm philosophy requires many iterations to converge if the initial nominal is far from the optimal. As an alternative to this method, a percentage correction procedure can be used. After the i-th correction is calculated, the norm of the i-th unknown variables and the norm of the i-th correction vector are calculated. The correction vector is scaled so that the norm of the correction is some percentage, possible 30%, of the norm of the unknown variables. This correction is accepted even if the terminal norm increases. If the norm of the correction is less than the specified percentage of the guessed variables then the full correction vector is accepted. From computational experience this last method requires considerably fewer iterations to converge than the first method does. The percentage correction procedure is used throughout this report.

2.3 Numerical Integration and Inversion Routines

The two basic numerical procedures associated with optimization using the MPF are numerical integration and matrix inversion. Convergence of the method is closely associated with the ability of the computational procedure to accurately integrate large systems of equations. The numerical integration is most important, since if accurate results are not obtained here, the matrix inversion is meaningless

One of the problems encountered using the MPF is the instability of the perturbation equations, which is discussed in the next section. Since stability is a major difficulty for the MPF, a numerically stable integration method would seem to be a necessity. A group of methods which are numerically stable are the Adams predictor-corrector methods considered in Ref. 46. These methods are strongly stable and hence suitable for integration over long intervals if round off errors can be controlled.

The integration routine used is a fourth order Adams predictor-corrector[44] with a fourth order Runge-Kutta starter. Both a fixed step integrator (FSI) and a variable step integrator (VSI) are considered. For the VSI, both an upper and a lower error bound are specified. A single step truncation error estimate is calculated for the predictor-corrector. If this error estimate for an integration step is larger than the upper error bound, then the step size is halved. The Runge-Kutta routine is used again as a starter with the smaller step size. If the error estimate is smaller than the lower bound, the step size is doubled and the Runge-Kutta method is required to generate starting values again. The FSI integrator uses the Runge-Kutta method as a started then switches control entirely to the predictor-corrector method.

The VSI routine is used for most of the integration in this investigation because it allows better control of integration errors.

For small error bounds, round off error is very important. Partial double precision arithmetic is used in the integration routine to help control round off errors. Values of the dependent variables are stored in double precision and all other computation is single precision. A description of a fixed step size version of this routine is in Ref. 33.

All computation is performed using the CDC 6600 computer at The University of Texas at Austin. The CDC 6600 has a single precision word length of 14 digits. Thus the partial double precision integration routine should give good control of round off errors. For a small relative error criteria accurate integration should be obtained.

The second numerical procedure required by the MPF is a matrix inversion routine, or a routine to solve a linear system of algebraic equations. The routine used does not calculate an inverse matrix. It solves the linear system directly using Gaussian elimination. Again, since fairly large systems are to be solved, the inversion is performed in double precision to minimize round off errors.

2.4 Stability of the Perturbation Method

One of the main problems associated with using the MPF to solve TPBVP problems is the instability of the perturbation equations, Eq. (2.11). If the A-matrix is constant, then the solution for Φ in general consists of the sum of n linearly independent exponential terms. If A is time dependent, the solutions still exhibit exponential behavior. For many nonlinear problems, such as reentry, the A-matrix will have positive and negative eigenvalues over the entire interval of interest. Positive eigenvalues imply positive exponential type terms. If the equations are integrated over a sufficiently long interval, the large magnitude of the positive eigenvalues will completely dominate the solution for Φ. When this happens, information about the true solution of the Φ matrix is lost. Thus if the solution to one element of the Φ matrix is equal to the linear sum of a positive exponential term and a negative exponential term, then the numerical solution will exhibit the characteristics of the small exponential only over a fairly short time interval. The value of the negative exponential will become small in magnitude and will be lost in the numerical integration error of the total solution which due to the positive exponential term, will be large in magnitude. This behavior is easily demonstrated by a linear example considered by Fox.[43] A linear example is considered so that analytic solutions can then be compared with numerical results obtained using the MPF.

In order to investigate the effects of stability, the linear system

$$\begin{bmatrix} \dot{x}_1 \\ \dot{x}_2 \end{bmatrix} = \begin{bmatrix} 11 & 12 \\ 1 & 0 \end{bmatrix} \begin{bmatrix} x_1 \\ x_2 \end{bmatrix} + \begin{bmatrix} -12t - 11 \\ 0 \end{bmatrix} \tag{2.17}$$

with

$$x_2(0) = 1 \quad \text{and} \quad x_2(t_f) = t_f + e^{-t_f} \tag{2.18}$$

is considered. The general solution to the problem is

$$\begin{aligned} x_1 &= 1 - C_1 e^{-t} + 12C_2 e^{12t} \\ x_2 &= t + C_1 e^{-t} + C_2 e^{12t} \end{aligned} \tag{2.19}$$

where C_1 and C_2 are constants. For the specified boundary conditions, the solution requires that $C_1 = 1$ and $C_2 = 0$.

The problem will now be solved by the perturbation method. This requires guessing $x_1(0)$ and integrating Eqs. (2.17) from $t = 0$ to $t = t_f$. The linear perturbation equations

$$\begin{bmatrix} \delta\dot{x}_1 \\ \delta\dot{x}_2 \end{bmatrix} = A \begin{bmatrix} \delta x_1 \\ \delta x_2 \end{bmatrix} \tag{2.20}$$

where $A = \begin{bmatrix} 11 & 12 \\ 1 & 0 \end{bmatrix}$

are integrated with the initial conditions

$$\delta x_1(0) = 1 \quad , \ \delta x_2(0) = 0 \tag{2.21}$$

Then a correction to $x_1(0)$ is calculated to make

$$h = x_2(t_f) - [t_f + e^{-t_f}] = 0 \tag{2.22}$$

The linear change in h is $\Delta h = \frac{\partial h}{\partial x(t_f)} \delta x(t_f) + \dot{h}(t_f)\Delta t_f$. Since t_f and $x_2(0)$ are specified, $\Delta t_f = 0$ and $\delta x_2(0) = 0$. Hence, Δh reduces to the following expression.

$$\Delta h = \frac{\partial h}{\partial x(t_f)} \Phi_1(t_f,0)\delta x_1(0) \tag{2.23}$$

where $\Delta h = -\{x_2(t_f) - [t_f + e^{-t_f}]\}$ and $\frac{\partial h}{\partial x(t_f)} = [0,1]$. Φ_1 in this case is a vector solution of Eqs. (2.20) with boundary conditions given by Eq. (2.21)

The system of equations and boundary conditions are linear, so the desired solution should be obtained after one correction using the perturbation equations. Thus Eq. (2.23) is solved for the correction to $x_1(0)$. This correction is added to the guessed value of $x_1(0)$. This should produce the true solution for $x_1(0)$ and hence the desired solution to the problem.

The question of interest is whether or not this can be done numerically, i.e., does one correction, for a guessed value of $x_1(0)$, give the exact solution?

For the initial conditions $\delta x_1(0) = 1$ and $\delta x_2(0) = 0$, the solution to the linear perturbation equations is

$$\begin{aligned} \delta x_1 &= +1/13\ e^{-t} + 12/13\ e^{12t} \\ \delta x_2 &= -1/13\ e^{-t} + 1/13\ e^{12t} \end{aligned} \tag{2.24}$$

The eigenvalues are seen to be 12 and -1.

If the other vector of the transition matrix is calculated for $\delta x_1(0) = 0$ and $\delta x_2(0) = 1$, the solution is

$$\begin{aligned} \delta x_1 &= -12/13\ e^{-t} + 12/13\ e^{12t} \\ \delta x_2 &= 12/13\ e^{-t} + 1/13\ e^{12t} \end{aligned} \tag{2.25}$$

For large time, that is for t sufficiently large that the small exponent is on the order of the integration errors, the two solutions become linearly dependent. Thus if t is sufficiently large that e^{-t} is on the order of the integration error for Eqs. (2.24) and (2.25) all information of the small exponent is lost from the solutions of these equations. At this point, the entire transition matrix no longer gives an accurate representation of all perturbations about the nominal trajectory. Convergence problems might be expected. Eqs. (2.24), however, still give a very accurate description of how changes in $\delta x_1(0)$ propagate along a nominal. As long as this equation can be integrated accurately, accurate corrections to $\delta x_1(0)$ should be expected. The MPF does not require the entire transition matrix to accurately represent all perturbations about a guessed nominal. In this case it only requires that half of the transition matrix give a true representation of how changes in the unknown initial variables alter the nominal trajectory.

As a second example, consider the same differential equations with the boundary conditions $x_2(0) = 0$ and $x_2(t_f) = t_f + e^{-t_f} - e^{12t_f}$. The solution is

$$\begin{aligned} x_1(t_f) &= 1.0 - e^{-t_f} - 12e^{12t_f} \\ x_2(t_f) &= t_f + e^{-t_f} - e^{12t_f} \end{aligned} \tag{2.26}$$

The important factor affecting convengence of the two problems is the desired boundary conditions. The desired solution for Case 1 requires that $C_2 = 0$, or the coefficient of the large exponential term be zero. For Case 2 the coefficient of the large exponential term is not zero. Numerical results for these two problems are shown in Table 1 for several values of t_f. The guess for $x_1(0)$ is 1.0 for all cases.

The results show that corrections calculated to $x_1(0)$ are very accurate for Case 1 (13 digits at least) even over long time intervals. Terminal accuracy is destroyed, however, by the fact that even if the coefficient of the large exponent is very small, approximately 10^{-13}, over long time intervals this term still becomes important. Since the computer has a finite word length, the coefficient of the large exponential term will never be identically zero. Even if it is initially set equal to zero, the finite word length of the machine produces a solution after the first integration step which does not correspond exactly to the solution desired. Thus after one integration step, the coefficient of the large exponential cannot be identically zero. Over a sufficiently long interval the large exponential will appear in the numerical solution. This term cannot be removed from the solution obtained in the manner described above. The MPF does, however, calculate an accurate correction for $x_1(0)$ even over long time intervals. The unstable perturbation equations can be used to predict accurately how changes in $x_1(0)$ change the final values of x_1 and x_2 for the example considered.

For the second problem considered, however, terminal accuracy is maintained even over long time intervals. This solution does not require that the coefficient of the large exponential be zero and accuracy is not as difficult to maintain.

When the MPF is used to solve other TPBVP's, the difficulties encountered in trying to integrate the state equations for Case 1 could occur in connection with the perturbation equations. If the boundary conditions for the perturbation equations require the coefficient of a positive exponential term to be zero, in general it will be impossible to numerically obtain the true solution over a long time interval. If this problem arises, the calculation of accurate corrections to guessed initial variables will be extremely difficult.

If the system had consisted of four state variables with two boundary conditions at each end, another problem could occur. As shown earlier, for the example, over long time intervals the rows of the entire Φ matrix become linearly dependent. If one large positive exponential existed for the four state variables mentioned above, both of the two required solutions to the perturbation equations could become linearly related over long time intervals. In this case, the difference in the eigenvalues of the A-matrix, the time interval of interest, the machine word length, and the required boundary conditions for the perturbation equations would all be relavent factors in determining whether or not the MPF would solve the problem accurately.

Since the Riccati transformation is often mentioned as an alternative to the MPF, and since it is claimed that the Riccati transformation uncouples the perturbation equations and leads to stability, the example is solved also by this method. The transformation is

$$\delta x_2 = W\delta x_1 + r\delta x_2(t_f) \tag{2.27}$$

and the differential equations for W and r are

$$\begin{aligned} &\dot{W} + W(A_{11} - A_{22}) + W^2 A_{12} - A_{21} = 0 \\ &\dot{r} + r(WA_{12} - A_{22}) = 0 \\ &W(t_f) = 0 \quad , \quad r(t_f) = 1 \end{aligned} \tag{2.28}$$

where subscripts on the A's denote rows and columns of the A matrix. The correction to $x_1(0)$ is then

$$\delta x_1(0) = - \frac{r(0)}{W(0)} \delta x_2(t_f) \tag{2.29}$$

The A's are constant and thus for the example the differential equations for W and r do not depend on the guessed nominal for the state equations. Results for the Riccati solution are presented also in Table 1. In all cases the results obtained using the Riccati transformation are not as accurate as those obtained using the MPF. The analytic solution for the Riccati variables is

$$W = 1/12 \left\{ \frac{1 - e^{13(t_f-t)}}{1 + 1/12\, e^{13(t_f-t)}} \right\}$$

and

$$r = 13/12 e^{(t_f-t)} \{1 + 1/2 e^{13(t_f-t)}\}^{-1}$$

For large t_f, W approaches minus one. As the difference between the true solutions of W and minus one gets small, the difference is lost in the integration error. Again, information about the true solution of a differential equation is lost due to a finite word length machine. If the numerically integrated value of W(0) is compared with the analytic solution, they agree to 9 or 10 digits for all of the cases. The numerically integrated values of r(0), however, only agree with the true solutions to 6 or 7 digits. Hence the loss of accuracy in r(0) causes the correction to $x_1(0)$ calculated by the Riccati transformation to be less accurate than the correction calculated by the MPF.

Method	Problem No.	t_f	ITERATION 1 Accuracy* of x_{2f}	ITERATION 1 Accuracy of x_{10}	ITERATION 2 Accuracy of x_{2f}	ITERATION 2 Accuracy of x_{10}
MPF	1	1.0	10	13	11	13
MPF	1	1.5	7	14	9	14
MPF	1	2.0	4	14	6	14
Riccati	1	1.0	3	7	7	10
Riccati	1	1.5	1	7	4	10
Riccati	1	2.0	0	7	1	10
MPF	2	1.0	11	7	11	7
MPF	2	1.5	11	7	11	7
MPF	2	2.0	11	7	11	7
Riccati	2	1.0	7	7	11	7
Riccati	2	1.5	7	7	11	7
Riccati	2	2.0	7	7	11	7

*Accuracy denotes number of correct digits determined by the method, compared to true analytical solution.

TABLE 1. Comparison of Accuracy Obtained Using the MPF and Riccati Transformation for the Linear Example

Note that in integrating the Riccati equation, it is put in the form

$$\frac{dW}{A_{12}W^2 + (A_{11} - A_{22})W - A_{21}} = - dt \tag{2.31}$$

As long as $4(-A_{21})(A_{12}) - (A_{11} - A_{22})^2$ is negative, the general solution is of the form

$$W = \frac{b_1 + C_1 e^{b_2 t}}{b_3 - C_1 e^{b_2 t}} \tag{2.32}$$

where b_1, b_2, and b_3 are constants determined by the A elements. The constant of integration is C_1. If b_2 is large and negative the solution approaches $\frac{b_1}{b_3}$ for large t_f. If b_2 is large and positive, the solution approaches -1. In either case, for sufficiently large t_f, information about the solution will be lost. This loss of information about the true solution of W could be causing the difficulty in the accuracy of the numerically integrated value of r.

Another alternative to the method used earlier is to integrate the perturbation equations backwards. If the equations are integrated backwards, the boundary conditions become

$$\delta x_2(t_f) = 0 \quad , \quad \delta x_1(t_f) = 1 \tag{2.33}$$

and the solution to Eq. (2.20) becomes

$$\begin{aligned} \delta x_1 &= 1/13e^{(t_f-t)} + 12/13e^{-12(t_f-t)} \\ \delta x_2 &= -1/13e^{(t_f-t)} + 1/13e^{-12(t_f-t)} \end{aligned} \tag{2.34}$$

Comparing these with Eqs. (2.24) it is seen that the signs on the exponents have been changed. The end result of the integration, however, is the same. For large time intervals $e^{-12(t_f-t_o)}$ becomes much smaller than $e^{(t_f-t)}$. When its value is on the order of the round off error, all information of the large negative exponential is lost. Thus, if information is lost from having positive exponentials swamp negative exponentials during forward integration, information will also be lost in backward integration.

For the specific boundary conditions chosen for Case 1, however, the coefficient of the large exponential should be zero. For a finite word length machine, as discussed earlier, it will never be identically zero. The e^{12t} term will eventually destroy terminal accuracy if the integration is done in a forward direction. If the integration of the state equations is done backwards, this term, e^{12t}, becomes $e^{-12(t_f-t)}$ and thus decreases instead of increasing. The undesired solution decreases and is lost in the integration error instead of increasing and destroying terminal accuracy as it does when the integration is done in a forward direction. Thus the integration of the equations should be done backwards for the specified boundary conditions. On the other hand, if the boundary conditions required that the coefficient of the smaller exponential, e^{-t}, vanish then integration should be done in a forward direction. If the integration is done backwards, then the desired solution, $e^{-12(t_f-t)}$, would eventually be corrupted by $e^{(t_f-t)}$ for large time.

The main point is that the choice of forward or backward integration depends on the boundary conditions which must be satisfied. For nonlinear problems, analytic solutions cannot, in general, be obtained.

The interaction of boundary conditions and the exponential type terms is not known. It is clear from the example that for general boundary conditions, integration can be corrupted in both directions. Hence if problems are encountered when integration is done in one direction, it might be advisable to try integrating the equations in the opposite direction. Initially, however, one direction of integration does not seem to be favored over the other.

As mentioned earlier, stability is affected by the word length of the machine. If the word length of the machine had been eight digits instead of fourteen, the coefficient of the large exponential would have been approximately 10^{-7} instead of 10^{-13}. Hence the large exponential term would build up much faster. If stability is a problem, increasing the word length should improve the numerical integration characteristics.

In summary, stability of the integration of both the state equation and the perturbation equation is a problem for the MPF. Over sufficiently long time intervals large exponentials, if they exist in the perturbation solutions, may completely swamp smaller exponentials. Over shorter intervals, if an accurate representation of the true behavior of the perturbation equations may be obtained numerically, then accurate results may be calculated using the MPF. It is seen also that the Riccati transformation does not always improve stability problems. In this case results obtained using the Riccati transformation are worse than those obtained using the MPF. The solution to stability problems is not backward integration since again information about the solution to the perturbation equations can be lost over long intervals. This does not imply that integrating the equations backwards might not be useful in some circumstances. It is shown that backward integration for Case 1 of the example gives a much better representation of the smaller exponential than forward integration. Thus in some cases backward integration would be useful for either state or perturbation equations.

For problems involving a large number of variables, the question of stability seems to be whether or not a sufficient number (n for the optimization problem described earlier) of linearly independent solutions can be obtained to the perturbation equations. As mentioned earlier, this depends on the eigenvalues, time interval of interest, boundary conditions, and machine word length. Machine word length is usually fixed except for the possibility of going to double precision arithmetic. For some problems this would seem to be very beneficial. Two possibilities of improving the other conditions will now be considered.

First, if the time interval of interest is so long that independent solutions cannot be obtained to the perturbation equations, the interval may be divided into two segments. Missing boundary conditions for the TPBVP may be guessed at both the initial and the final times. The state and perturbation equations are integrated from the initial time and from the final time to an intermediate time. Then the guessed boundary conditions at both ends are corrected to make the states continuous at the intermediate time. This method is suggested by Fox.[43] It requires guessing $2n + 1$ variables for the optimization problem defined earlier but it should improve the accuracy of the Φ integration since Φ need not be integrated over the entire trajectory.

An alternate approach is similar to regularization. A time transformation

$$t' = \frac{dt}{d\tau} = R(x) \qquad (2.35)$$

is made where R is a scalar function of the x's. The differential equations associated with the optimization problem and the perturbation equations are derived.

The problem is to extremize

$$I = \int_{t_o}^{t_f} [H - \lambda^T \dot{x}]dt \qquad (2.36)$$

subject to $\frac{dt}{d\tau} = R(x)$. Then

$$I = \int_{\tau_o}^{\tau_f} [HR - \lambda^T \dot{x}R]d\tau \qquad (2.37)$$

but $\dot{x}R = \dot{x}\frac{dt}{d\tau} = x'$ and

$$I = \int_{\tau}^{\tau_f} [\overline{H} - \lambda^T x']d\tau \qquad (2.38)$$

where $\overline{H} = HR$. Now attach Eq. (2.35) to the integral using the multiplier λ_t and define x to be the old x's and t, and λ to be the old λ's and λ_t. If H is independent of t and t_f is free then τ_f is free and $\lambda_t = 0$. Thus Eq. (2.35) adds nothing to the problem and may be integrated separately after the optimization procedure to determine the actual time.

If the first variation of Eq. (2.38) is required to vanish then

$$x' = \bar{H}_\lambda^T \quad , \quad \lambda' = -\bar{H}_x^T \quad , \quad H_u R = 0 \tag{2.39}$$

or

$$\begin{aligned} x' &= \dot{x}R \\ \lambda' &= \dot{\lambda}R - HR_x^T \\ H_u &= 0 \end{aligned} \tag{2.40}$$

The variational equations are

$$\begin{aligned} \delta x' &= \delta\dot{x}R + \dot{x}\delta R \\ \delta\lambda' &= \delta\dot{\lambda}R + \dot{\lambda}\delta R - \delta HR_x^T - H\delta R_x^T \end{aligned} \tag{2.41}$$

For H independent of time and t_f free, $H = 0$, and $\delta H = 0$ along an optimal. Hence the same equations would be obtained along an optimal if the nonlinear equations $\dot{z} = F(z)$ were transformed to $z' = F(z)R$ and then the variational equations were obtained. The important point is that the characteristics of the A matrix are altered by the transformation. It might be possible to choose the transformation $R(x)$ to improve integration characteristics of both the nonlinear equations and the linear perturbation equations.

Neither of these methods has been fully tested. They are mentioned here primarily as topics for future research.

CHAPTER 3

UNCONSTRAINED REENTRY OPTIMIZATION

3.1 Reentry Problem

Numerical optimization of a large system of nonlinear equations is a difficult task. With this in mind, the model used to obtain the state equations for reentry should be as simple as possible while retaining the dominant characteristics of the actual reentry problem. Thus the model will consist of an inverse square gravitational force field for the earth. The atmosphere will be assumed to vary exponentially with altitude. For the reentry vehicle, constant lift and drag coefficients are used and the only control of the vehicle is the roll angle. For fairly short reentry trajectories these assumptions give a good representation of the actual Apollo reentry problem, while keeping the model sufficiently simple that numerical solutions may be obtained.

In order to determine the differential equations governing the reentry trajectory, consider a fixed spherical coordinate system located at the center of the earth. The position of the vehicle is then located by r, the distance from the center of the coordinate system to the center of mass of the vehicle, θ, the longitude, and ϕ, the latitude. (See Fig. 1).

The magnitude of the velocity of the vehicle is represented by V. The flight path angle is γ and the heading angle is ψ. These are shown in Fig. 2. The body fixed coordinate system is designated by the unit vectors e_X, e_Y, and e_Z. With these variables the equations governing reentry are

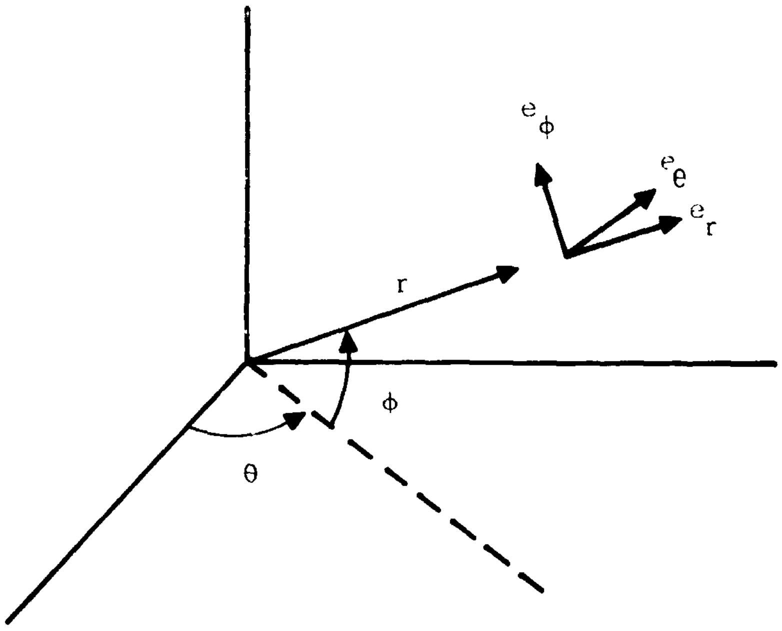
e_ϕ
e_θ
e_r
r
ϕ
θ

FIG. 1. Spherical Earth Centered Coordinate System

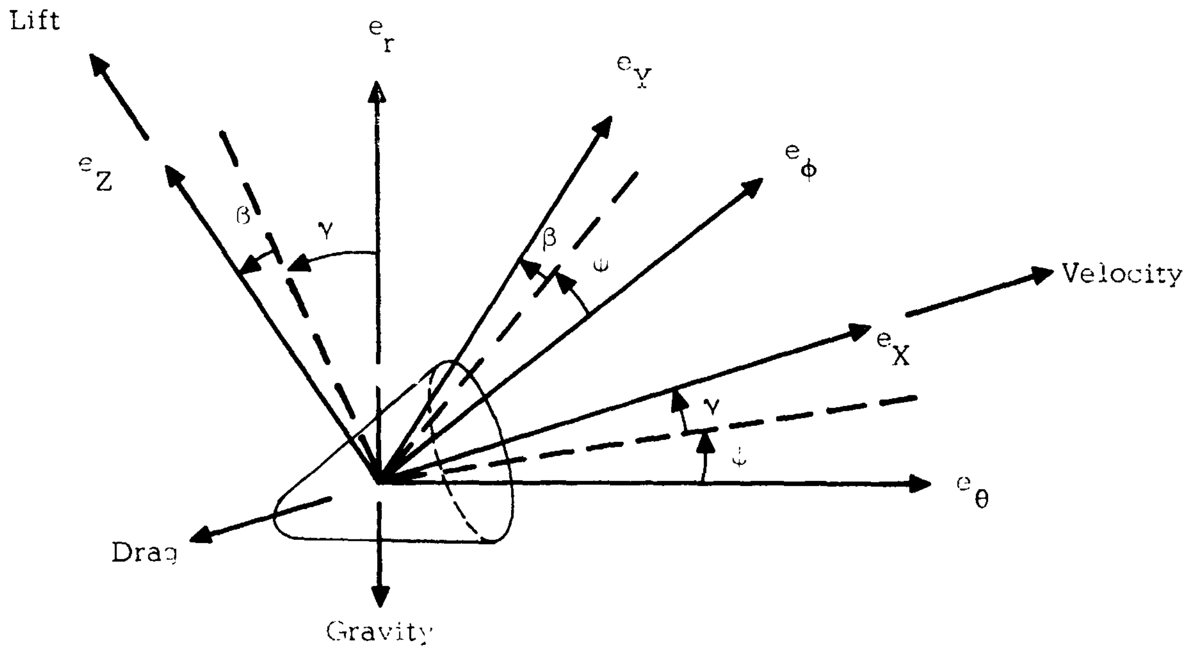
Lift
e_r
e_Y
e_Z
e_ϕ
β
γ
β
ψ
Velocity
e_X
γ
ψ
e_θ
Drag
Gravity

FIG. 2. Body Coordinate System For Reentry Vehicle

$$\begin{aligned}
\dot{r} &= V \sin \gamma \\
\dot{\theta} &= \frac{V \cos \gamma \cos \psi}{r \cos \phi} \\
\dot{\phi} &= \frac{V \cos \gamma \sin \psi}{r} \\
\dot{V} &= -\frac{\mu \sin \gamma}{r^2} - D \\
\dot{\gamma} &= -\frac{\mu \cos \gamma}{r^2 V} + \frac{V \cos \gamma}{r} + \frac{L}{V} \cos \beta \\
\dot{\psi} &= -\frac{V \cos \gamma \cos \psi \sin \phi}{r \cos \phi} - \frac{L \sin \beta}{V \cos \gamma}
\end{aligned} \tag{3.1}$$

where μ is the gravitational constant, L is the lift per unit mass of the vehicle, D is the drag per unit mass, and β is the control angle shown in Fig. 2. The lift and drag per unit mass are

$$L = \frac{1}{2} C_L \rho S^* V^2 \ , \quad D = \frac{1}{2} C_D \rho S^* V^2 \tag{3.2}$$

where S^* is the reference area divided by the mass of the vehicle, C_L is the lift coefficient, C_D is the drag coefficient, and ρ is the density of the atmosphere. An exponential atmosphere is assumed so that

$$\rho = \rho_o e^{-k(r-r_e)} \tag{3.3}$$

where ρ_o is the density at sea level, k is a constant, and r_e is the radius of the earth. The numerical values for the C_D, C_L, and S^* are chosen to represent an Apollo-type reentry vehicle. Values for the density are chosen to represent the actual atmosphere over the altitudes of interest for reentry. (See Ref. 11). All numerical values are shown in Appendix A.

Since the two basic problems associated with reentry are the heating and the aerodynamically induced acceleration the quantity to be minimized is

$$I = \int_{t_0}^{t_f} [(L^2 + D^2)^{1/2} + \lambda_0 \dot{Q}_c]dt \tag{3.4}$$

where $\dot{Q}_c$ is the convective heating rate and λ_0 is a constant chosen to give a relative weighting to the deceleration and the heating term. In this investigation the two terms are given an approximately equal weighting. Since the convective heating is substantially larger than the other forms of heating for reentry with initial velocities on the order of 36,000 ft./sec.[18], it is the only type of heating considered here. The approximation for the heating term used is[18]

$$\dot{Q}_c = 20\rho^{1/2} \left(\frac{V}{1000}\right)^3 \frac{\text{BTU}}{\text{ft.}^2\text{-sec.}} \tag{3.5}$$

where ρ is in slugs/ft.^{3} and V is in ft./sec. For all numerical computation the heating term times the weighting constant will be written as $\lambda_0 \rho^{1/2} V^3$ where the unit of length for ρ and V is in miles. Thus the numerical value of λ_0 shown in Appendix A includes both the scaling factor and the numerical constants and unit conversion factors associated with $\dot{Q}_c$.

The important quantities associated with the deceleration during reentry are the cumulative deceleration and the maximum values of the deceleration.[20] An astronaut can take fairly high accelerations if they are applied over short time intervals. Thus the integral of the acceleration is a reasonable quantity in the performance index to represent the acceleration-time interval relationship.

The reentry trajectory must satisfy a specified set of boundary conditions. The initial conditions are fixed and given. These initial conditions for reentry are the terminal conditions for the Apollo transearth coast trajectory. Corrections are made during the transearth coast to ensure that the initial conditions for reentry will be very close to the desired conditions. Hence these conditions remain approximately constant for all Apollo lunar trajectories. Reentry begins at an altitude of 400,000 ft., a velocity of 36,000 ft./sec., and a flight path angle of -6.5 degs. The other state variables θ, ϕ, and ψ are initially set equal to zero for convenience.

Terminal conditions include specification of latitude and longitude so that the reentry vehicle may land near a recovery vessel. The velocity is fixed also since a small specified terminal velocity is required before opening the landing parachute. The final time and other terminal variables are left open. The terminal conditions are expressed as

$$\begin{aligned} \theta_f &= \theta_{fs} \\ \phi_f &= \phi_{fs} \\ V_f &= V_{fs} \end{aligned} \tag{3.6}$$

where s denotes specified conditions.

Before applying the MPF to the reentry problem, the optimization problem must be reduced to the TPBVP. The Hamiltonian for the reentry problem is

$$H = \lambda_r[VS\gamma] + \lambda_\theta\left[\frac{VC\gamma C\psi}{rC\phi}\right] + \lambda_\phi\left[\frac{VC\gamma S\psi}{r}\right]$$

$$+ \lambda_V\left[-\frac{\mu S\gamma}{r^2} - D\right] + \lambda_\gamma\left[-\frac{\mu C\gamma}{r^2V} + \frac{VC\gamma}{r} + \frac{L}{V}C\beta\right] \qquad (3.7)$$

$$+ \lambda_\psi\left[-\frac{VC\gamma C\psi S\phi}{rC\phi} - \frac{LS\beta}{VC\gamma}\right] + Q$$

where $C\gamma = \cos\gamma$ $\quad S\gamma = \sin\gamma$, etc.

The equations for the multipliers are:

$$\dot\lambda_r = \frac{VC\gamma C\psi}{r^2C\phi}\lambda_\theta + \frac{VC\gamma S\psi}{r^2}\lambda_\phi - \left(\frac{2\mu S\gamma}{r^3} - \frac{S^*}{2}C_D\rho_r V^2\right)\lambda_V$$

$$- \left(\frac{2\mu C\gamma}{r^3V} - \frac{VC\gamma}{r^2} + \frac{S^*}{2}C_L\rho_r VC\beta\right)\lambda_\gamma$$

$$- \left(\frac{VC\gamma C\psi S\phi}{r^2C\phi} - \frac{S^*}{2}C_L\rho_r V\frac{S\beta}{C\gamma}\right)\lambda_\psi - Q_r$$

$$\dot\lambda_\theta = 0$$

$$\dot\lambda_\phi = -\frac{VC\gamma C\psi S\phi}{rC^2\phi} \qquad \frac{VC\gamma C\psi}{r}\lambda_\psi \qquad (3.8)$$

$$\dot\lambda_V = -S\gamma\lambda_r - \frac{C\gamma C\psi}{rC\phi} \qquad \frac{C\gamma S\psi}{r}\lambda_\phi$$

$$+ S^*C_D\rho V\lambda_V - \left[\frac{\mu C\gamma}{r^2V^2} + \frac{C\gamma}{r} + \frac{S^*}{2}C_L\rho C\beta\right]\lambda_\gamma$$

$$+ \left[\frac{VC\gamma C\psi S\phi}{rC\phi} + \frac{S^*}{2} C_L \rho \frac{S\beta}{C\gamma}\right]\lambda_\psi - Q_V$$

$$\dot{\lambda}_\gamma = - VC\gamma\lambda_r + \frac{VS\gamma C\psi}{rC\phi}\lambda_\theta + \frac{VS\lambda S\psi}{r}\lambda_\phi + \frac{\mu C\gamma}{r^2}\lambda_V$$

$$- \left(\frac{\mu S\gamma}{r^2 V} - \frac{VS\gamma}{r}\right)\lambda_\gamma - \left(\frac{VS\gamma C\psi S\phi}{rC\phi} - \frac{S^*}{2} C_L V \frac{S\gamma S\beta}{C^2\gamma}\right)\lambda_\psi$$

$$\dot{\lambda}_\psi = \frac{VC\gamma S\psi}{rC\phi}\lambda_\theta - \frac{VC\gamma C\psi}{r}\lambda_\phi - \frac{VC\gamma S\psi S\phi}{rC\phi}\lambda_\psi$$

where

$$Q_r = \frac{S^*}{2}(C_L^2 + C_D^2)^{1/2}\rho_r V^2 + 1/2\lambda_o\rho^{-1/2}\rho_r V^3$$

$$Q_V = S^*(C_L^2 + C_D^2)^{1/2}\rho V + 3\lambda_o\rho^{1/2}V^2$$

and

$$\rho_r = - k\rho$$

The optimal control is determined by requiring that $H_\beta = 0$ and $H_{\beta\beta} \geq 0$. From these conditions it follows that

$$\sin\beta = \frac{\lambda_\psi}{(\lambda_\psi^2 + \lambda_\gamma^2 C^2\gamma)^{1/2}} \qquad \cos\beta = \frac{-C\gamma\lambda_\gamma}{(\lambda_\psi^2 + \lambda_\gamma^2 C^2\gamma)^{1/2}}$$

(3.9)

If the expressions for sin β and cos β are used in the differential equations for the states and multipliers, a system of 12 first order coupled differential equations is obtained. The transversality conditions associated with the problem lead to the following additional conditions.

$$\lambda_r(t_f) = 0, \; \lambda_\gamma(t_f) = 0, \; \lambda_\psi(t_f) = 0, \text{ and } H(t_f) = 0 \tag{3.10}$$

The TPBVP now consists of the 12 differential equations, Eqs. (3.1) and (3.8) with β eliminated by using Eqs. (3.9), the fixed initial state and time (7 conditions), and terminal boundary conditions, Eqs. (3.6) and (3.10) (7 conditions).

The coefficients for the perturbations equations are obtained by taking the partial derivatives with respect to the states and multipliers of Eqs. (3.1) and (3.8) after β has been eliminated. These are shown in Appendix B.

The definition of the reentry problem to be considered is now complete. In summary, the control angle, β, must be determined so that the integration of the state equations, Eqs. (3.1), from the specified initial conditions to the terminal conditions, (Eqs. (3.6), yields a minimal value for the performance index, Eq. (3.4).

3.2 Numerical Accuracy Studies

The perturbation method outlined in Chapter 2 is used to calculate optimal reentry trajectories for Apollo-type missions. Before the results are presented some of the numerical problems encountered in generating optimal solutions should be discussed. The perturbation method, as do most numerical optimization methods, requires two basic numerical procedures; i.e., the integration of a system of first order ordinary differential equations, and the inversion of a matrix. The ability of the method to converge to optimal solutions is very dependent on the accuracy obtained during these two procedures.

For reentry, most of the problems in calculating optimal trajectories are a result of the numerical integration procedure. For each iteration, the nonlinear equations including the state and Lagrange multiplier equations, and the linear perturbation equations must be integrated. Reentry for Apollo lunar return trajectories is characterized by high accelerations and heating rates. These cause large variations in the derivatives of x and λ making numerical integration very difficult. Hence the first problem is the development of an integration routine which can accurately integrate the nonlinear equations, Eqs. (3.1) and (3.8). The accuracy of the integration of the nonlinear equations is determined by using a fixed step size and a variable step size version of the integration routine discussed in Section (2.4). The accuracy of the integration is checked as follows: a nominal trajectory characterized by specified initial values of x, λ, and t_f is selected. The values used are shown in Table 4 as the nominal values. For the FSI, an integration step size is selected and the nonlinear equations are integrated to a specified t_f. The step size is decreased and the equations are reintegrated. As the step size is decreased, changes in the final values of x and λ should become smaller and smaller until round off errors become a factor.

For the VSI, the same procedure is followed by decreasing the relative single step error criteria. Again, as the upper error bound decreases, the step size along the trajectory decreases. Changes in x_f and λ_f should become smaller as the step size is decreased until round off errors become important.

For the nominal shown in Table 4, a fixed step size of 0.25 seconds or a variable step size error bound, ϵ, of $10^{-10} \leq \epsilon \leq 10^{-8}$ is found to produce six digit accuracy by this method. Any further decrease in the step size or upper error bound produces changes in the seventh digit or less. The integration time for the FSI is 5.6 seconds and is 4.0 seconds for the VSI.

The accuracy of the integration is checked also for several other initial values of the multipliers. In all cases, the VSI using error bounds listed above performs better (requires less time for integration) than a FSI with a step size which gave comparable accuracy.

The accuracy of the integration using the VSI is checked also by a second method. The equations are integrated to a specified t_f with given initial values of x and λ. These final values of x and λ are then used as initial conditions to integrate the equations backwards from t_f to t_o. Values of x and λ at t_o calculated from the backwards integration are compared with the original initial conditions. These numbers should agree if the integration of the equations is accurate. For the nominal just discussed the variables at t_o agree to six digits.

The results of the initial analysis of the integration accuracy indicate that the nonlinear equations can be integrated accurately. The best approach is the variable step size integrator. This allows sufficient accuracy while requiring less time than the FSI to integrate the equations for reentry.

The second question concerning the integration accuracy is associated with the integration of the linear perturbation equations. Since the time dependent coefficients of the linear system are dependent on the values of x and λ, accurate integration of the nonlinear [illegible] is necessary for accurate integration of the linear system.

accurate integration of the nonlinear equations is not sufficient for accurate integration of the linear equations. The accuracy of the linear equations can be checked in the same manner as the accuracy of the nonlinear equations. Since only unit perturbations in the initial values of the λ's are required, all comparisons are based on just this part of the Φ matrix. An error bound of 10^{-8} to 10^{-10} produces 6 digits which are not altered by decreasing the error bound.

Numerical partial derivatives are calculated also in order to check the accuracy of the linear system. The nominal previously computed is compared with another integration of the nonlinear equations with a small change in one of the initial multipliers. For instance, a change of 1.0E-6 is made in λ_{r_0}. The first row of the Φ_2 matrix should then be approximately equal to

$$\frac{z_f \Big|_{\lambda_{r_o} + 1.0E-6} - z_f \Big|_{\lambda_{r_o}}}{1.0E-6}$$

The agreement between the numerical partials and the Φ matrix for the nominal discussed above is at least 3 digits. This indicates that the linear system is probably analytically correct. Similar accuracy is obtained for other columns of the Φ matrix.

An alternate method of checking the accuracy of the Φ integration will now be considered. Several authors have recommended that for reentry optimization, the equations should be integrated backwards, i.e., integrate back out of the atmosphere instead of into it. This suggests the application of the adjoint method.[31] The equations adjoint to Eq. (2.11) are

$$\dot{Y} = - [\frac{\partial F}{\partial z}]^T Y \tag{3.11}$$

where Y is a 2n vector of adjoint functions.

If the system

$$\dot{\Theta} = - [\frac{\partial F}{\partial z}]^T \Theta \tag{3.12}$$

where Θ is a 2n x(n + 1) matrix of adjoint functions with boundary conditions

$$\Theta_f^T = [\frac{\partial h}{\partial z_f}] \tag{3.13}$$

is integrated from t_f to t_o, the solution of Eq. (2.12) can be

$$\Delta h = \Theta^T(t_o,t_f)\left[\begin{array}{c}0\\ \hdashline \delta\lambda_o\end{array}\right] + \dot{h}\,\Delta t_f \tag{3.14}$$

At this point, it is noted that $n + 1$ integrations of Eq. (3.11) are required for the adjoint method. If, however, the Hamiltonian is independent of time then

$$\dot{H} = \left(\frac{\partial H}{\partial z}\right)\dot{z} = 0 \tag{3.15}$$

implying that the Hamiltonian is a constant and thus

$$H = \text{const} = H_o = H_f \tag{3.16}$$

Since a boundary condition is $H_f = 0$ this also implies $H_o = 0$ or to first order

$$\Delta H = \frac{\partial H}{\partial \lambda_o}\,\delta\lambda_o \tag{3.17}$$

since $\delta x_o = 0$ and $\Delta t_o = 0$.

This determines one row of the linear system, Eq. (2.12), without any integration. Consequently only n integrations of Eq. (3.11) are required if the Hamiltonian is constant. Eq. (3.17) can be used also with the perturbation method, but this does not decrease the number of integrations required for MPF.

If these n integrations are made, the coefficients of the linear system obtained by this method can be compared with the coefficients obtained by the perturbation method. Note that this does not compare all of the integration required for either of Eqs. (2.11) or (3.11) but only the elements of the integration which are to be used in solving the linear system of equations. These, however, are the important elements of the integration and as far as the optimization procedure is concerned, are the only elements which affect convergence of the method.

If the linear system generated by MPF and that generated by the adjoint method are compared for the previous nominal, all elements of the system agree to at least five digits. The correction vectors calculated by the two methods agree to six digits.

The ability to reproduce the linear system generated by MPF by the adjoint method and by numerical partial derivatives should indicate that sufficient accuracy is being obtained to allow convergence of the method.

Eigenvalues are calculated for the A matrix at specified intervals along the nominal trajectory. A representative set of eigenvalues is shown in Table 2. Over the entire trajectory, four and occassionally six of the eigenvalues are very small. Note that each large, positive, real part of an eigenvalue has a corresponding negative real part of an eigenvalue. The small exponentials correspond to approximately constant solutions. As long as the time interval is sufficiently short so that the exponential type terms accurately represent linear perturbations, good results may be expected.

The second numerical procedure used extensively by the optimization method is that of matrix inversion. Since the ratio of the largest eigenvalue to the smallest one gives an indication of the

Real	Imaginary	Real	Imaginary
-1.013E-2	4.984E-2	1.305E-3	0.0
-1.013E-2	-4.984E-2	-1.305E-3	0.0
1.013E-2	4.984E-2	1.282E-14	9.219E-4
1.013E-2	-4.984E-2	1.282E-14	-9.219E-4
9.573E-3	0.0	-4.457E-15	0.0

TABLE 2. Eigenvalues of the A Matrix for a Reentry Trajectory

Real	Imaginary
-5.566E+1	0.0
-5.223	2.346
-5.223	-2.346
1.013	0.0
-1.640E-3	0.0
5.690E-4	0.0
-7.350E-4	0.0

TABLE 3. Eigenvalues of the Linear System for a Reentry Trajectory

difficulty in inverting a matrix, eigenvalues are calculated for the linear system produced by the nominal used for the integration accuracy studies. The magnitude of the largest eigenvalue is 55.7 and the smallest is 7.3E-4. (See Table 3). These values are typical of eigenvalues obtained on other nominals. Since the ratio is on the order of 10^5 and the word length of the CDC 6600 is 14 digits, inversion of the matrix should not be a problem.

3.3 Numerical Results

The numerical values of physical constants are shown in Appendix A. Initial values of the states are selected to represent Apollo reentry conditions for lunar return missions. These are

$$\begin{aligned}
r_o &= 4035.75758 \text{ miles (400,000 feet altitude)} \\
\theta_o &= 0.0 \text{ radians} \\
\phi_o &= 0.0 \text{ radians} \\
V_o &= 6.81818182 \text{ miles/sec. (36,000 ft./sec.)} \\
\gamma_o &= -\ 0.113446401 \text{ radians } (-6.5°) \\
\psi_o &= 0.0 \text{ radians}
\end{aligned} \tag{3.18}$$

Terminal conditions are

$$\begin{aligned}
\theta_{fs} &= 0.33 \text{ radians} \\
\phi_{fs} &= -\ 0.025 \text{ radians} \\
V_{fs} &= 0.5 \text{ miles/sec.}
\end{aligned} \tag{3.19}$$

Initial values of the multipliers and final time are selected from Ref. 51. Both a gradient method and sweep method are used to obtain these initial values. The mass of the vehicle in that study is different from the one considered here. Since this nominal integrates through a singularity ($\gamma = -90°$) at $t = 400$ sec., the guess for t_f is changed to 380 sec. The initial nominal values and the converged values are shown in Table 4.

Eight iterations are required to decrease the terminal norm ($h^T h$) from 5.4 to 4.2E-11.

Plots of the state variables are shown in Figs. 3 and 4. Fig. 5 shows the control, acceleration, and convective heating rate. The maximum deceleration is 16.0 g's. The maximum heating rate is 804.6 BTU/ft.^{2}-sec. and the total heat absorbed by the vehicle is 48657.0 BTU/ft.^{2}.

All trajectories obtained have the same general characteristics of the one shown. They are skip trajectories with high peak accelerations and heating rates. The initial entry into the atmosphere is sufficiently deep so that the terminal phase of the ballistic segment of the trajectory is approximately at the specified terminal longitude. As the specified final value of the longitude increases, so does the skip altitude. For large values of θ_{fs}, most of the reentry time is spent on the ballistic skip segment. Also during the initial entry phase, the lift vector is oriented so that the final value of the latitude is approximately the specified value. Increasing θ_{fs} and ϕ_{fs} increases the performance index. Thus short inplane trajectories produce minimal values for the performance index. Changing the final

Variable	Nominal Values	Converged Values
λ_r	3.98397469E-3	-1.24748687E-3
λ_θ	-8.95206071	-9.17150992
λ_ϕ	8.31654552	26.5110657
λ_V	2.52107557	2.35519683
λ_γ	16.9208133	13.8236235
λ_ψ	3.25899074	8.83828355
t_f	380.0	391.80724

Terminal Conditions: θ_f = 0.33 radians, ϕ_f = -0.025 radians,
V_f = 0.5 miles/sec.

TABLE 4. Nominal and Converged Multipliers for Optimal Reentry Trajectory

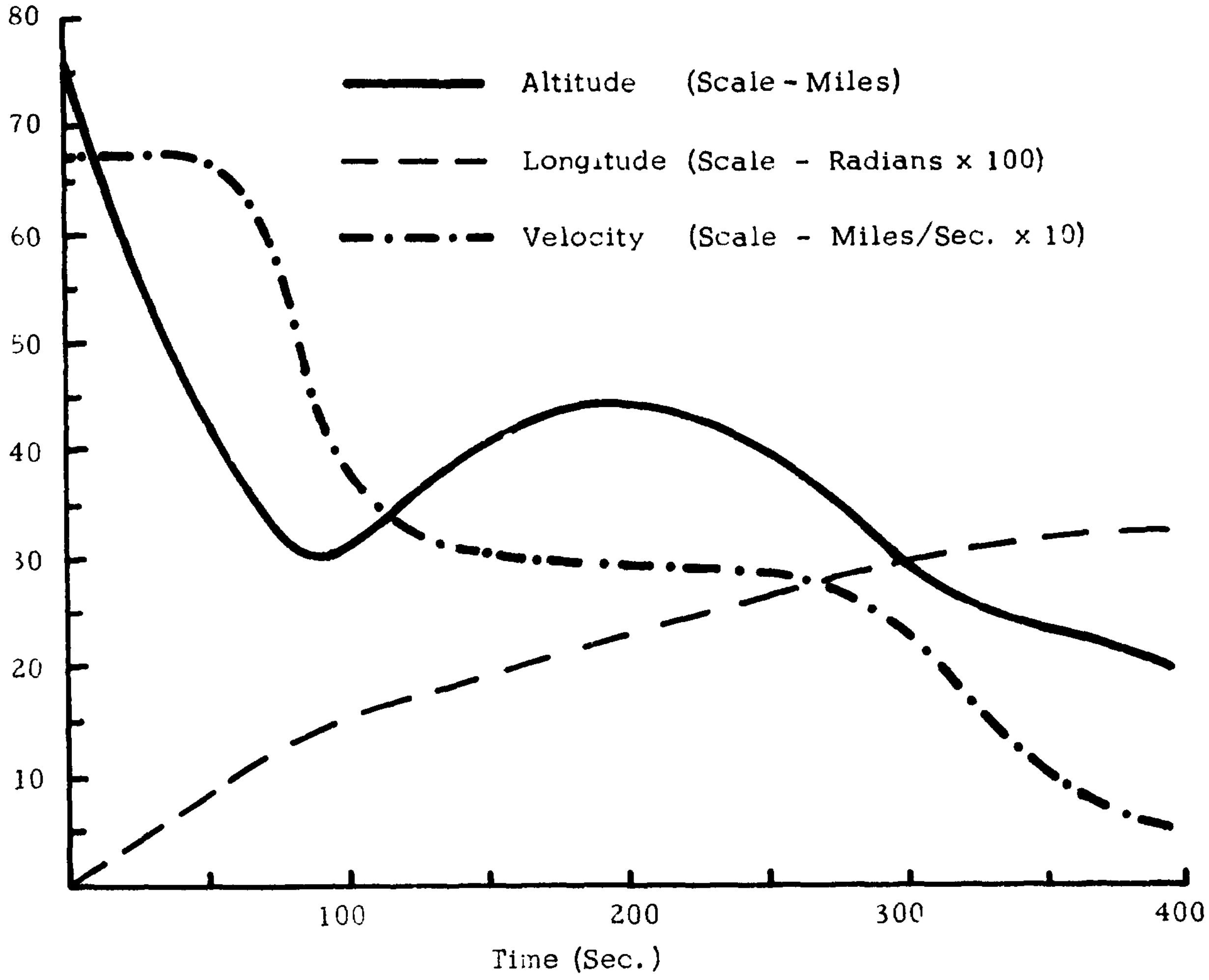

FIG. 3. State Variables r, θ, and V for Optimal Reentry Trajectory

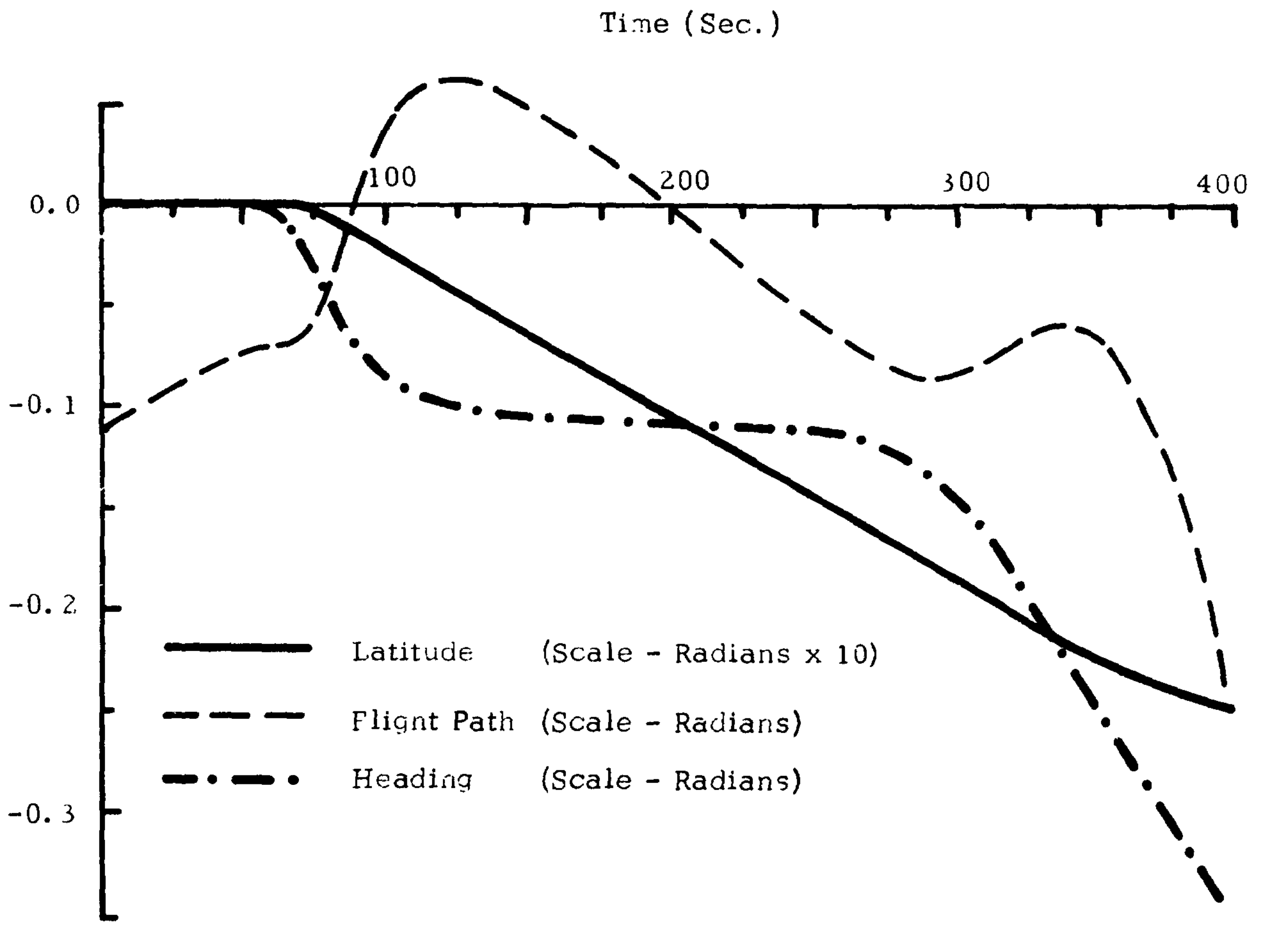

FIG. 4. State Variables, ϕ, γ, and ψ for Optimal Reentry Trajectory

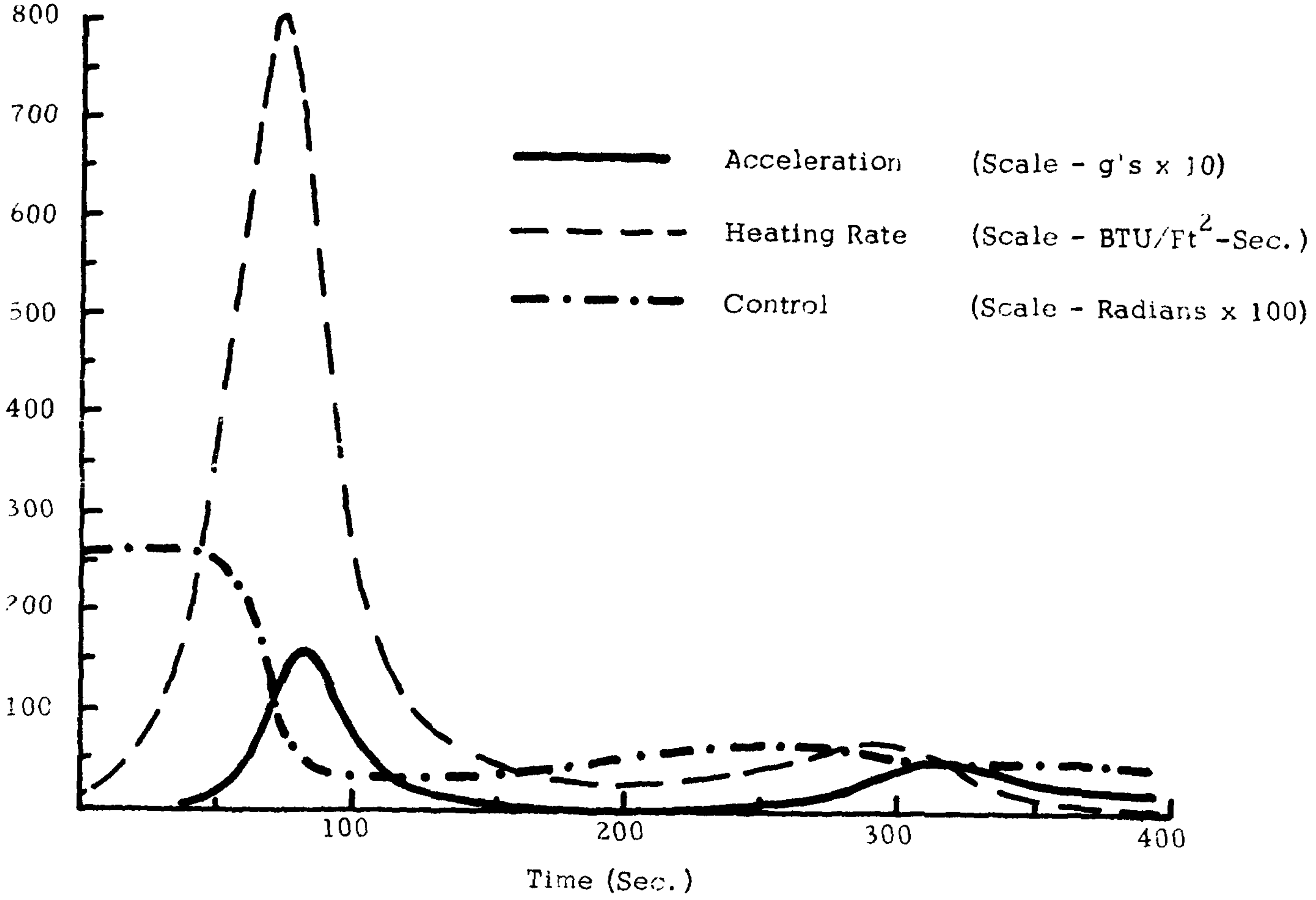

FIG. 5. Control, Acceleration, and Heating Rate for Optimal Reentry Trajectory

velocity changes the performance index only slightly since lowering the velocity just causes the trajectory to terminate at a slightly lower altitude. The heating rate and acceleration are small at this phase of the trajectory, and integrating the equations further into the atmosphere adds very little to the performance index.

It is relatively easy to vary terminal conditions and other parameters and obtain near by solutions using the MPF method. Changing the terminal conditions to $\theta_{fs} = 0.4$ radians and $V_{fs} = 0.2$ miles/sec. and using the multipliers from the previous converged trajectory requires 15 iterations to converge to the new conditions.

A problem is encountered when the converged multipliers for $\theta_{fs} = 0.4$ radians and $V_{fs} = 0.2$ miles/sec. are used as initial guesses for the trajectory with $\theta_{fs} = 0.5$ radians and $V_{fs} = 0.2$ miles/sec. The MPF diverges for this case. The terminal norm plotted against the number of iterations is shown in Fig. 6. After the third iteration, γ is approximately -90°. The state equations, Eq. (3.1) show that a singularity exists in the $\dot{\psi}$ equation when $\gamma = \pm 90°$. If during the iteration process the singularity is encountered, convergence of the method is very uncertain. Two methods of avoiding this difficulty will now be discussed.

First, when the singularity is approached, the guess for the final time may be decreased. After iteration 21, if the value of the final time is changed from 541.365408 sec. to 500.0 sec., convergence occurs in 7 iterations. This change is sufficient to avoid the singularity and hence to allow convergence.

A better method of avoiding the singularity is to remove it

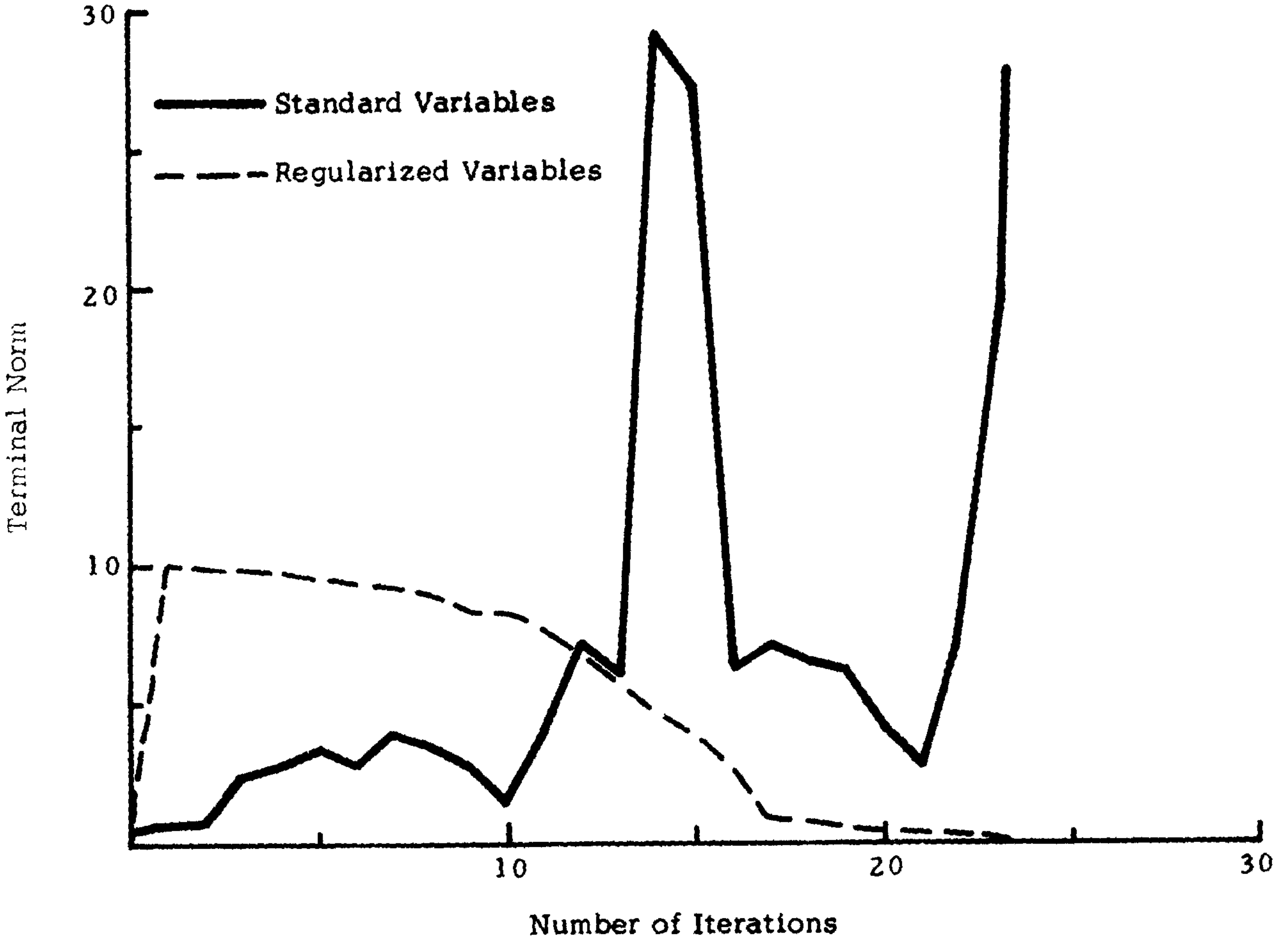

FIG. 6. Terminal Norm vs. Number of Iterations for Regularized and Standard Variables

from the differential equations. The change of independent variables discussed in Section (2.4) may be used to remove the singularity. This process is known as regularization. The advantages of regularization for the calculation of optimal interplanetary transfers are presented in Ref. 50. Since the velocity also approaches a very small value at the final time, the transformation used is

$$\frac{dt}{d\tau} = V \cos \gamma \tag{3.20}$$

Then the change of variables

$$\bar{V} = V^2 \tag{3.21}$$

is made. The state equations become:

$$\begin{aligned}
r' &= \bar{V}C\gamma S\gamma \\
\theta' &= \frac{\bar{V}C^2\gamma C\psi}{rC\phi} \\
\phi' &= \frac{\bar{V}C^2\gamma S\psi}{r} \\
\bar{V}' &= -2\,\frac{\mu}{r^2}\,\bar{V}C\gamma S\gamma - S^*C_D\rho\bar{V}^2C\gamma \\
\gamma' &= -\frac{\mu}{r^2}\,C^2\gamma\,\frac{\bar{V}C^2\gamma}{r} + \frac{1}{2}\,S^*C_L\rho\bar{V}C\gamma C\beta \\
\psi' &= \frac{\bar{V}C^2\gamma C\psi S\phi}{rC\phi} - \frac{1}{2}\,S^*C_L\rho\bar{V}S\beta
\end{aligned} \tag{3.22}$$

No singularities are approached for this set of equations since ϕ is always small and r is never less than the radius of the earth. The multiplier equations are shown in Appendix F.

Since a change of variables is made, an initial guess for $\lambda_{\bar{V}}$ is required. The Hamiltonian in the new system must still be constant and zero. Since all terms of the Hamiltonian remain unchanged except those containing λ_V and $\lambda_{\bar{V}}$, these terms are equated. Thus if the Hamiltonian is zero in the V system, it will be zero in the $\bar{V}$ system if

$$\lambda_V \dot{V} = \lambda_{\bar{V}} \dot{\bar{V}} \tag{3.23}$$

Since $\bar{V} = V^2$ then $\dot{\bar{V}} = 2V\dot{V}$ or

$$\lambda_{\bar{V}} = \frac{\lambda_V}{2V} \tag{3.24}$$

Boundary conditions for τ are the same as those for t, that is $\tau_o = 0$ and τ_f is free. Since t does not appear in the state equations, Eq. (3.20) need not be integrated until a converged trajectory is obtained. A value of τ_f is guessed instead of t_f for the iteration process and corrections are calculated to τ_f using

$$\Delta h = \left(\frac{\partial h}{\partial z}\right) \Phi_2(\tau_f, \tau_o)\ \delta\lambda_o + (h')\ \Delta\tau_f \tag{3.25}$$

The value for $\lambda_{\bar{V}}(\tau_o)$ is calculated using Eq. (3.24), and the converged trajectory for $\theta_{fs} = 0.4$ radians is generated with $\tau_f = 356.0$. This value of τ_f gives a terminal norm of 10^{-5}. The value of θ_{fs} is then changed to $\theta_{fs} = 0.5$ radians. The regularized equations are allowed to iterate toward a solution. The regularized variables converge after 30 iterations. The change in the terminal norm is shown in Fig. 6.

The computer time for one iteration is considerably longer using regularized variables. The regularized variables require 55.7 seconds per iteration and the standard variables require 25.7 seconds per iteration. For one integration of the nonlinear equations, 7.1 seconds is required for the regularized variables and 4.0 seconds are required for the standard variables. The computer time requirements listed above are for the last iteration before convergence at $\theta_{fs} = 0.5$ radians.

The regularized variables do converge, however, and the standard variables do not unless the singularity is avoided. The increase in computer time using regularized variables is because most of the trajectory is not near the singularity. The regularized state equations are more complex which implies more terms to be evaluated in both the multiplier and perturbation equations. Regularization thus does not improve integration characteristics when the trajectory is not near the singularity. An alternate approach to the one used above is to integrate the standard variables until the singularity is approached. The extra equation $\frac{d\tau}{dt} = \frac{1}{V \cos \gamma}$ is integrated to determine τ. When the singularity becomes a problem, switch to the regularized variables. This would require less computer time per iteration. The computer program is more complex since two systems of equations are required. If the singularity is approached, however, regularization does definitely improve convergence characteristics. The improved convergence characteristics would probably be worth the extra effort.

The reason for the problem encountered in changing θ_{fs} from 0.4 radians to 0.5 radians is seen from Figs. 7, 8, and 9. Two types of trajectories are produced. The shorter trajectory, $\theta_{fs} = 0.4$ radians is shown as Trajectory 1. The initial entry is sufficiently deep into the atmosphere that the ballistic skip undershoots the desired θ_{fs} (See Fig. 7). Control near the terminal phase is lifting upward as seen from Fig. 8. The vehicle lifts upward and glides outward to the desired longitude. The longer trajectory $\theta_{fs} = 0.5$ radians is shown as Trajectory 2. The initial entry is not as deep into the atmosphere as Trajectory 1. The trajectory appears as though it will overshoot the desired longitude. Then near the end of the trajectory the vehicle rolls the lift vector 180° and flies down toward the desired value of θ_{fs}. This causes γ to approach -90°. Trajectory 1 lifts up near the end of the trajectory and does not cause the singularity to be approached.

For the given values of ϕ_{fs} and V_{fs}, the change in the type of optimal trajectory obtained is at $\theta_{fs} = 0.415$ radians. For values of θ_{fs} less than this value trajectories similar to those shown as Trajectory 1 are obtained. For values of θ_{fs} greater than this, trajectories similar to those shown as Trajectory 2 are obtained.

Since several authors favor backward integration over forward integration for dissipative systems, the reentry problem is solved by the MPF starting at the final time. Guesses are made for the unknown variables at the final time and for the time interval. These unknowns, r_f, γ_f, ψ_f, λ_{θ_f}, λ_{ϕ_f}, λ_{V_f}, and t_o, where t_o now represents the time

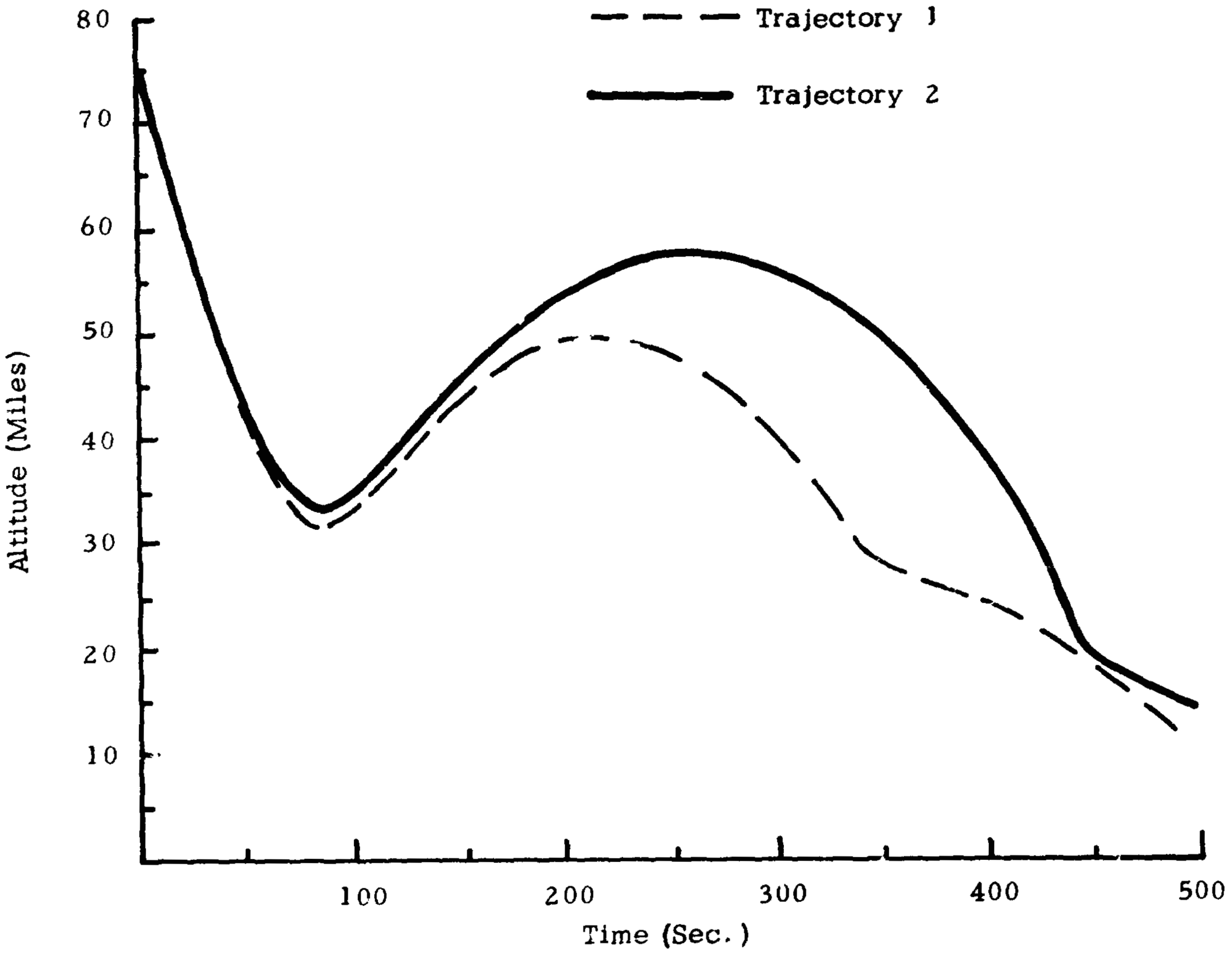

FIC Altitud. Histories for Two Types of Reentry Trajectories

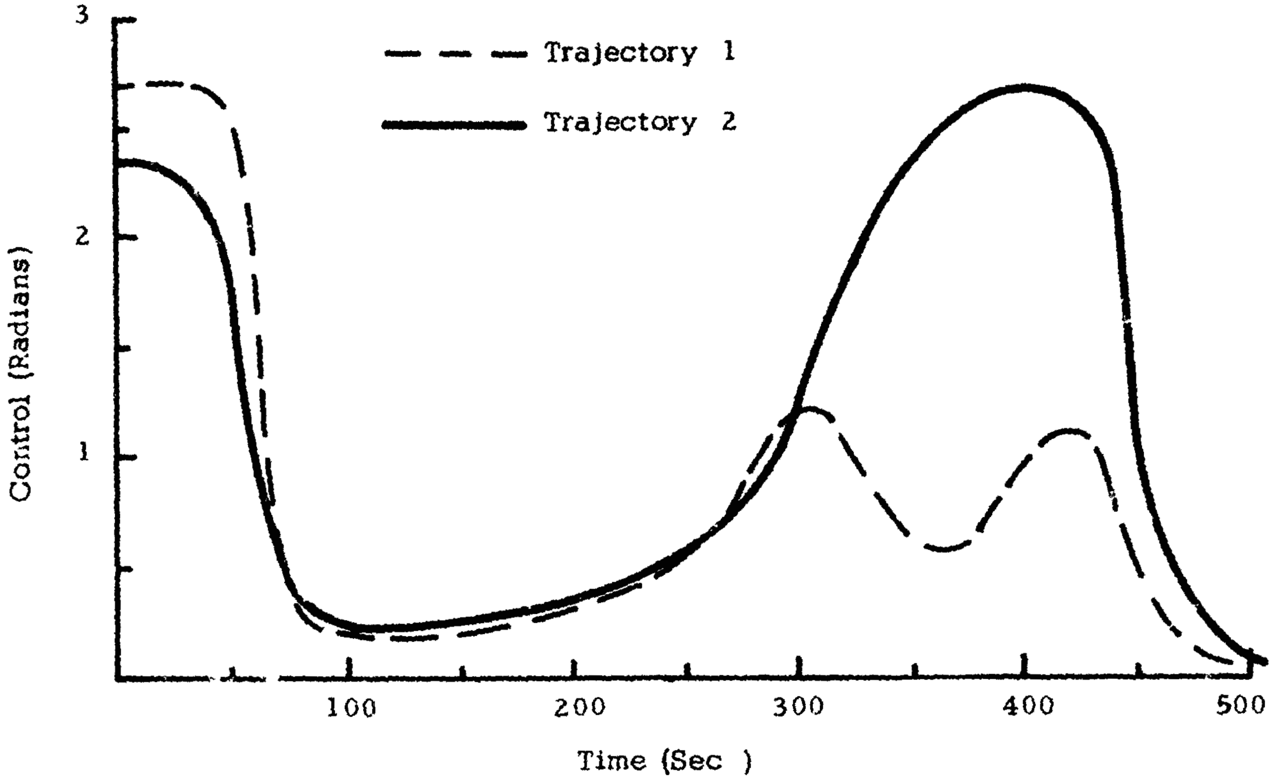

FIG 8. Control Histories for Two Types of Reentry Trajectories

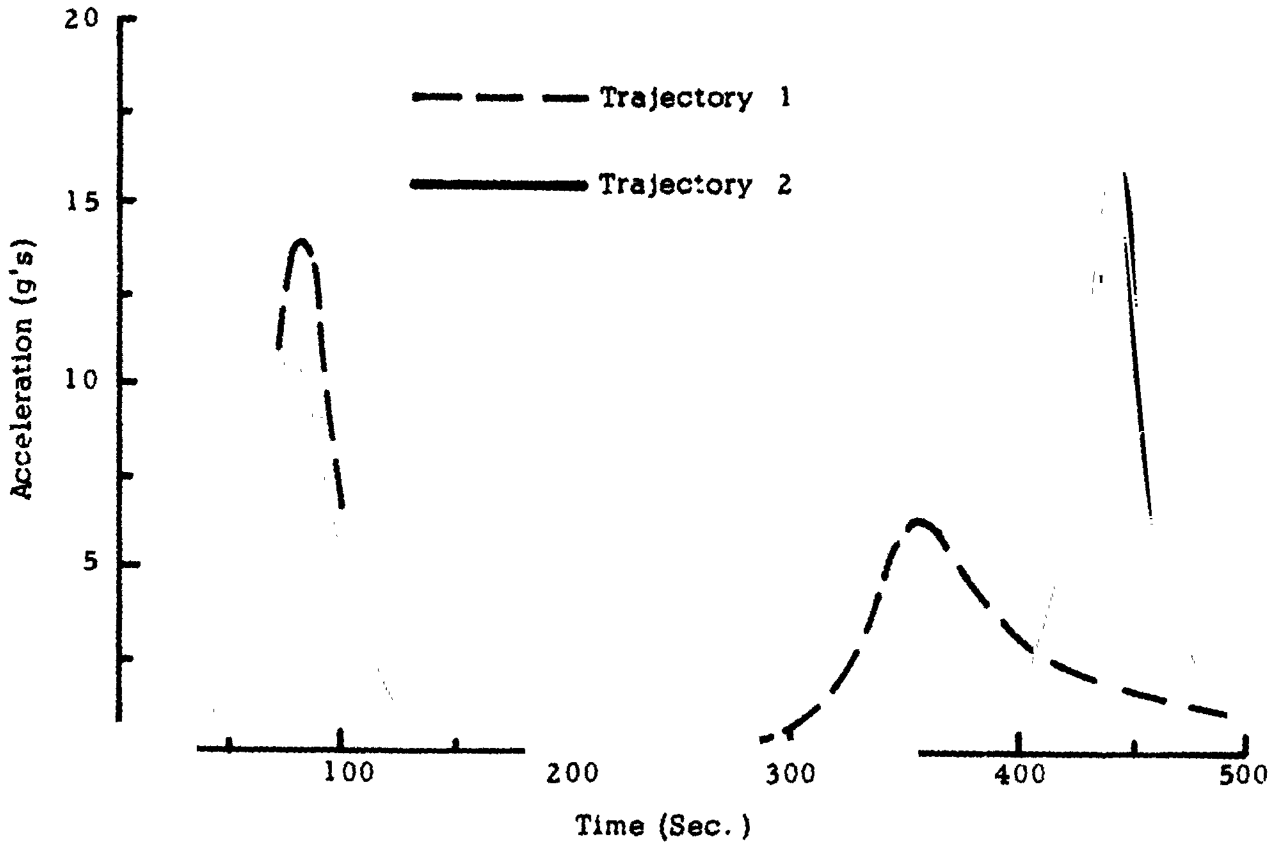

FIG. 9. Acceleration Histories for Two Types of Reentry Trajectories

at the initiation of the reentry trajectory, are corrected to drive the initial states to their specified values. A nominal trajectory produced by guessing unknown variables at t_o in general does not satisfy specified terminal conditions. A nominal produced by guessing unknown variables at t_f does not satisfy specified initial conditions. Hence the same initial nominal trajectory cannot be used for both the forward and backward iterations. Direct comparisons of the two approaches are thus not possible. From computational experience, however, there appears to be very little advantage, as far as convergence characteristics are concerned, in using either approach. Converged trajectories can be and have been obtained by either approach. The deciding factor would seem to be the specified boundary conditions. If initial states are fixed and extremals are required for various values of the terminal states, forward integration corrects an initial nominal trajectory which is acceptable and relatively accurate for reasonable changes in terminal conditions. For backward integration, changes in conditions at t_f could produce large changes in conditions at t_o thus requiring more iterations for convergence than forward integration. If various states at t_o are to be studied, then backward integration seems better suited to the problem.

The study presented in this chapter indicates that accurate numerical solutions can be obtained to the reentry optimization problem. Part of the success of the method in this study must be attributed to the computer used, i.e., the CDC 6600. Ref. 3 gives an indication of accuracy and integration time requirements for two dimensional optimization using a perturbation method on the IBM 7094, an eight digit machine. A lower energy, shorter trajectory is optimized in this reference. Leondes requires approximately 18 seconds per iteration. For the three dimensional model considered here, with a longer trajectory, 25 seconds are required per iteration. Leondes achieves three digit accuracy in his sensitivity functions (perturbation equations) and apparently has a great deal of trouble in converging trajectories. Five or six digit accuracy is obtained here and this appears to be sufficient to substantially improve convergence characteristics.

Trajectories presented in this chapter have the undesirable characteristic of high acceleration peaks. The trajectory shown has a maximum acceleration of 16 g's. This is above the generally accepted limit of 10 g's for manned reentry trajectories. Also the skip trajectories produced here do not allow control of the vehicle over the skip segment. Terminal conditions for this type of trajectory are difficult to predict due to atmospheric variations. Small changes in the atmosphere produces large changes in terminal conditions. In the following chapters, a method of improving the characteristics of the reentry trajectories will be discussed.

CHAPTER 4

STATE VARIABLE INEQUALITY CONSTRAINTS

4.1 Summary of Theory and Numerical Methods for SVIC

Unfortunately, most attempts to solve realistic problems in optimal control theory require the satisfaction of inequality constraints which are functions of the state and/or control variables. The reentry problem solved in Chapter 3 is an example of this situation. The peak acceleration experienced by the reentry vehicle is too high for manned reentry. Also the use of skip trajectories has been found to be extremely sensitive to atmospheric conditions. Exact reentry terminal conditions are difficult to predict for skip trajectories. Also, very little control of the trajectory is obtainable over the skip portion since the vehicle is outside of the sensible atmosphere. Thus reentry trajectories which remain in the atmosphere with small peak accelerations are desired.

Both of these constraints can be expressed as state variable inequality constraints (SVIC). The first constraint requires that the maximum acceleration be less than or equal to some prescribed maximum acceleration. For constant lift and drag coefficients, acceleration is a function only of altitude and velocity. The second constraint requires that the skip portion of the trajectory be less than or equal to a maximum skip altitude. Note that the control variable does not appear in either of the constraints. Constraints which contain the control variable explicitly will not be considered here.

Numerous developments of necessary conditions for a SVIC are given in the literature. Refs. 5, 8, 9, 16, 17, 23 consider this problem. Recently new necessary conditions have been derived by Jacobson, Lele, and Speyer.[47] A penalty function approach is used which does not require the assumption of finite boundary segments. If the order of the constraint is greater than two, they have shown that non-extremal solutions with finite boundary segments which satisfy all of the necessary conditions given in Ref. 23, may be obtained. For problems considered here, the order of the constraint is less than or equal to two. Hence the necessary conditions given in Ref. 23 are still applicable.

Several numerical methods have been used to obtain solutions to SVIC. These methods can generally be divided into penalty function methods and hard constraint methods. In the first case, a penalty term related to the constraint violation is added to the performance index. Then an attempt is made to drive the performance index to its minimum value which in a limiting sense should drive the constraint violation to zero. The penalty function technique has been used in connection with the gradient method[4,18,20,36,37] and quasilinearization.[25] The direct methods attempt to incorporate the constraint directly into the problem. A limiting process is not required. This method has been used with the gradient method[6,24,38] and perturbation method[41,40]. Comparison of penalty function techniques and hard constraint methods using a gradient method indicate that better convergence characteristics are obtained using the hard constraint method.[6]

An alternate approach to the numerical solution of optimal trajectories which satisfy SVIC is presented by Jacobson.[21] He uses a transformation technique based on early work by Valentine[12] to transform the SVIC into a singular arc problem. The singular arc problem is solved by a conjugate gradient method or some other method which will handle this type of problem. Jacobson[39] also has presented a penalty function method to solve the singular arc problem. The question of whether the penalty function solution of the singular arc problem or the direct penalty function solution of the SVIC is better, is not answered.

Another approach is that used by Speyer.[42] Some trajectories containing SVIC are separable. This implies that parts of the trajectory not on the constraint boundary may be solved independently and pieced together with the part on the boundary. With this approach, any method may be used to obtain the segments off of the boundary. However not all problems are separable.

To the author's knowledge attempts to develop second order methods to handle SVIC's directly for non-separable problems have been limited to the perturbation method or slight modifications of the perturbation method. Both of the methods referenced earlier apply the necessary conditions obtained in Ref. 5. They keep the full set of n Lagrange multipliers along the constraint boundary and assume that jumps in the multipliers occur at the time when the trajectory goes on the constraint. Both methods seem to exhibit good convergence characteristics for the problems considered, however, both references consider only very simple examples.

An alternate method of calculating optimal trajectories with SVIC based on necessary conditions shown in Ref. 23 and the perturbation method will be derived in the next section. This method reduces the state space and hence the number of multipliers while the trajectory is on a constraint. There are no jumps in multipliers at the entry time, as in the previous two methods; however, unknown multipliers do appear at the exit boundary. The necessary conditions for an extremal presented here have appeared previously in the literature. The modification of the perturbation method to calculate optimal constrained trajectories is new. It has not appeared in the literature before.

4.2 Necessary Conditions for SVIC

The necessary conditions for SVIC described below are derived in Ref. 23. A summary of the necessary conditions is presented for the sake of completeness and to familarize the reader with the notation to be used in the remainder of the dissertation. These conditions are derived by dividing the optimization problem into segments on the boundary and segments off the boundary. The state space is reduced for segments on the boundary implying a reduction in the number of multipliers required. Then the segments are tied together through corner conditions obtained by requiring that the first variation vanish. Only one boundary segment is considered since necessary conditions for all boundary arcs are identical to those obtained below. The problem statement is as follows:

Determine the control variable $u(t)$ over the interval $t_o \leq t \leq t_f$ to extremize

$$I = \int_{t_o}^{t_f} Q(x,t)dt + \overline{G}(x_f,t_f) \tag{4.1}$$

subject to $\dot{x} = f(x,u,t)$, $M(x_f,t_f) = 0$, $x(t_o) = x_{os}$, and $S(x,t) \leq 0$. The initial time is fixed. The definition of all terms except S is given in Section (1.1). The constraint S is a scalar function of the states and possible time and its value is required to be less than or equal to zero all along the trajectory.

Following accepted notation, a p-th order constraint is defined as one in which

$$\frac{\partial}{\partial u}\left[\frac{d^k S}{dt^k}\right] = 0 \quad , \quad k = 1, \ldots, p\text{-}1$$

and (4.2)

$$\frac{\partial}{\partial u}\left[\frac{d^p S}{dt^p}\right] \neq 0$$

Define

$$y = \begin{bmatrix} S \\ \vdots \\ S^{p-1} \end{bmatrix} \tag{4.3}$$

where $S^k = \dfrac{d^k S}{dt^k}$ and y is a p vector. The vector y is a function only of x and possibly t. Note that in order for S to be zero all along a boundary segment, it is required that $y = 0$ all along the boundary segment. Also the control must be determined from $S^p = 0$ to force the trajectory to remain on the boundary. Thus the number of variables required to describe the trajectory along a boundary arc is reduced from n to (n-p). Choose (n-p) states, Z, to describe the trajectory along the constraint. In general, the Z's will be chosen as (n-p) of the original states, x, which are not affected by the constraint. Thus

$$Z = \begin{bmatrix} Z_1(x,t) \\ \cdot \\ \cdot \\ \cdot \\ Z_{(n-p)}(x,t) \end{bmatrix} \tag{4.4}$$

and the Z's are chosen such that

$$\begin{vmatrix} \frac{\partial y}{\partial x} \\ \hline \frac{\partial Z}{\partial x} \end{vmatrix} \neq 0 \tag{4.5}$$

The last condition allows x to be determined as a function of y and Z.

The optimization problem can then be divided into arcs on the boundary and arcs off the boundary. On the boundary the state is determined from the conditions

$$\dot{Z} = g(Z,t) \quad , \quad y = 0 \tag{4.6}$$

where $g(Z,t)$ is the (n-p) vector of derivatives of the Z variables along the constraint boundary. The control is eliminated from the Z equations by using $S^p = 0$.

At this point it is assumed that an optimal trajectory exists that either touches the boundary at one or more points or has one or more intervals of finite length along the boundary. Necessary conditions for an optimal trajectory of this type are then derived. Then an attempt is made to determine a solution which satisfies these necessary conditions. In order to derive necessary conditions for the problem, only one segment on the SVIC boundary will be considered. Necessary conditions obtained, however, apply to any number of segments. The augmented performance index is written as

$$I = \int_{t_o}^{t_1^-} (H - \lambda^T \dot{x})dt + \int_{t_1^+}^{t_2^-} (G - \mu^T \dot{Z})dt$$

$$+ \int_{t_2^+}^{t_f} (H - \lambda^T \dot{x})dt + P \tag{4.7}$$

where $G = \mu^T g + Q(Z)$ and μ is a (n-p) vector of multipliers associated with the Z's. The segment on the boundary is from t_1 to t_2. The time t_1^- is the time just prior to the entry boundary time and t_1^+ is the time just after the entry boundary time. The time t_2^- is the time just prior to the exit boundary time and t_2^+ is the time just after the exit boundary time. The first variation of I is required to vanish. Thus

$$\delta I = 0 = (H - \lambda^T \dot{x})\Big|_{t_1^-} \Delta t_1^- - \lambda^T \delta x\Big|_{t_1^-}$$

$$- [(G - \mu^T \dot{Z})\Big|_{t_1^+} \Delta t_1^+ - \mu^T \delta Z\Big|_{t_1^+}]$$

$$+ (G - \mu^T \dot{Z})\Big|_{t_2^-} \Delta t_2^- - \mu^T \delta Z\Big|_{t_2^-}$$

$$- [(H - \lambda^T\dot{x})\Big|_{t_2^+} \Delta t_2^+ - \lambda^T \delta x\Big|_{t_2^+}]$$

$$+ (H - \lambda^T\dot{x})\Big|_{t_f} \Delta t_f - \lambda^T \delta x\Big|_{t_f} + \Delta P$$

$$+ \int_{t_o}^{t_1^-} [H_u \delta u + (H_\lambda - \dot{x}^T)\delta\lambda + (H_x + \dot{\lambda}^T)\delta x]dt$$

$$+ \int_{t_1^+}^{t_2^-} [(G_\mu - \dot{Z}^T)\delta\mu + (G_Z + \dot{\mu}^T)\delta Z]dt$$

$$+ \int_{t_2^+}^{t_f} [H_u \delta u + (H_\lambda - \dot{x}^T)\delta\lambda + (H_x + \dot{\lambda}^T)\delta x]dt \tag{4.8}$$

The necessary conditions for an extremal with a boundary segment arc thus:

At the initial time,

$$t = 0 \quad , \quad x(t_o) = x_{os} \; . \tag{4.9}$$

At the final time,

$$M = 0 \quad , \quad \lambda(t_f) = P_{x_f}^T \quad , \quad H + P_{t_f} = 0 \quad . \tag{4.10}$$

On unconstrained arcs,

$$\dot{x} = H_\lambda^T \quad , \quad \dot{\lambda} = - H_x^T \quad , \quad H_u = 0 \quad . \tag{4.11}$$

On constrained arcs,

$$\dot{Z} = G_{\mu}^{T} \quad , \quad \dot{\mu} = - G_{Z}^{T} \quad , \quad y = 0 \quad , \quad S^{p} = 0 \quad . \tag{4.12}$$

At each junction point,

$$\begin{gathered} H - G + \lambda^{T}(My_{t} + NZ_{t}) = 0 \quad , \quad \mu^{T} - \lambda^{T}N = 0 \\ y = 0 \quad , \quad Z = Z(x,t) \end{gathered} \tag{4.13}$$

where the matrices M and N are defined as

$$\left[M \;\middle|\; N \right] = \left[\frac{y_{x}}{Z_{x}} \right]^{-1} \tag{4.14}$$

M is an $n \times p$ matrix and N is an $n \times (n-p)$ matrix.

All of the conditions are easily varified from Eq. (4.8) except the boundary conditions. These will be derived at t_1 to show the procedure required. Since

$$\Delta x = \delta x + \dot{x}\Delta t \quad , \quad \Delta Z = \delta Z + \dot{Z}\Delta t \tag{4.15}$$

at the boundary, the terms at t_1 may be written as

$$H\Big|_{t_1^-} \Delta t_1^- - \lambda\Delta x\Big|_{t_1^-} - \left[G\Big|_{t_1^+} \Delta t_1^+ - \mu^{T}\Delta Z\Big|_{t_1^+}\right] \tag{4.16}$$

The ΔZ's are independent, however the Δx's are not since from continuity of x's across t_1 they are related through $y = 0$. To first order then

$$\begin{bmatrix} \Delta y \\ \Delta Z \end{bmatrix} = \begin{bmatrix} y_x \\ Z_x \end{bmatrix} \Delta x + \begin{bmatrix} y_t \\ Z_t \end{bmatrix} \Delta t \qquad (4.17)$$

and from Eq. (4.5) this can be solved for Δx as

$$\Delta x = [\, M \vdots N \,] \begin{bmatrix} \Delta y - y_t \Delta t \\ \Delta Z - Z_t \Delta t \end{bmatrix} \qquad (4.18)$$

At t_1, or any corner, $\Delta y = 0$, and the terms involving t_1 become

$$[H - G + \lambda^T(My_{t_1} + NZ_{t_1})]\Big|_{t_1} \Delta t_1 + (\mu^T - \lambda^T N)\Delta Z\Big|_{t_1} \qquad (4.19)$$

where for continuous t, it is required that $\Delta t_1^- = \Delta t_1^+$. The boundary conditions follow directly from the above expression. Note that as a boundary is entered the multipliers μ are uniquely determined from Eq. (4.13). As the boundary is left, p of the λ's cannot be determined directly from the boundary conditions. In Chapter 2, the solution to an unconstrained optimal trajectory is characterized as a TPBVP. Here necessary conditions for an optimal trajectory with a SVIC are formulated as a multi-point boundary value problem. Modifications to the standard MPF to include these additional conditions are considered in the next section.

4.3 Application of Perturbation Method to SVIC

A perturbation method will now be derived to solve the intermediate boundary value problem described by Eqs. (4.9) through (4.13). Again this will be derived for only one SVIC boundary segment. The extension to more than one segment is straight forward.

Corresponding to the standard MPF method, unknown multipliers and unknown boundary times will be guessed. At the boundary exit, either p of the λ's or all of the λ's may be guessed. If all the λ's are guessed the equation relating λ's and μ's may be considered as boundary conditions to be satisfied by the iteration procedure. The latter procedure will be followed here. The initial multipliers, multipliers at the boundary exit, the boundary entry time, boundary exit time, and final time will all be guessed. A nominal trajectory is produced by integrating the $\dot{x}$ and $\dot{\lambda}$ equations from t_o to t_1 using specified values for x_o and guessed values for λ_o. At t_1, Z and μ are determined from $Z = Z(x,t)$ and $\mu^T = \lambda^T N$. The equations for $\dot{Z}$ and $\dot{\mu}$ are integrated from t_1 to t_2. At t_2, x is determined from $Z = Z(x,t)$ and $y = 0$. The values of λ at t_2 are guessed and the $\dot{x}$ and $\dot{\lambda}$ equations are integrated from t_2 to t_f. Corrections to the guessed variables, λ_o, λ_{t_2}, t_1, t_2, and t_f are calculated to drive all the unsatisfied boundary conditions to zero. These corrections to the variables are related to desired changes in the unsatisfied boundary conditions using linear perturbation theory. The method is then iterated until convergence or divergence occurs. Boundary conditions which will not be satisfied by the nominal are given below.

At the boundary entry time, $Z = Z(x,t)$ determines Z and $\mu^T = \lambda^T N$ determines μ. Unsatisfied boundary conditions (p+1), for the nominal trajectory are

$$h_1 = \begin{bmatrix} H - G + \lambda^T (My_t + NZ_t) \\ y \end{bmatrix}_{t_1} = 0 \qquad (4.20)$$

At the exit time, $Z = Z(x,t)$ and $y(x,t) = 0$ determine x at t_2. This leaves $(n-p+1)$ unsatisfied boundary conditions

$$h_2 = \begin{bmatrix} H - G + \lambda^T(My_t + NZ_t) \\ \\ \mu^T - \lambda^T N \end{bmatrix}_{t_2} = 0 \qquad \text{[illegible]1)}$$

At the final time, the usual boundary conditions (n+1) obtained in Section (2.1) are still applicable and are expressed as

$$h_f = 0 \tag{4.22}$$

The vector h_f consists of the same conditions defined by Eq. (2.10). This gives $(2n+3)$ boundary conditions and $(2n+3)$ unknowns which are $\lambda(t_o)$, $\lambda(t_2)$, t_1, t_2, and t_f. Corrections in these quantities are now related to desired changes in boundary conditions. Define

$$z = \left[\frac{x}{\lambda}\right] \quad , \quad v = \left[\frac{Z}{\mu}\right] \tag{4.23}$$

and from linear perturbations

$$\delta z_1 = \Phi(1,0)\delta z_o \; , \; \delta v_2 = \Phi(2,1)\delta v_1 \; , \; \delta z_f = \Phi(f,2)\delta z_2 \tag{4.24}$$

where $\Phi(1,0)$ and $\Phi(f,2)$ are $2n \times 2n$ matrices and $\Phi(2,1)$ is a $2(n-p) \times 2(n-p)$ matrix. Here $\Phi(a,b)$ denotes the solution of the appropriate set of perturbation equations, Eqs. (2.14), which have been integrated from t_b to t_a with the initial conditions at t_b set equal to the identity matrix.

At the boundary t_1

$$v(z) = \begin{bmatrix} Z(x,\lambda) \\ \mu(x,\lambda) \end{bmatrix} \tag{4.25}$$

and

$$\Delta v = \frac{\partial v}{\partial z} \Delta z + \frac{\partial v}{\partial t} \Delta t \tag{4.26}$$

The boundary conditions are now expanded about the nominal and related to guessed quantities. For the conditions at t_1,

$$\Delta h_1 = \frac{\partial h_1}{\partial z_1} \Delta z_1 + \frac{\partial h_1}{\partial t_1} \Delta t_1 \tag{4.27}$$

or

$$\Delta h_1 = \frac{\partial h_1}{\partial z_1} \delta z_1 + \dot{h}_1 \Delta t_1$$

Using the Φ matrix

$$\Delta h_1 = \frac{\partial h_1}{\partial z_1} \Phi(1,0)\ \delta z_o + \dot{h}_1 \Delta t_1 \tag{4.28}$$

Since $\delta z_o = [\frac{0}{\delta \lambda_o}]$, only the last n columns of the $\Phi(1,0)$ matrix are required and

$$\Delta h_1 = \frac{\partial h_1}{\partial z_1} \Phi_2(1,0)\delta\lambda_o + \dot{h}_1 \Delta t_1 \tag{4.29}$$

Similarly for t_2,

$$\Delta h_2 = \frac{\partial h_2}{\partial v_2} \Delta v_2 + \frac{\partial h_2}{\partial \lambda_2} \Delta\lambda_2 + \frac{\partial h_2}{\partial t_2} \Delta t_2 \tag{4.30}$$

where the corrections to $\lambda(t_2)$ are separated from other terms at t_2 since corrections to $\lambda(t_2)$ must be calculated.

Since $\Delta v_2 = \delta v_2 + \dot{v}_2 \Delta t_2$ and $\delta v_2 = \Phi(2,1)\delta v_1$ then

$$\Delta h_2 = \frac{\partial h_2}{\partial v_2}\,\Phi(2,1)\delta v_1 + \frac{\partial h_2}{\partial \lambda_2}\,\Delta\lambda_2 + \left(\frac{\partial h_2}{\partial t_2} + \frac{\partial h_2}{\partial v_2}\,\dot{v}_2\right)\Delta t_2 \tag{4.31}$$

Again $\delta v_1 = \Delta v_1 - \dot{v}_1 \Delta t_1$ and $\Delta v_1 = \frac{\partial v_1}{\partial z_1}\,\Delta z_1 + \frac{\partial v_1}{\partial t_1}\,\Delta t_1$ so that

$$\begin{aligned}\Delta h_2 = {} & \frac{\partial h_2}{\partial \lambda_2}\,\Delta\lambda_2 + \frac{\partial h_2}{\partial v_2}\,\Phi(2,1)\,\frac{\partial v_1}{\partial z_1}\,\Phi_2(1,0)\delta\lambda_o \\ & - \frac{\partial h_2}{\partial v_2}\,\Phi(2,1)\,\left[\dot{v}_1 - \frac{\partial v_1}{\partial t_1} - \frac{\partial v_1}{\partial z_1}\,\dot{z}_1\right]\Delta t_1 \\ & + \left(\frac{\partial h_2}{\partial t_2} + \frac{\partial h_2}{\partial v_2}\,\dot{v}_2\right)\Delta t_2\end{aligned} \tag{4.32}$$

Note that total changes, $\Delta\lambda_2$, are calculated for the multipliers at t_2. Changes in h_2 are linearly related to changes in $\lambda(t_o)$, $\lambda(t_2)$, t_1, and t_2.

For the final time,

$$\begin{aligned}\Delta h_f &= \frac{\partial h_f}{\partial z_f}\,\delta z_f + \dot{h}_f \Delta t_f \\ &= \frac{\partial h_f}{\partial z_f}\,\Phi(f,2)\delta z_2 + \dot{h}_f \Delta t_f\end{aligned} \tag{4.33}$$

Define $\frac{\partial h_f}{\partial z_f}\,\Phi(f,2) = [\bar{\Phi}_1(f,2) \mid \bar{\Phi}_2(f,2)]$

where $\bar{\Phi}_1(f,2)$ and $\bar{\Phi}_2(f,2)$ are $(n+1) \times n$ matrices. Then

$$\begin{aligned}\Delta h_f &= \bar{\Phi}_1(f,2)\delta x_2 + \bar{\Phi}_2(f,2)\delta\lambda_2 + \dot{h}_f \Delta t_f \\ &= \bar{\Phi}_1(f,2)\Delta x_2 + \bar{\Phi}_2(f,2)\Delta\lambda_2 - [\bar{\Phi}_1(f,2)\dot{x}_2 + \bar{\Phi}_2(f,2)\dot{\lambda}_2]\Delta t_2 + \dot{h}_f \Delta t_f\end{aligned} \tag{4.34}$$

Again using Eq. (4.18)

$$\Delta x_2 = (-My_t - NZ_t)\Big|_{t_2} \Delta t_2 + N_2 \Delta Z_2 \tag{4.35}$$

Define $\bar{N}_2$ such that

$$N_2 \Delta Z_2 = \bar{N}_2 \Delta v_2 \quad \text{or} \quad \bar{N}_2 = [N_2 \;\vdots\; 0] \tag{4.36}$$

$\bar{N}_2$ is an $n \times 2(n-p)$ matrix. Then

$$\begin{aligned} \Delta h_f = {} & \bar{\Phi}_1(f,2)\bar{N}_2 \delta v_2 + \bar{\Phi}_2(f,2)\Delta\lambda_2 \\ & - [\bar{\Phi}_1(f,2)\dot{x}_2 + \bar{\Phi}_2(f,2)\dot{\lambda}_2 - \bar{\Phi}_1(f,2)(\bar{N}_2 v_2 \\ & + My_t + NZ_t)]\Delta t_2 + \dot{h}_f \Delta t_f \end{aligned} \tag{4.37}$$

And

$$\begin{aligned} \Delta h_f = {} & \bar{\Phi}_2(f,2)\Delta\lambda_2 + \bar{\Phi}_1(f,2)\bar{N}_2 \Phi(2,1) \frac{\partial v_1}{\partial z_1} \Phi_2(1,0)\delta\lambda_o \\ & \{\bar{\Phi}_1(f,2)\bar{N}_2 \Phi(2,1)[\dot{v}_1 - \frac{\partial v_1}{\partial t_1} - \frac{\partial v_1}{\partial z_1} \dot{z}_1]\}\Delta t_1 \\ & -\{\bar{\Phi}_1(f,2)\dot{x}_2 + \bar{\Phi}_2(f,2)\dot{\lambda}_2 - \bar{\Phi}_1(f,2)\bar{N}\dot{v}_2 \\ & + My_t + NZ_t\}\Delta t_2 + \dot{h}_f \Delta t_f \end{aligned} \tag{4.38}$$

The three vector equations, Eqs. (4.29), (4.32), and (4.38) must be solved simultaneously, for the corrections to the guessed quantities. These corrections are added to the guessed variables and the procedure continues iterating until all of the h's are zero.

The entire fundamental matrix must be integrated from t_1 to t_2 and from t_2 to t_f. Thus more integration is required for constrained trajectories.

The major disadvantage of this method is the necessity of guessing the number of boundary arcs and their approximate location. For many problems, however, unconstrained optimal trajectories may be obtained. These unconstrained trajectories provide insight into the location of boundary segments. They also provide reasonable estimates for boundary entry and exit times. If some apriori information about the location of boundary arcs is available, the convergence characteristics of the method, presented in the remainder of this investigation, indicate that it is a feasible method for attacking SVIC's.

4.4 Example Problem (Constrained Brachistochrone)

The example problem chosen to illustrate the algorithm is the constrained Brachistochrone problem. This problem is chosen because it has been considered by several other authors and hence numerical results can be compared. Other papers that have considered this problem or a slight variation of it are Refs. 5, 25, 41, 38. Ref. 5 presents an analytical solution. The statement of the problem is as follows:

Minimize

$$I = t_f - t_o \tag{4.39}$$

subject to

$$\begin{aligned} \dot{x}_1 &= x_2^{1/2} \cos u \\ \dot{x}_2 &= x_2^{1/2} \sin u \end{aligned} \tag{4.40}$$

with boundary conditions

$$t_o = 0.1$$

$$x_1(t_o) = x_{1s} \quad , \quad x_2(t_o) = x_{2s} \tag{4.41}$$

$$x_1(t_f) = 1$$

and inequality constraint

$$S = x_2 - x_1 \tan C_1 - C_2 \leq 0 \tag{4.42}$$

where C_1 and C_2 are constants.

This is a first order constraint since

$$\dot{S} = x_2^{1/2}[\sin u - \cos u \tan C_1] \tag{4.43}$$

and thus on the constraint boundary $u = C_1$.

Define

$$y = S = x_2 - x_1 \tan C_1 - C_2 \tag{4.44}$$

and choose $Z = x_2$ as the state variable on the boundary. Note that

$$\left| \begin{array}{c} \frac{\partial y}{\partial x} \\ \hline \frac{\partial Z}{\partial x} \end{array} \right| = - \tan C_1 \tag{4.45}$$

which is not zero for $C_1 \neq 0$. The state equation on the boundary is then

$$\dot{Z} = Z^{1/2} \sin C_1 \tag{4.46}$$

The Hamiltonian off the boundary is

$$H = \lambda_1[(x_2)^{1/2} \cos u] + \lambda_2[(x_2)^{1/2} \sin u] \tag{4.47}$$

and the conditions $H_u = 0$ and $H_{uu} \geq$ determine the optimal choice of the control variable as

$$\sin u = \frac{-\lambda_2}{(\lambda_1^2 + \lambda_2^2)^{1/2}} \, , \quad \cos u = \frac{-\lambda_1}{(\lambda_1^2 + \lambda_2^2)^{1/2}} \tag{4.48}$$

On the boundary the Hamiltonian is

$$G = \mu[Z^{1/2} \sin C_1] \tag{4.49}$$

Necessary conditions for a minimal trajectory are given below. At t_o the selected initial conditions are

$$\begin{aligned} t_o &= 0.1 \\ x_1(t_o) &= [C_3 t_o - 1/2 \sin(2C_3 t_o)]/4C_3^2 \\ x_2(t_o) &= \sin^2(C_3 t_o)/4C_3^2 \end{aligned} \tag{4.50}$$

where C_3 is a constant. On the unconstrained arc

$$\begin{aligned} \dot{x}_1 &= (x_2)^{1/2} \cos u \\ \dot{x}_2 &= (x_2)^{1/2} \sin u \\ \dot{\lambda}_1 &= 0 \\ \dot{\lambda}_2 &= -\frac{1}{(x_2)^{1/2}} [\lambda_1 \cos u + \lambda_2 \sin u] \end{aligned} \tag{4.51}$$

where sin u and cos u are defined in terms of λ_1 and λ_2 by Eq. (4.48). On the constrained arc

$$\dot{Z} = Z^{1/2} \sin C_1$$

$$\dot{\mu} = - \frac{\mu \sin C_1}{2\, Z^{1/2}} \tag{4.52}$$

At the final time

$$\begin{aligned} x_1(t_f) - 1 &= 0 \\ \lambda_2(t_f) &= 0 \\ H(t_f) + 1 &= 0 \end{aligned} \tag{4.53}$$

At intermediate boundaries

$$\begin{aligned} &H - G = 0 \\ &y = x_2 - x_1 \tan C_1 - C_2 = 0 \\ &\mu - \frac{\lambda_1}{\tan C_1} - \lambda_2 = 0 \\ &Z - x_2 = 0 \end{aligned} \tag{4.54}$$

The problem now is to generate a nominal trajectory and use the modified perturbation method developed in the previous section to iterate toward a trajectory which satisfies all of the conditions listed above. Before this is done, the boundary conditions are altered slightly. Since Eqs. (4.40) and (4.46) do not contain t explicitly, both H and G are constant. Then the first of Eqs. (4.54) may be used to show that requiring $H(t_o) + 1 = 0$ is equivalent to requiring $H(t_f) + 1 = 0$. This boundary condition will be applied at t_o below. Also, the condition $H = G$ at intermediate boundaries requires that the control be continuous at these boundaries. Thus requiring that $\lambda_1 \tan C_1 - \lambda_2 = 0$ is equivalent to requiring that the Hamiltonian be continuous. The condition will be applied in this manner.

In order to generate a nominal trajectory, one boundary segment is assumed. Guesses are made for $\lambda(t_o)$, $\lambda(t_2)$, t_1, t_2, and t_f. (7 variables). Eqs. (4.51) can then be integrated from t_o to t_1. At t_1, Z and μ are determined from the last two equations of Eqs. (4.54). Eqs. (4.52) are integrated from t_1 to t_2. At t_2, $x(t_2)$ is determined from the second and fourth equations of Eq. (4.54). Using this and the guess for $\lambda(t_2)$, Eqs. (4.51) are integrated from t_2 to t_f. The boundary conditions not satisfied by this nominal are

$$h_o = H(t_o) + 1 = 0 \tag{4.55}$$

$$h_1 = \begin{bmatrix} x_2 - x_1 \tan C_1 - C_2 \\ \lambda_1 \tan C_1 - \lambda_2 \end{bmatrix}_{t_1} = 0 \tag{4.56}$$

$$h_2 = \begin{bmatrix} \mu - \dfrac{\lambda_1}{\tan C_1} - \lambda_2 \\ \lambda_1 \tan C_1 - \lambda_2 \end{bmatrix}_{t_2} = 0 \tag{4.57}$$

and

$$h_f = \begin{bmatrix} x_1 - 1 \\ \lambda_2 \end{bmatrix}_{t_f} = 0 \tag{4.58}$$

The modified perturbation method derived in the previous chapter is used to relate the changes $\delta\lambda_1(t_o)$, $\delta\lambda_2(t_o)$, $\Delta\lambda_1(t_2)$, $\Delta\lambda_2(t_2)$, Δt_1, Δt_2, and Δt_f to desired changes in the boundary conditions. The coefficients of the linear perturbation equations and derivatives of the h's are shown in Appendix C.

The VSI with an error bound of 10^{-8} and 10^{-10} is used for the integration. A 30% correction scheme based on the norm of all the multipliers is used during the iteration.

The initial nominal values of the multipliers and times are shown in Table 5 along with the converged values. This trajectory is calculated for $C_1 = \arcsin [1/(5)^{1/2}]$, $C_2 = 0.2$, and $C_3 = 1/4[10(C_1 + 2 - \frac{\pi}{2})]^{1/2}$. (Case 1) and also for $C_2 = 0.1$ (Case 2). Starting with the nominal shown in Table 5, five iterations are required to converge Case 1. Starting with the converged values for Case 1, four iterations are required to converge Case 2. Convergence implies that the square root of the sum of the squares of all h's is less than 10^{-7}. Each iteration, including the integration of the nonlinear equations, all perturbation equations, and solving the linear system required 1.9 seconds of computer time. These results agree with those presented in Ref. 41 to at least seven digits. Plots of the state variables for the converged trajectories are shown in Fig. 10.

This example shows that the method does converge and that convergence near an optimal is quite rapid.

Variable	Nominal	CASE 1	CASE 2
$\lambda_1(t_o)$	- 1.5	- 1.49403214	- 2.11215421
$\lambda_2(t_o)$	-20.0	-19.9627889	-19.906769
$\lambda_1(t_2)$	- 1.0	- 1.3265554	- 1.43284396
$\lambda_2(t_2)$	-10.0	-0.663276291	- 0.71642038
t_1	1.48	1.4820961	1.0477710
t_2	1.9	1.8201062	1.9465189
t_f	2.52	2.5191296	2.5936887

Case 1: $C_2 = 0.2$

Case 2: $C_2 = 0.1$

TABLE 5. Nominal and Converged Multipliers for Constrained Brachistochrone

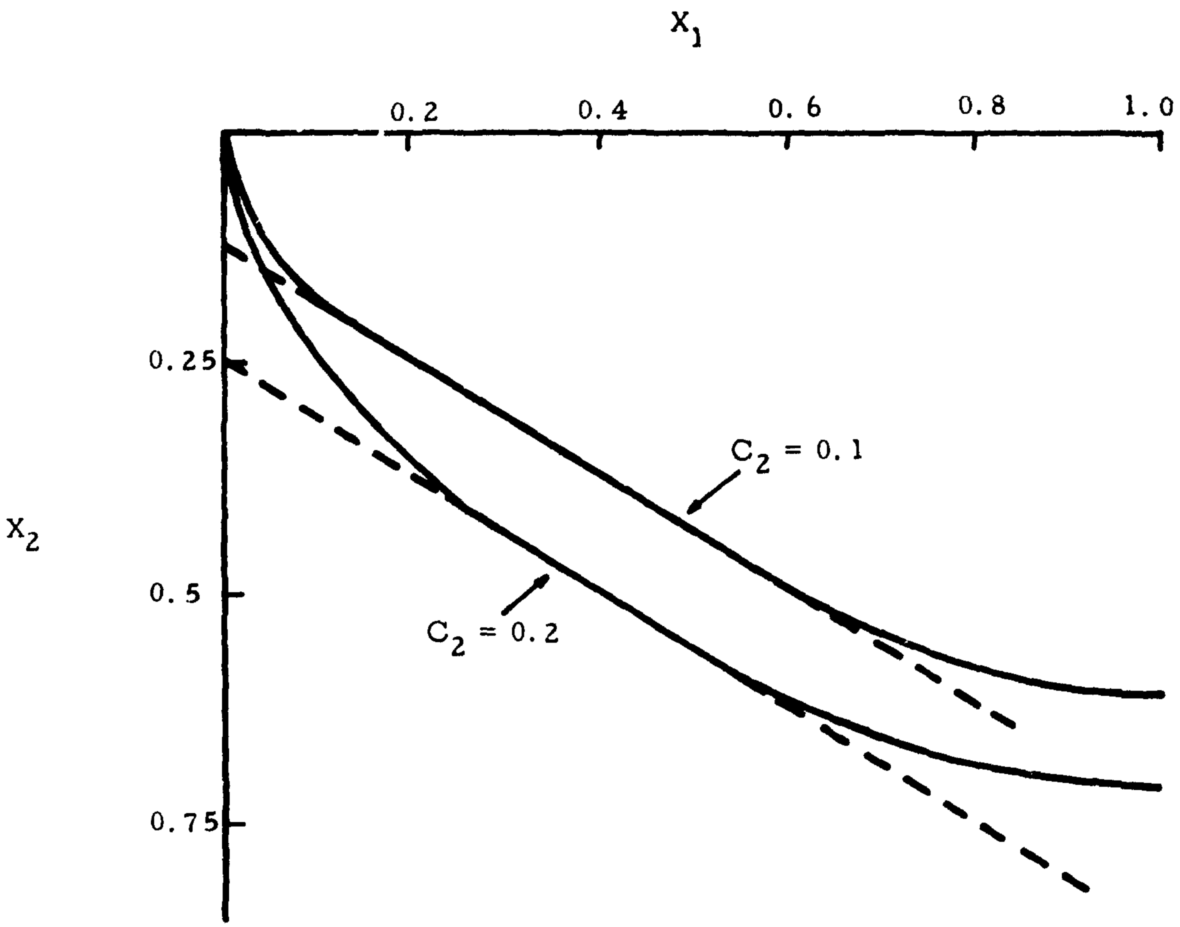

FIG. 10. State Variables for Optimal Constrained Brachistochrone

CHAPTER 5

ALTITUDE CONSTRAINED REENTRY

5.1 Theoretical Development

The numerical method developed in the previous chapter to solve optimal control problems with SVIC will now be applied to the reentry problem. The SVIC will require the altitude over the skip segment to be less than or equal to some specified maximum altitude. As mentioned earlier, both altitude and acceleration constraints should be considered for the reentry problem since both low peak accelerations and reentry trajectories which remain in the sensible atmosphere are desired. Ref. 18 shows that an altitude SVIC has the effect of accomplishing both of these goals. Hence it is chosen for the following study. The SVIC is thus

$$S(x,t) = r - r_d \leq 0 \tag{5.1}$$

where r_d denotes a specified altitude. Since the initial altitutde r_o will be larger than r_d, the constraint applies only after the reentry altitude becomes less than or equal to the constraint altitude. This is a second order constraint as seen from taking derivatives of S.

$$\dot{S} = \dot{h} = V \sin \gamma = 0 \tag{5.2}$$

implying $\gamma = 0$. Also

$$\ddot{S} = \ddot{h} = \dot{V} \sin \gamma + (V \cos \gamma)\dot{\gamma} = 0 \tag{5.3}$$

implying $\dot{\gamma} = 0$, or

$$\cos\beta = \frac{\dfrac{\mu}{r_d^2V^2} - \dfrac{1}{r_d}}{\dfrac{1}{2}\,S^*C_L\rho_d} \quad , \quad \sin\beta = (1 - \cos^2\beta)^{1/2} \tag{5.4}$$

The plus sign has been chosen for sin β since for this study, only negative values of ϕ are considered. It would seem reasonable to have the vehicle roll in the direction of the desired terminal value of ϕ, which in this case implies that sin β should be positive.

On the altitude constraint, the Z variables are chosen as θ, ϕ, V, and ψ. This is the natural choice for the Z variables since this choice gives a one to one correspondence between the μ vector and 4 variables in the λ vector as will be shown later. The equations for $\dot{Z}$ are thus

$$\begin{aligned}
\dot{\theta} &= \frac{VC\psi}{r_dC\phi} \\
\dot{\phi} &= \frac{VS\psi}{r_d} \\
\dot{V} &= -(1/2\ S^*C_D)\rho_dV^2 \\
\dot{\psi} &= -\frac{VC\psi\tan\phi}{r_d} - (1/2\ S^*C_L)\rho_dVS\beta
\end{aligned} \tag{5.5}$$

and the y equations are

$$y_1 = r - r_d = 0 \quad , \quad y_2 = \gamma = 0 \tag{5.6}$$

The Hamiltonian on the constraint is defined as

$$\begin{aligned} G = {} & \mu_\theta\left[\frac{VC\psi}{r_d C\phi}\right] + \mu_\phi\left[\frac{VS\psi}{r_d}\right] + \mu_V[-1/2S^*C_D\rho_d V^2] \\ & + \mu_\psi\left[-\frac{VC\psi \tan\phi}{r_d} - 1/2S^*C_L\rho_d VS\beta\right] \\ & + \frac{S^*}{2}(C_L^2 + C_D^2)^{1/2}\rho_d V^2 + \lambda_o \rho_d^{1/2} V^3 \end{aligned} \tag{5.7}$$

The equations for $\dot{\mu}$ are

$$\begin{aligned} \dot{\mu}_\theta & = 0 \\ \dot{\mu}_\phi & = -\frac{VC\psi S\phi}{r_d C^2\phi}\mu_\theta + \frac{VC\psi}{r_d C^2\phi}\mu_\psi \\ \dot{\mu}_V & = -\frac{C\psi}{r_d C\phi}\mu_\theta - \frac{S\psi}{r_d}\mu_\phi + S^*C_D\rho_s V\mu_V \\ & \quad - \left\{\frac{C\psi \tan\phi}{r_d} + \left(\frac{S^*C_L}{2}\right)\rho_d\left[S\beta + V\left(\frac{2C_1C\beta}{V^3S\beta}\right)\right]\right\}\mu_\psi \\ & \quad - 2C_2V - 3C_3V^2 \\ \dot{\mu}_\psi & = \frac{VS\psi}{r_d C\phi}\mu_\theta - \frac{VC\psi}{r_d}\mu_\phi - \frac{VS\psi \tan\phi}{r_d}\mu_\psi \end{aligned} \tag{5.8}$$

where $$C_1 = \frac{\mu}{r_d^2(1/2\ S^*C_L)\rho_d} \quad , \quad C_2 = 1/2\ S^*(C_L^2 + C_D^2)^{1/2}\rho_d$$

$$C_3 = \lambda_o\rho_d^{1/2} \tag{5.9}$$

and ρ_d is the density at the specified altitude. The variational equations for the boundary segment are shown in Appendix D. Boundary conditions at entering and exiting times require continuity of the states and also

$$\mu_\theta = \lambda_\theta \quad , \quad \mu_\phi = \lambda_\phi \quad , \quad \mu_V = \lambda_V \quad , \quad \mu_\psi = \lambda_\psi$$

$$G = H \quad , \quad r - r_d = 0 \quad , \quad \gamma = 0 \tag{5.10}$$

A nominal trajectory must now be produced. Again one boundary arc is assumed. The first four conditions of Eq. (5.10) can be satisfied on every integration. At t_1 the final values of λ are used as the initial values of μ. At t_2, final values of μ are used as initial values for four of the λ's. Thus only two of the λ variables must be guessed at t_2. Also, at t_2, the integration of the x equations is begun with $r = r_d$ and $\gamma = 0$. Hence the only intermediate boundary conditions which cannot be satisfied on every iteration are:

$$\text{at } t_1 \quad , \quad G = H \quad , \quad r - r_d = 0 \quad , \quad \gamma = 0 \quad , \tag{5.11}$$

$$\text{at } t_2 \quad , \quad G = H \ . \tag{5.12}$$

Unknowns associated with the problem include the initial values of λ (6 variables), λ_r and λ_γ at t_2 (2 variables), and the times t_1, t_2, and t_f. Thus there are 11 unknowns. Boundary conditions consist of the 7 original terminal conditions for the unconstrained problem and the four conditions shown above, or a total of eleven boundary conditions. The number of boundary conditions is thus equal to the number of unknowns and a well posed problem exists.

Again for numerical results, conditions on the Hamiltonian are applied in a different manner The Hamiltonian is required to be zero initially, i.e. $H(t_o) = 0$. The continuous Hamiltonian at both boundary times requires that the control be continuous at the boundaries. This condition may be expressed as

$$\left[\frac{\mu}{\frac{1}{2} S^* C_L r_d^2 \rho_d V^2} - \frac{1}{\frac{1}{2} S^* C_L r_d \rho_d} \right] \left[\lambda_\psi^2 + \lambda_\gamma^2 \right] + \lambda_\gamma = 0 \qquad (5.13)$$

All necessary conditions on the Hamiltonian will be satisfied if these three conditions are satisfied. See Appendix E for a summary of boundary conditions and derivatives of the boundary conditions.

For this problem, all the multipliers at the exit time are not guessed. In order to decrease the dimensionality of the linear system to be solved, only the two multipliers λ_r and λ_γ and guessed. The theory developed in the previous chapter must be altered slightly to include this change. The effects of $\Delta\lambda_r(t_2)$ and $\Delta\lambda_\gamma(t_2)$ are separated out and changes in the other λ's at t_2 are propagated in the same manner as in the previous chapter. If the two vector

$$\lambda_u = \left[\frac{\lambda_r}{\lambda_\gamma} \right]_{t_2} \qquad (5.14)$$

is defined then the linear equations for h with y_t and Z_t equal to zero become

$$\Delta h_o = \frac{\partial h_o}{\partial \lambda_o}\, \delta\lambda_o \tag{5.15}$$

$$\Delta h_1 = \frac{\partial h_1}{\partial z_1}\, \Phi_2(1,0)\delta\lambda_o + \dot{h}_1 \Delta t_1 \tag{5.16}$$

$$\begin{aligned}\Delta h_2 = {} & \frac{\partial h_2}{\partial \lambda_u}\, \Delta\lambda_u + \frac{\partial h_2}{\partial v_2}\, \Phi(2,1)\left(\frac{\partial v_1}{\partial z_1}\right)\Phi_2(1,0)\delta\lambda_o \\ & + \frac{\partial h_2}{\partial v_2}\, \Phi(2,1)\left[\frac{\partial v_1}{\partial z_1}\, \dot{z}_1 - \dot{v}_1\right]\Delta t_1 + \frac{\partial h_2}{\partial v_2}\, \dot{v}_2 \Delta t_2\end{aligned} \tag{5.17}$$

$$\begin{aligned}\Delta h_f = {} & \underline{\Phi}(f,2)\Delta\lambda_u + \bar{\Phi}(f,2)\Phi(2,1)\, \frac{\partial v_1}{\partial z_1}\, \Phi_2(1,0)\delta\lambda_o \\ & + \bar{\Phi}(f,2)\Phi(2,1)\left[\frac{\partial v_1}{\partial z_1}\, \dot{z}_1 - \dot{v}_1\right]\Delta t_1 \\ & + \left[\bar{\Phi}(f,2)\dot{v}_2 - \frac{\partial h_f}{\partial z_f}\, \Phi(2,1)\dot{z}_2\right]\Delta t_2 + \dot{h}_f \Delta t_f\end{aligned} \tag{5.18}$$

where

$$\bar{\Phi}(f,2) = \frac{\partial h_f}{\partial z_f}\, \Phi(f,2)B_1$$

and

$$B_1 = \left[\begin{array}{cccc:cccc} 0 & 0 & 0 & 0 & & & & \\ 1 & 0 & 0 & 0 & & & & \\ 0 & 1 & 0 & 0 & & 0 & & \\ 0 & 0 & 1 & 0 & & & & \\ 0 & 0 & 0 & 1 & & & & \\ \hdashline & & & & 0 & 0 & 0 & 0 \\ & & & & 1 & 0 & 0 & 0 \\ & 0 & & & 0 & 1 & 0 & 0 \\ & & & & 0 & 0 & 1 & 0 \\ & & & & 0 & 0 & 0 & 0 \\ & & & & 0 & 0 & 0 & 1 \end{array}\right]$$

B_1 is a 12 x 8 matrix, and $\bar{\Phi}(f,2)$ is a 6 x 8 matrix. Also

$$\underline{\Phi}(f,2) = \frac{\partial h_f}{\partial z_f} \Phi(f,2) B_2 \qquad (5.20)$$

where

$$B_2 = \begin{bmatrix} 0 & 0 \\ 0 & 0 \\ 0 & 0 \\ 0 & 0 \\ 0 & 0 \\ 0 & 0 \\ 1 & 0 \\ 0 & 0 \\ 0 & 0 \\ 0 & 0 \\ 0 & 1 \\ 0 & 0 \end{bmatrix}$$

B_2 is a 12 x 2 matrix and $\underline{\Phi}(f,2)$ is a 6 x 2 matrix.

Thus $\underline{\Phi}(f,2)$ separates out the coefficients for $\Delta\lambda_u$ and $\bar{\Phi}(f,2)$ includes the other terms after realizing that Δr_2 and $\Delta\gamma_2$ are zero. All other terms correspond directly to the previous development.

5.2 Numerical Results

The same numerical values for the initial conditions and terminal conditions used in Chapter 3 will be used for the constrained trajectory. The terminal conditions are $\theta_{fs} = 0.33$ radians, $\phi_{fs} = -0.025$ radians, and $V_{fs} = 0.5$ miles/sec.

The initial multipliers for the unconstrained trajectory will be used as initial multipliers for the iteration procedure here. These values, guesses for the unknown vector λ_u , and guesses for t_1, t_2, and t_f are shown in Table 6. The constraint altitude chosen is $r_d = 3995.0$ miles.

Approximately 32 seconds is required for each iteration of the constrained reentry trajectory. A plot of the terminal norm vs. the number of iterations is shown in Fig. 11. The method requires 104 iterations to converge. The norm for the last 10 iterations is shown in Table 7. Plots of the states, control, acceleration, and heating rate are shown in Figs. 12, 13, and 14.

The modified MPF does very well for the first few iterations and then the norm begins to decrease very slowly for a considerable number of iterations. Over this interval the signs on the corrections of most of the variables oscillate back and forth from plus to minus. Elements of the linear system produced by the transition matrices change only in about the third or fourth digits. The flight path angle at t_f over this interval is near -60°. It is changing very rapidly near the end of the trajectory and if the equations are integrated for a few more seconds past the nominal final time, it quickly approaches -90°. A singularity exists in the equations at -90° and accurate integration near this singularity is very difficult. The iteration continues for about 70 iterations slowly increasing γ. After the flight path angle is changed to -35° the method begins to converge very rapidly again.

Variable	Nominal Value	Converged Value
λ_{r_o}	-1.26588E-3	-1.2772884E-2
λ_{θ_o}	-9.181666	-7.40988123
λ_{ϕ_o}	26.5966	3.3857227
λ_{V_o}	2.35619	3.15221059
λ_{γ_o}	13.82719	-1.20936003
λ_{ψ_o}	8.84954	9.63840795E-1
λ_{r_2}	1.0E-2	5.33051908E-3
λ_{γ_2}	-1.0E-1	-8.16314647E-1
t_1	70.0	85.0966654
t_2	150.0	184.938154
t_f	320.0	383.410663

Terminal Conditions: $\theta_{fs} = 0.33$ rads, $\phi_{fs} = -0.025$ rads,
$V_{fs} = 0.5$ miles/sec.

Altitude Constraint: $r_d = 3995.0$ miles

TABLE 6. Nominal and Converged Multipliers for Constrained Reentry

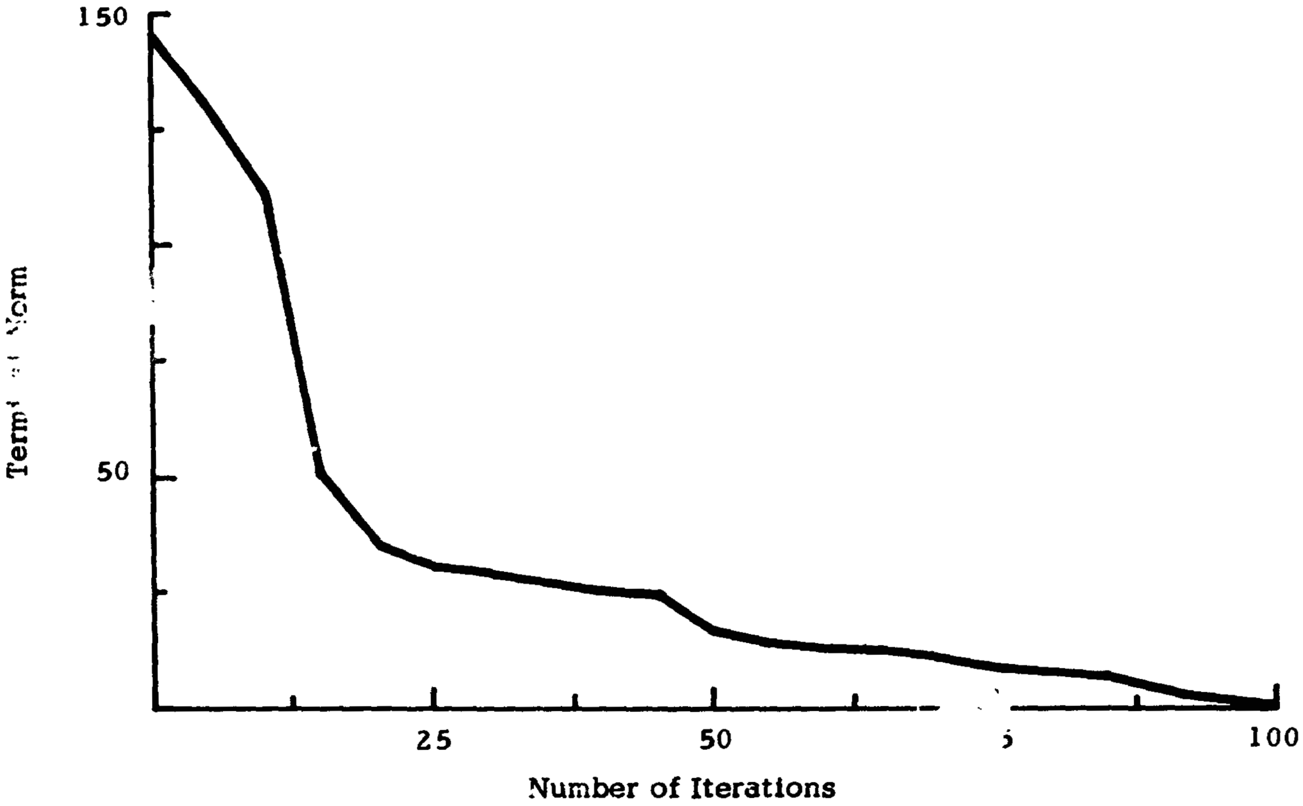

FIG. 11. Terminal Norm vs. Number of Iterations for Constrained Reentry

Iteration	Terminal Norm $(h^T h)^{1/2}$
95	1.3286
96	1.1601
97	8.9962E-1
98	6.4966E-1
99	4.0133E-1
100	1.9503E-1
101	1.2640E-2
102	1.3522E-4
103	1.854E-6
104	7.8315E-10

TABLE 7. Terminal Norm for Last Ten Iterations of Constrained Reentry

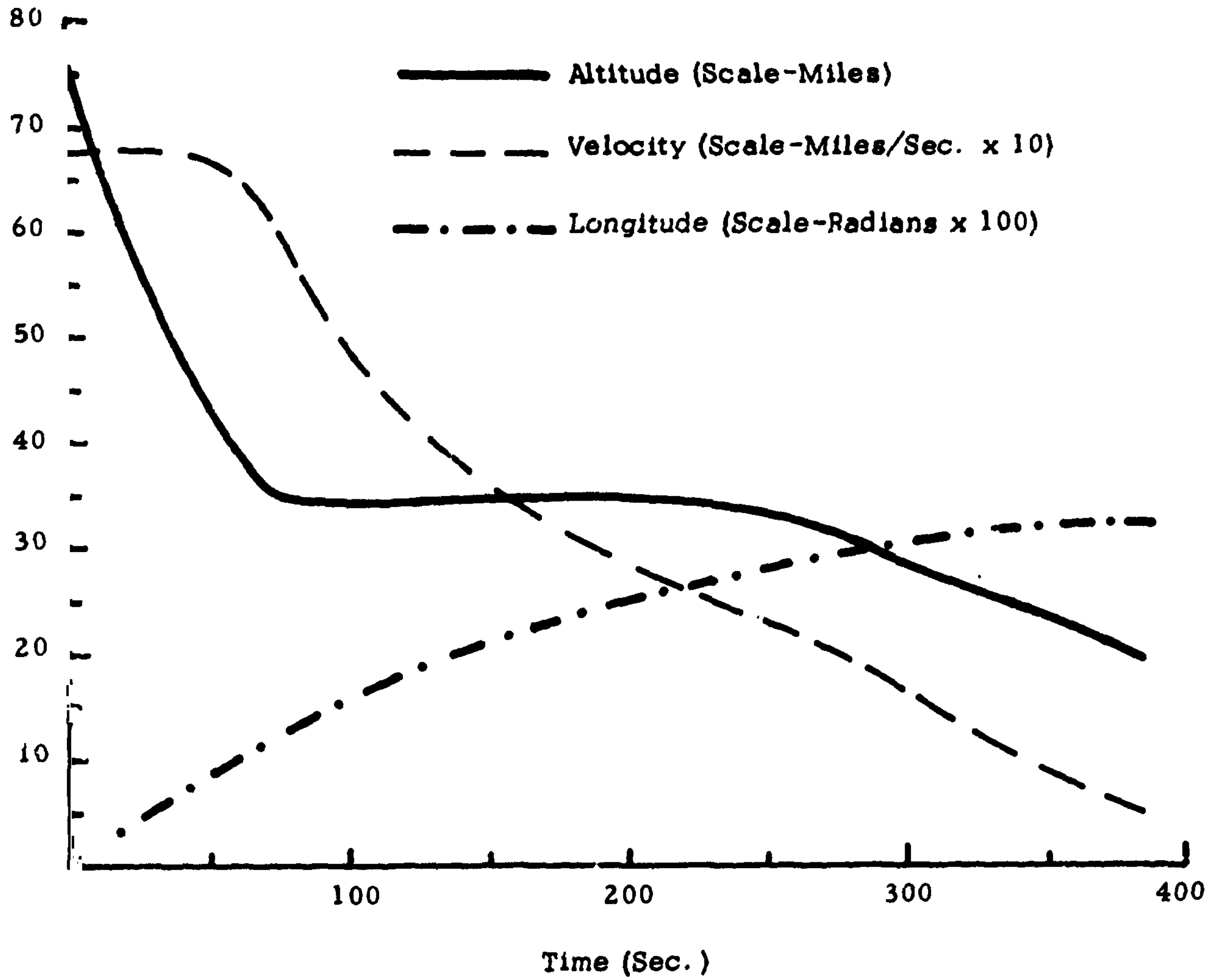

FIG. 12. State Variables r, θ, and V for Optimal, Constrained Reentry

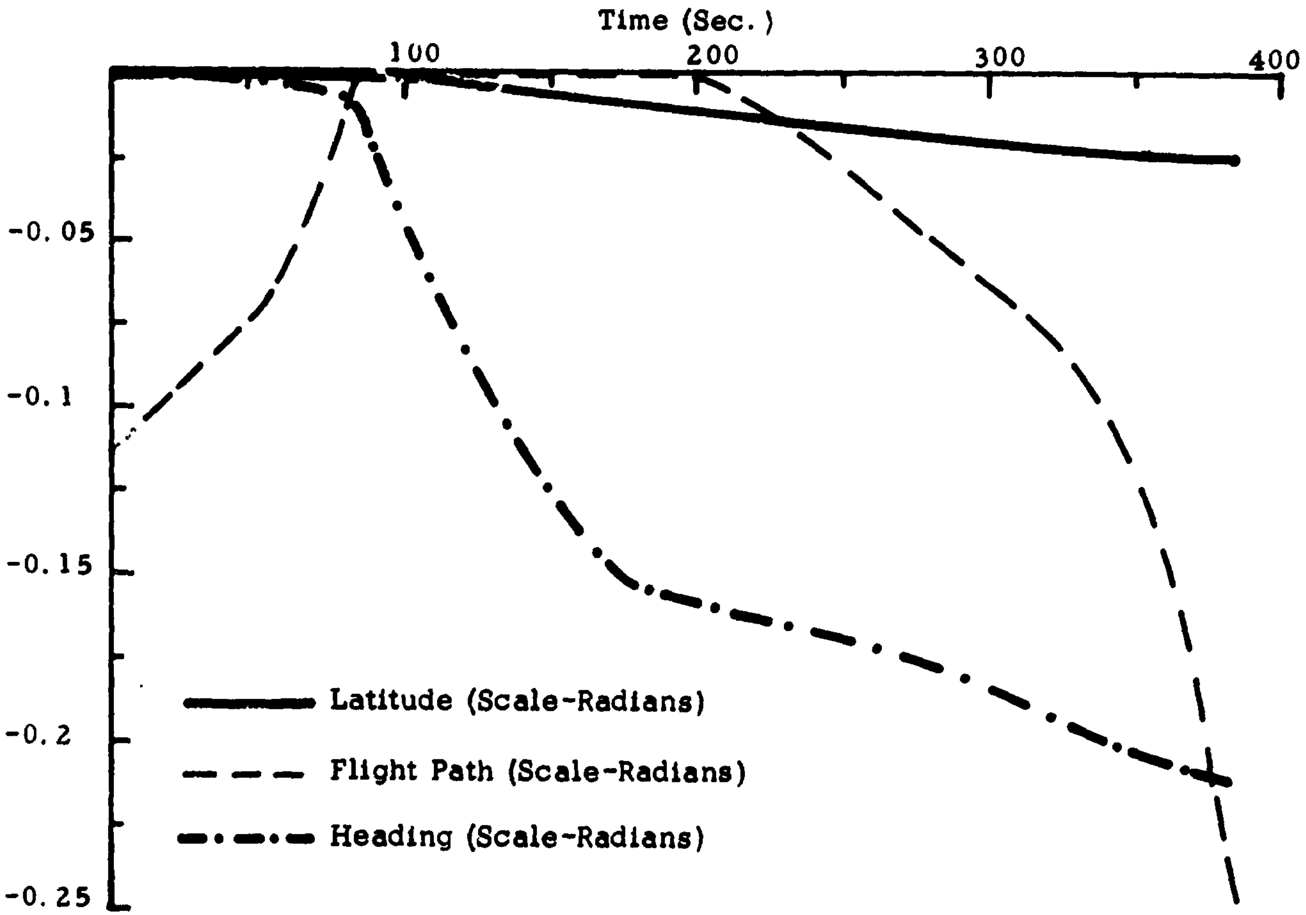

FIG. 13. State Variables ϕ, γ, and ψ for Optimal Constrained Reentry Trajectory

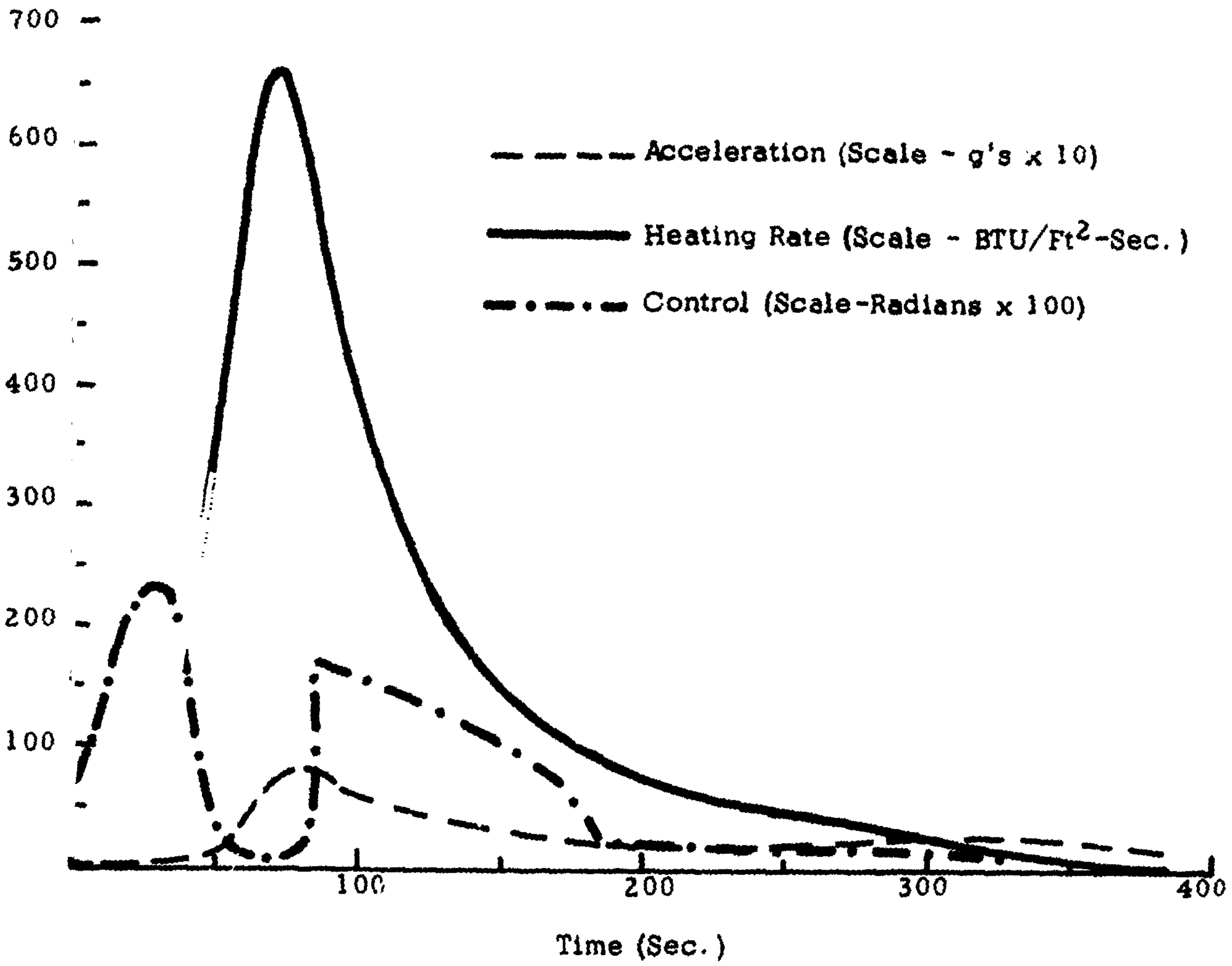

FIG. 14. Control, Acceleration, and Heating Rate for Optimal, Constrained Reentry Trajectory

Another problem is that large corrections oscillating from plus to minus are calculated for t_2. The control along the boundary segment is calculated from Eq. (5.4). If the time calculated for t_2 is sufficiently large, the velocity along the boundary becomes small enough to make the absolute value of cos β greater than one. This indicates that the vehicle cannot fly at a specified altitude for an infinite time interval. If the value of t_2 is larger than the maximum time interval that the vehicle can remain on the boundary then sin β becomes imaginary.

For the iterations above, the nominal value of t_2 approaches [illegible] after 30 iterations. From this point on, if large positive corrections are accepted for t_2 an imaginary value of sin β is obtained. Thus even though corrections to t_2 are oscillating from plus to minus, allowing fairly large corrections (7.0 seconds) results in nominal trajectories which require imaginary control. Requiring small corrections for t_2 and hence the rest of the correction vector slows down the convergence process and is partially responsible for the large number of iterations required for convergence.

These two problems also effect convergence for other near by optimal trajectories. When the flight path angle begins to change rapidly and approach -90°, iteration problems are encountered. It is believed that integration accuracy and hence convergence characteristics would be improved by regularizing the nonlinear reentry Eqs. (3.1). This could be accomplished by using the transformation $R(x) = \cos \gamma$ in Eq. (2.30) and transforming the independent variable from t to τ as done in Section (3.3). Only the segment of the trajectory from t_2

to t_f would need to be regularized since this is the only segment which approaches the singularity.

Since the performance index is the integral of the acceleration and heating rate, the terminal phase of the trajectory (near -90°) does not substantially change its value. Both the acceleration and heating rate are sufficiently small by this time, that very little is added to the performance index when the terminal phase of the trajectory is approached.

Since the entire transition matrix is integrated from t_1 to t_2 and from t_2 to t_f, it may be inverted at t_2 and t_f as a check on the instability of the perturbation equations. This is done for several trajectories during the previous iteration and each time both matrices are full rank. Positive real eigenvalues exist over both segments. The intervals are sufficiently short that the unstable nature of the equations has not caused the Φ matrices to become singular.

From Figs. 5 and 14 it is seen that the altitude constraint does decrease the acceleration peaks. The maximum acceleration is 8.3 g's for the constrained trajectories. The heating for the constrained trajectories is greater than that for the unconstrained trajectories. The maximum heating rate is 664 BTU/ft.^{2}-sec., and the total heat absorbed for this trajectory is 56233.11 BTU/ft.^{2}

Trajectories obtained with the altitude SVIC represent realistic reentry trajectories. The maximum acceleration peak is sufficiently small, and over most of the trajectory, the acceleration is two or three g's. The heating is sufficiently small for present heat shields. Most of the trajectory is in the sensible atmosphere allowing reasonable control of the vehicle throughout the trajectory.

The method used to generate solutions to problems with SVIC in this report can produce solutions which violate the constraint. If the values of the terminal conditions are not consistent with the inequality constraint, trajectories which remain on the constraint for a short segment, and then violate the constraint, may be produced. For instance, the altitude constraint limits the range capabilities of the vehicle. If values of θ_{fs} and ϕ_{fs} are specified which cannot be reached if the vehicle remains below the altitude constraint, the method will converge to a trajectory with a short segment on the boundary. After the boundary segment, the vehicle will roll the lift vector upward and penetrate the constraint in order to satisfy the boundary conditions. The method does converge, however, and the solution obtained does give the user a trajectory with, in general, a small constraint violation. From observing the trajectory it will usually be apparent that the terminal conditions and constraint are inconsistent. The converged trajectory gives good estimates of variables to be used for a consistent set of conditions.

In order to check the ability of the new method to converge to near by optimal trajectories, r_d is changed to 3995.3 miles and θ_{fs} is changed to 0.34 radians. The converged values shown in Table 6 are used as initial guesses for the unknown variables. The trajectory produced after the third iteration integrates through the singularity

(γ = -90°) near the end of the trajectory. The method diverges at this point. If the converged values shown in Table 6 are used and the final time, t_f, is changed to 360.0 sec., the method converges to the new optimal in 17 iterations. Changing the guess for t_f from 383.4 sec. to 360.0 sec. allows the method to iterate without encountering the singularity. Thus near by optimal trajectories can be produced with a relatively few number of iterations if the singularity is avoided.

Plots of the altitude, control, and acceleration for the Apollo 10 trajectory are shown in Ref. 48. These graphs are compared with the same plots for the optimal constrained trajectory computed with r_d = 3995.3 miles, θ_{fs} = 0.34 radians, ϕ_{fs} = -0.025 radians, and V_{fs} = 0.5 miles/sec. in Figs. 15, 16, and 17. The two trajectories are quite similar. From Fig. 16 it is seen that the Apollo vehicle rolls both to the right and to the left in an attempt to land in approximately the same plane as the one it is in when it begins to reenter the atmosphere. The calculated optimal trajectories roll only in one direction and hence land out of the initial flight plane, in this case by -0.025 radians.

The other difference in the two trajectories is the short skip segment at t = 250 sec. for the Apollo trajectory. (See Fig. 15). This skip is responsible for the small acceleration near the peak of the skip and also for the high acceleration as the vehicle flies back into the dense atmosphere. The accelerations are shown in Fig. 17. Trajectories which have the small skip segment in this location are obtained by the modified MPF if a final value of

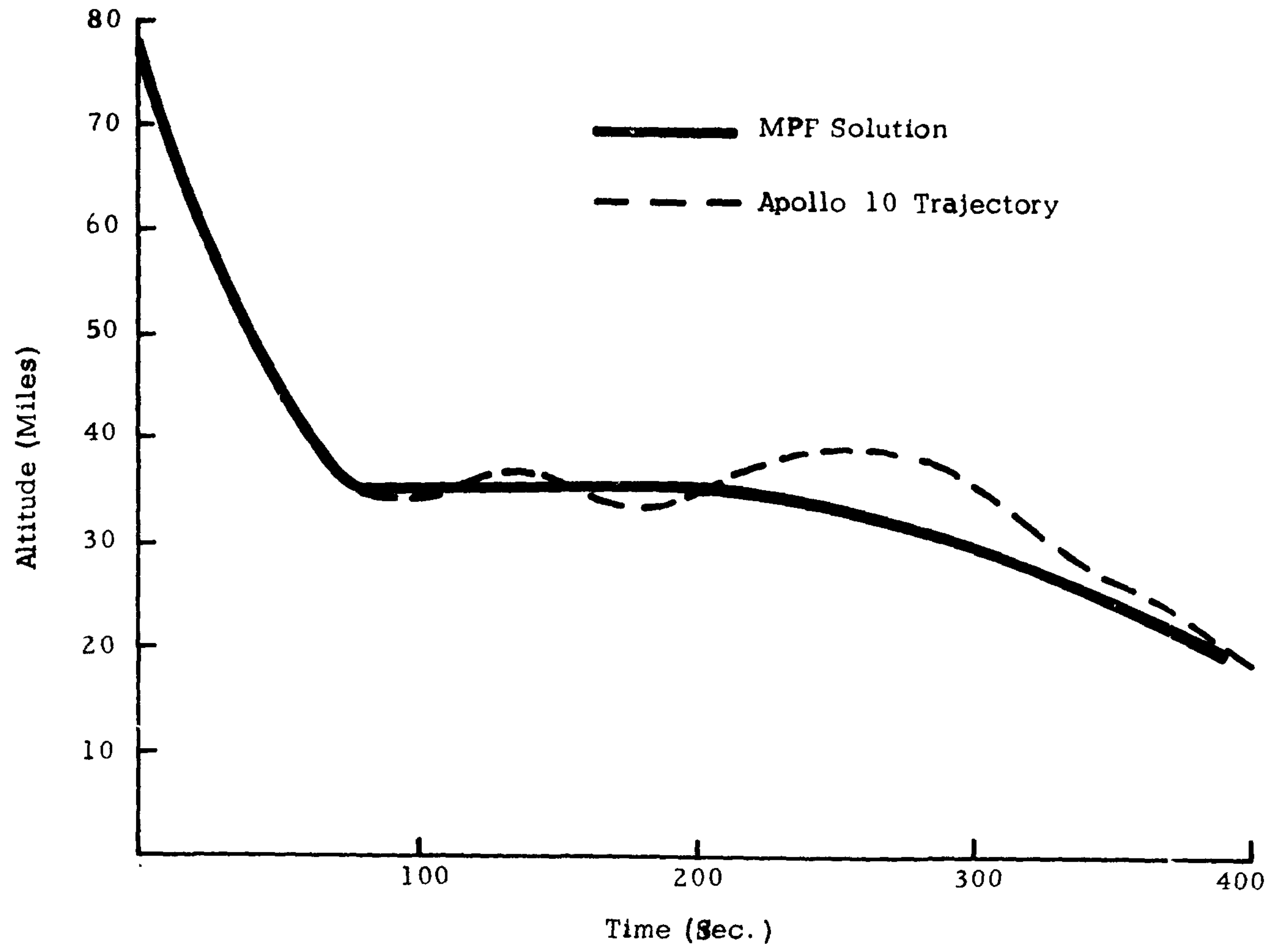

FIG. 15. Comparison of Altitude H' ies for Constrained Optimal Trajectory and Apollo 1 tory

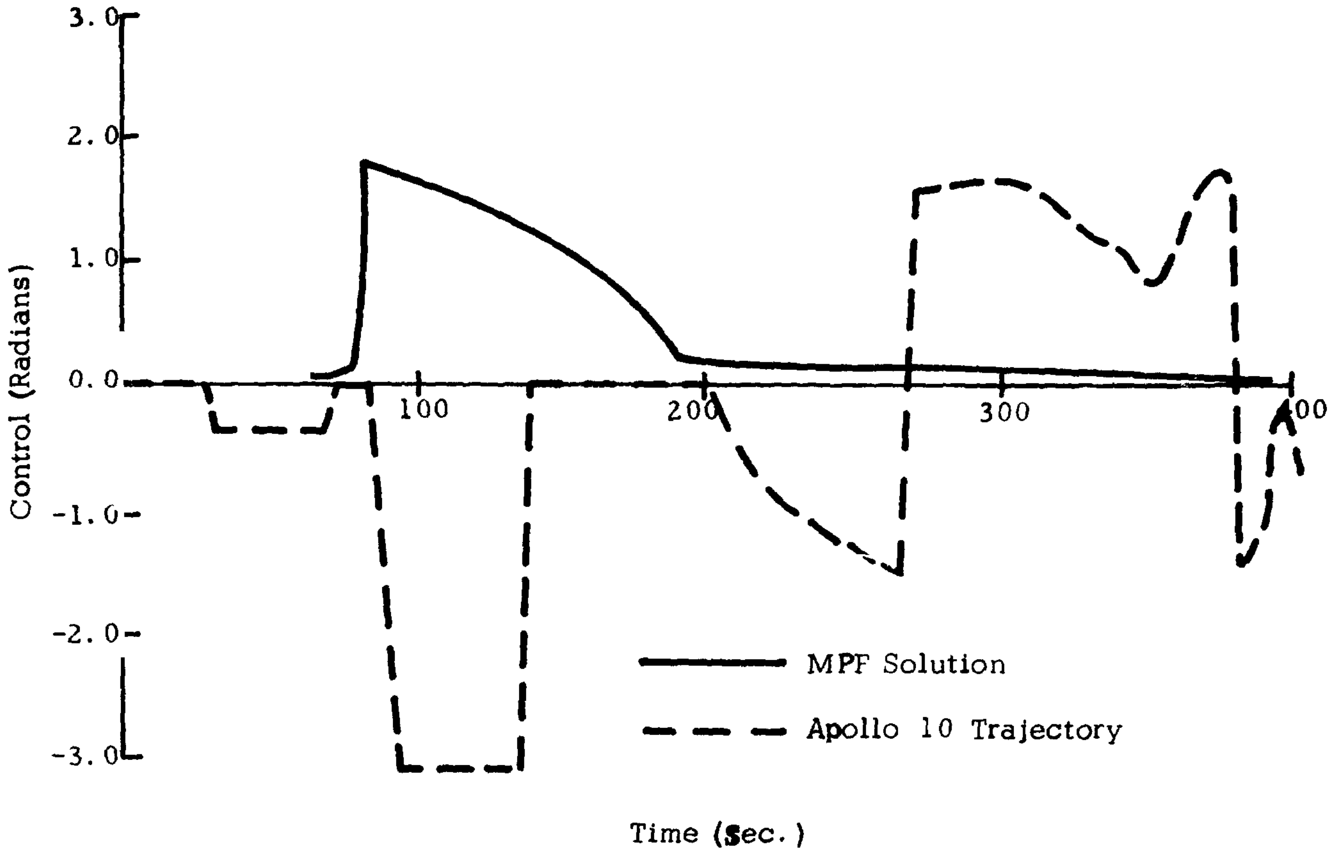

FIG. 16. Comparison of Control Programs for Constrained Optimal Trajectory and Apollo 10 Trajectory

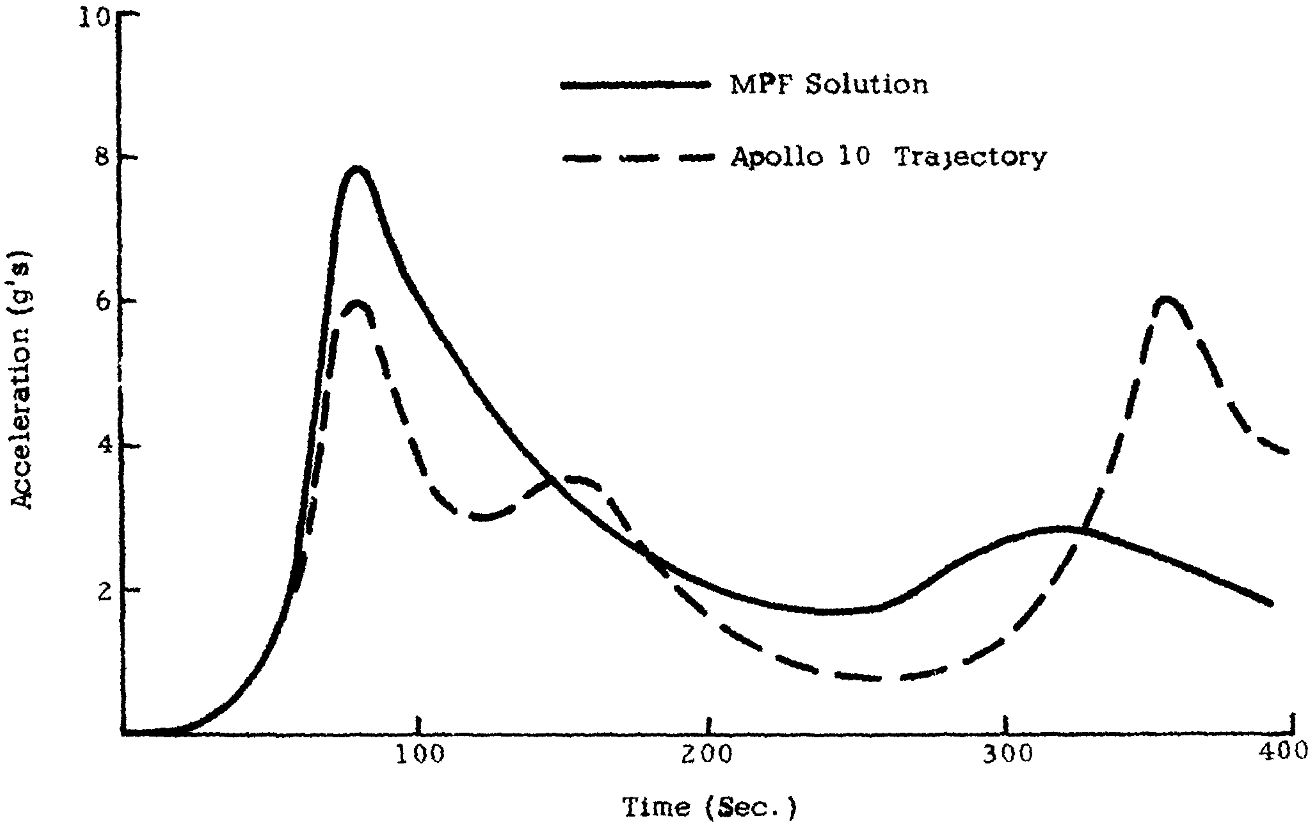

FIG. 17. Comparison of Acceleration Histories for Constrained Optimal Trajectory and Apollo 10 Trajectory

θ_{fs} is specified which cannot be reached by the vehicle if it remains below the altitude constraint.

The results of this comparison show that the choice of the performance index used here and the inclusion of the altitude constraint can be used to generate realistic optimal reentry trajectories.

CHAPTER 6

RESULTS AND CONCLUSIONS

6.1 Summary

The perturbation method is used to solve a three dimensional atmospheric reentry problem. From the results of this study it is determined that state variable inequality constraints are necessary in order to produce reentry trajectories with acceptable maximum acceleration peaks and trajectories which do not skip out of the sensible atmosphere. A modified perturbation method is developed to include SVIC. The method is checked by solving a constrained Brachistochrone problem. It is then used to solve the reentry problem with an altitude constraint over the skip segment of the trajectory.

The stability problem for the linear perturbation equations is considered. A linear TPBVP is solved in order to illustrate the unstable nature of some linear systems of equations.

A regularizing transformation is used to improve the accuracy of the numerical integration of the reentry equations when singularities in the differential equations are approached.

6.2 Results and Conclusions

1. The perturbation method can be used to produce accurate optimal trajectories for the reentry problem. Numerical experiments indicate that if a sufficiently small integration step size is used the reentry equations can be integrated accurately. A comparison of the perturbation method and adjoint method indicate that both methods

produce equivalent results for the reentry problem.

2. The perturbation method can be used to solve an unstable TPBVP. A linear, unstable TPBVP is considered and better results are obtained using the MPF than the Riccati transformation to solve this problem. The machine word length, the desired boundary conditions, the ratio of the eigenvalues of the A matrix, and the time interval all affect the ability of the MPF to solve unstable TPBVP. Without knowledge of the desired solution of a linear system of equations, the advantages of forward or backward integration can only be determined by numerical experiments. For the reentry problem, one direction of integration does not seem to produce better results than the other direction.

3. Regularization improves the accuracy obtained by numerical integration near singularities. In many cases, the improvement is sufficient to allow the regularized variables to converge when the standard variables diverge for the reentry problem.

4. A variation of the standard perturbation method developed to handle SVIC can be used to generate accurate optimal constrained trajectories. The method is used to solve both a constrained Brachistochrone problem and an altitude constrained reentry problem.

5. Placing a constraint on the skip altitude of a reentry trajectory for an Apollo-type vehicle returning from a lunar mission substantially decreases the acceleration peaks. Trajectories produced with the constraint have acceptable heating and acceleration histories. They remain in the sensible atmosphere which allows the vehicle to be controlled all along the trajectory. Optimal trajectories

obtained are very similar to present Apollo reentry trajectories.

6.3 Recommendations for Future Study

1. More work needs to be done on the stability problem for the MPF. The smoothing transformation discussed in Section (2.4) should be investigated as a possible means of improving the stability of the linear equations. Patching solutions at an intermediate time offers a solution to some integration problems and should be considered as an alternative to the standard MPF. The Riccati transformation, often listed as an alternative to the unstable linear perturbation method is not nearly as effective for solving the unstable example considered here as is the MPF. Further analysis of the difficulties experienced by the Riccati method would seem to be in order.

2. The reentry equations between t_2 and t_f for the altitude constrained reentry should be regularized. Nominal trajectories are very close to the singularity at $\gamma = -90°$. Convergence of the method proposed for solving SVIC would probably be considerably better if the singularity were not present in the equations.

3. Integration time for the constrained trajectories can be decreased by "matching" the trajectory at an intermediate point t_2. Presently the entire Φ matrix must be integrated from t_2 to t_f. This requires 2n integrations of the perturbation equations. As suggested in Section (2.4), unknown variables at t_f may be guessed. The state and perturbation equations are then integrated from t_f to t_2 and states at t_2 are matched with those obtained by forward integration from t_o to t_2. Then only perturbation in n unknown

variables between t_f and t_2 must be obtained. A 15 x 15 linear system must be solved instead of an 11 x 11, but less integration is required. The advantage of one approach over the other should be determined. More quantities must be guessed in the approach presented here, but if an unconstrained optimal is known, reasonable guesses may be available. Then the method proposed here may have some advantages.

4. The effects of a more realistic model for the reentry trajectory, on the optimal trajectories obtained here, should be determined. A better atmospheric model should be considered. The effects of variable lift and drag coefficients should be determined.

APPENDICES

APPENDIX A

Numerical values used for the reentry problem are

$C_L = 0.35$

$C_D = 1.3$

$k = 4.2E-5$ 1/ft.

$\mu = 1.4076519E\ 16$ ft.^{3}/sec.^{2}

$S^* = \frac{1}{(2.05)(1.3)}$ ft.^{2}/slug

$\rho_o = 0.0027$ slug/ft.^{3}

$\lambda_o = 1.053829E-6$ $1/(\text{slug-miles})^{1/2}$

$r_e = 3960.0$ miles

APPENDIX B

Linear perturbation equations for reentry satisfy the differential equation $\delta\dot{z} = A\delta z$ where elements of A are defined below. All elements of A not shown are zero. $A_{i,j}$ denotes the ith row and the jth column of the A matrix

$$A_{1,4} = S\gamma$$

$$A_{1,5} = VC\gamma$$

$$A_{2,1} = -\frac{VC\gamma C\psi}{r^2 C\phi}$$

$$A_{2,3} = \frac{VC\gamma C\psi S\phi}{rC^2\phi}$$

$$A_{2,4} = \frac{C\gamma C\psi}{rC\phi}$$

$$A_{2,5} = -\frac{VS\gamma C\psi}{rC\phi}$$

$$A_{2,6} = -\frac{VC\gamma S\psi}{rC\phi}$$

$$A_{3,1} = -\frac{VC\gamma S\psi}{r^2}$$

$$A_{3,4} = \frac{C\gamma S\psi}{r}$$

$$A_{3,5} = -\frac{VS\gamma S\psi}{r}$$

$$A_{3,6} = \frac{VC\gamma C\psi}{r}$$

$$A_{4,1} = \frac{2\mu S\gamma}{r^3} - D_r$$

$$\Lambda_{4,4} = -D_V$$

$$\Lambda_{4,5} = -\frac{\mu C\gamma}{r^2}$$

$$\Lambda_{5,1} = \frac{2\mu C\gamma}{r^3 V} - \frac{VC\gamma}{r^2} + \left(\frac{L}{V}\right)_r C\beta$$

$$\Lambda_{5,4} = \frac{\mu C\gamma}{r^2 V^2} + \frac{C\gamma}{r} + \left(\frac{L}{V}\right)_V C\beta$$

$$\Lambda_{5,5} = \left(\frac{\mu}{r^2 V} - \frac{V}{r}\right)S\gamma - \frac{L}{V}\,\frac{(\lambda_\gamma S\gamma)S^2\beta}{(\lambda_\psi^2 + \lambda_\gamma^2 C^2\gamma)^{1/2}}$$

$$\Lambda_{6,1} = \frac{VC\gamma C\psi S\phi}{r^2 C^2\phi} - \left(\frac{L}{V}\right)_r \frac{S\beta}{C\gamma}$$

$$\Lambda_{6,3} = -\frac{VC\gamma C\psi}{rC^2\phi}$$

$$\Lambda_{6,4} = -\frac{C\gamma C\psi S\phi}{rC\phi} - \left(\frac{L}{V}\right)_V \frac{S\beta}{C\gamma}$$

$$\Lambda_{6,5} = +\frac{VS\gamma C\psi S\phi}{rC\phi} - \left(\frac{L}{V}\right)\frac{S\beta S\gamma}{C^2\gamma}(1 + C^2\beta)$$

$$\Lambda_{6,6} = \frac{VC\gamma S\psi S\phi}{rC\phi}$$

$$\Lambda_{5,11} = -\left(\frac{L}{V}\right)\frac{S^2\beta C\gamma}{(\lambda_\psi^2 + \lambda_\gamma^2 C^2\gamma)^{1/2}}$$

$$\Lambda_{5,12} = -\left(\frac{L}{V}\right)\frac{S\beta C\beta}{(\lambda_\psi^2 + \lambda_\gamma^2 C^2\gamma)^{1/2}}$$

$$\Lambda_{6,11} = \Lambda_{5,12}$$

$$\Lambda_{6,12} = -\left(\frac{L}{V}\right) \frac{C^2\beta}{C\gamma(\lambda_\psi^2 + \lambda_\gamma^2 C^2\gamma)^{1/2}}$$

$$\Lambda_{7,1} = -\frac{2VC\gamma C\psi}{r^3 C\phi}\lambda_\theta - \frac{2VC\gamma S\psi}{r^3}\lambda_\phi + \frac{6\mu S\gamma}{r^4}\lambda_V$$

$$+ D_{rr}\lambda_V + \frac{6\mu C\gamma}{r^4 V}\lambda_\gamma - \frac{2VC\gamma}{r^3}\lambda_\gamma - \left(\frac{L}{V}\right)_{rr} C\beta\lambda_\gamma$$

$$+ \frac{2VC\gamma C\psi S\phi}{r^3 C\phi}\lambda_\psi + \left(\frac{L}{V}\right)_{rr}\frac{S\beta}{C\gamma}\lambda_\psi - Q_{rr}$$

$$\Lambda_{7,3} = \frac{VC\gamma C\psi S\phi}{r^2 C^2\phi}\lambda_\theta - \frac{VC\gamma C\psi}{r^2 C^2\phi}\lambda_\psi$$

$$\Lambda_{7,4} = \frac{C\gamma C\psi}{r^2 C\phi}\lambda_\theta + \frac{C\gamma S\psi}{r^2}\lambda_\phi + D_{rV}\lambda_V + \frac{2\mu C\gamma}{r^3 V^2}\lambda_\gamma$$

$$+ \frac{C\gamma}{r^2}\lambda_\gamma - \left(\frac{L}{V}\right)_{rV} C\beta\lambda_\gamma - \frac{C\gamma C\psi S\phi}{r^2 C\phi}\lambda_\psi$$

$$+ \left(\frac{L}{V}\right)_{rV}\frac{S\beta}{C\gamma}\lambda_\psi - Q_{rV}$$

$$\Lambda_{7,5} = -\frac{VS\gamma C\psi}{r^2 C\phi}\lambda_\theta - \frac{VS\gamma S\psi}{r^2}\lambda_\phi - \frac{2\mu C\gamma}{r^3}\lambda_V$$

$$+ \frac{2\mu S\gamma}{r^3 V}\lambda_\gamma - \frac{VS\gamma}{r^2}\lambda_\gamma + \frac{VS\gamma C\psi S\phi}{r^2 C\phi}\lambda_\psi$$

$$+ \left(\frac{L}{V}\right)_r \frac{S\beta S\gamma}{C^2\gamma}\lambda_\psi$$

$$\Lambda_{7,6} = -\frac{VC\gamma S\psi}{r^2C\phi}\lambda_\theta + \frac{VC\gamma C\psi}{r^2}\lambda_\phi + \frac{VC\gamma S\psi S\phi}{r^2C\phi}\lambda_\psi$$

$$\Lambda_{9,1} = \Lambda_{7,3}$$

$$\Lambda_{9,3} = -\frac{VC\gamma C\psi}{rC^3\phi}(1 + S^2\phi)\lambda_\theta + \frac{2VC\gamma C\psi S\phi}{rC^3\phi}\lambda_\psi$$

$$\Lambda_{9,4} = -\frac{C\gamma C\psi S\phi}{rC^2\phi}\lambda_\theta + \frac{C\gamma C\psi}{rC^2\phi}\lambda_\psi$$

$$\Lambda_{9,5} = \frac{VS\gamma C\psi S\phi}{rC^2\phi}\lambda_\theta - \frac{VS\gamma C\psi}{rC^2\phi}\lambda_\psi$$

$$\Lambda_{9,6} = \frac{VC\gamma S\psi S\phi}{rC^2\phi}\lambda_\theta - \frac{VC\gamma S\psi}{rC^2\phi}\lambda_\psi$$

$$\Lambda_{10,1} = \Lambda_{7,4}$$

$$\Lambda_{10,3} = \Lambda_{9,4}$$

$$\Lambda_{10,4} = -D_{VV}\lambda_V + \frac{2\mu C\gamma}{r^2V^3}\lambda_\gamma - Q_{VV}$$

$$\Lambda_{10,5} = -C\gamma\lambda_r + \frac{S\gamma C\psi}{rC\phi}\lambda_\theta + \frac{S\gamma S\psi}{r}\lambda_\phi + \left(\frac{\mu S\gamma}{r^2V^2} + \frac{S\gamma}{r}\right)\lambda_\gamma$$

$$- \frac{S\gamma C\psi S\phi}{rC\phi}\lambda_\psi + \left(\frac{L}{V}\right)_V \frac{S\beta S\gamma}{C^2\gamma}\lambda_\psi$$

$$\Lambda_{10,6} = \frac{C\gamma S\psi}{rC\phi}\lambda_\theta - \frac{C\gamma C\psi}{r}\lambda_\phi - \frac{C\gamma S\psi S\phi}{rC\phi}\lambda_\psi$$

$$\Lambda_{11,1} = \Lambda_{7,5}$$

$$\Lambda_{11,3} = \Lambda_{9,5}$$

$$A_{11,4} = \Lambda_{10,5}$$

$$\Lambda_{11,5} = VS\gamma\lambda_r + \frac{VC\gamma C\psi}{rC\phi}\lambda_\theta + \frac{VC\gamma S\psi}{r}\lambda_\phi$$

$$- \frac{\mu S\gamma}{r^2}\lambda_V - \left(\frac{\mu}{r^2 V} - \frac{V}{r}\right)C\gamma\lambda_\gamma - \frac{VC\gamma C\psi S\phi}{rC\phi}\lambda_\psi$$

$$+ \left(\frac{L}{V}\right)\frac{S\beta(1 + S^2\gamma)}{C^3\gamma}\lambda_\psi + \left(\frac{L}{V}\right)\frac{C^2\beta S^2\gamma\lambda_\psi^2}{C^3\gamma(\lambda_\psi^2 + \lambda_\gamma^2 C^2\gamma)^{1/2}}$$

$$\Lambda_{11,6} = -\frac{VS\gamma S\psi}{rC\phi}\lambda_\theta + \frac{VS\gamma C\psi}{r}\lambda_\phi + \frac{VS\gamma S\psi S\phi}{C\phi}\lambda_\psi$$

$$A_{12,1} = \Lambda_{7,6}$$

$$A_{12,3} = \Lambda_{9,6}$$

$$A_{12,4} = A_{10,6}$$

$$\Lambda_{12,5} = A_{11,6}$$

$$\Lambda_{12,6} = \frac{VC\gamma C\psi}{rC\phi}\lambda_\theta + \frac{VC\gamma S\psi}{r}\lambda_\phi - \frac{VC\gamma C\psi S\phi}{rC\phi}\lambda_\psi$$

and $\Lambda_{i+6,\, j+6} = -\Lambda_{j,i}$ $i = 1,6;$ $j = 1,6$

where

$$Q_{VV} = S^*(C_L^2 + C_D^2)^{1/2}\ \rho + 6\lambda_o\rho^{1/2}V$$

$$Q_{Vr} = Q_{rV} = S^*(C_L^2 + C_D^2)^{1/2}\ \rho_r V + 3/2\lambda_o\rho^{-1/2}\rho_r V^2$$

$$Q_{rr} = \frac{1}{2}\ S^*(C_L^2 + C_D^2)^{1/2}\ \rho_{rr}V^2 + 1/2\lambda_o V^3\ (\rho^{-1/2}\rho_{rr} - 1/2\rho^{-3/2}\rho_r^2)$$

$$\rho_r = -\ k\rho \quad , \quad \rho_{rr} = k^2\rho$$

$$(\tfrac{L}{V})_V = \frac{1}{2}\ S^*\ C_L\rho \quad , \quad (\tfrac{L}{V})_r = \frac{1}{2}\ S^*\ C_L\rho_r V$$

$$D_r = \frac{1}{2}\ S^*\ C_D\rho_r V^2 \quad , \quad D_V = S^*\ C_D\rho V$$

$$(\tfrac{L}{V})_{VV} = 0 \quad , \quad (\tfrac{L}{V})_{Vr} = \frac{1}{2}\ S^*\ C_L\rho_r$$

$$(\tfrac{L}{V})_{rr} = \frac{1}{2}\ S^*\ C_L\rho_{rr}V \quad , \quad D_{rr} = \frac{1}{2}\ S^*\ C_D\rho_{rr}V^2$$

$$D_{VV} = C_D S^*\rho \quad , \quad D_{rV} = C_D S^*\rho_r V$$

APPENDIX C

The perturbation equations for the constrained Brachistochrone are of the form $\delta\dot{z} = A\delta z$. Elements of the A matrix are as follows:

Off the boundary

$$A_{1,2} = \frac{\cos u}{2(x_2)^{1/2}}$$

$$A_{1,3} = -(x_2)^{1/2} \frac{\sin^2 u}{(\lambda_1^2 + \lambda_2^2)^{1/2}}$$

$$A_{1,4} = (x_2)^{1/2} \frac{\sin u \cos u}{(\lambda_1^2 + \lambda_2^2)^{1/2}}$$

$$A_{2,2} = \frac{\sin u}{2(x_2)^{1/2}}$$

$$A_{2,3} = (x_2)^{1/2} \frac{\sin u \cos u}{(\lambda_1^2 + \lambda_2^2)^{1/2}} \tag{C.1}$$

$$A_{2,4} = -(x_2)^{1/2} \frac{\cos^2 u}{(\lambda_1^2 + \lambda_2^2)^{1/2}}$$

$$A_{4,2} = 1/4(x_2)^{-3/2} (\lambda_1 \cos u + \lambda_2 \sin u)$$

$$A_{4,3} = -\frac{\cos u}{2(x_2)^{1/2}}$$

$$A_{4,4} = -\frac{\sin u}{2(x_2)^{1/2}}$$

On the boundary

$$A_{11} = 1/2 \frac{\sin C_1}{(Z)^{1/2}}$$

$$A_{21} = \frac{\mu \sin C_1}{4(Z)^{3/2}} \tag{C.2}$$

$$A_{22} = -\frac{\sin C_1}{2(Z)^{1/2}}$$

and all A's not defined are zero.

At t_o, the boundary condition is

$$h_o = [H(t_o) + 1] \tag{C.3}$$

Thus

$$\frac{\partial h_o}{\partial \lambda_o} = [\dot{x}_1, \dot{x}_2]_{t_o} \tag{C.4}$$

and

$$\dot{h}_o = 0 \tag{C.5}$$

At t_1, the boundary conditions are

$$h_1 = \begin{bmatrix} x_2 - x_1 \tan C_1 - C_2 \\ \lambda_1 \tan C_1 - \lambda_2 \end{bmatrix}_{t_1} \tag{C.6}$$

Thus

$$\frac{\partial h_1}{\partial z_1} = \begin{bmatrix} -\tan C_1 \;, & 1 \;, & 0 \;, & 0 \\ 0 \;, & 0 \;, & \tan C_1 \;, & -1 \end{bmatrix}_{t_1} \qquad (C.7)$$

and

$$\dot{h}_1 = \begin{bmatrix} \dot{x}_2 - \dot{x}_1 \tan C_1 \\ \dot{\lambda}_1 \tan C_1 - \dot{\lambda}_2 \end{bmatrix}_{t_1} \qquad (C.8)$$

At t_2, the boundary conditions are

$$h_2 = \begin{bmatrix} \mu - \dfrac{\lambda_1}{\tan C_1} - \lambda_2 \\ \\ \lambda_1 \tan C_1 - \lambda_2 \end{bmatrix}_{t_2} \qquad (C.9)$$

Thus

$$\frac{\partial h_2}{\partial \lambda_{t_2}} = \begin{bmatrix} \dfrac{-1}{\tan C_1} \;, & -1 \\ \tan C_1 & -1 \end{bmatrix}_{t_2} \qquad (C.10)$$

and

$$\frac{\partial h_2}{\partial v_2} = \begin{bmatrix} 0 \;, & 1 \\ 0 \;, & 0 \end{bmatrix} \qquad (C.11)$$

At t_f, the boundary conditions are

$$h_f = \begin{bmatrix} x_1 - 1 \\ \lambda_2 \end{bmatrix}_{t_f} \qquad (C.12)$$

Thus

$$\frac{\partial h_f}{\partial z_f} = \begin{bmatrix} 1 & , & 0 & , & 0 & , & 0 \\ 0 & , & 0 & , & 0 & , & 1 \end{bmatrix} \tag{C.13}$$

and

$$\dot{h}_f = \begin{bmatrix} \dot{x}_1 \\ \dot{\lambda}_2 \end{bmatrix}_{t_f} \tag{C.14}$$

APPENDIX D

The coefficients of the linear perturbation equations for the constrained segment of the reentry trajectory are

$$A_{1,2} = \frac{VC\psi S\phi}{r_d C^2\phi}$$

$$A_{1,3} = \frac{C\psi}{r_d C\phi}$$

$$A_{1,4} = -\frac{VS\psi}{r_d C\phi}$$

$$A_{2,3} = \frac{S\psi}{r_d}$$

$$A_{2,4} = \frac{VC\psi}{r_d}$$

$$A_{3,3} = -S^*C_D\rho_d V$$

$$A_{4,2} = -\frac{VC\psi}{r_d C^2\phi}$$

$$A_{4,3} = -\frac{C\psi S\phi}{r_d C\phi} - \frac{1}{2}S^*C_L\rho_d\ (S_\beta + \frac{2C_1 C\beta}{V^2 S\beta})$$

$$A_{4,4} = \frac{VS\psi S\phi}{r_d C\phi}$$

and

$$A_{i+4,\ j+4} = -A_{j,i} \qquad i = 1,4; \quad j = 1,4$$

$$A_{6,2} = -\frac{VC\psi}{r_d C^3\phi}(1 + S^2\phi)\mu_\theta + \frac{2VC\psi S\phi}{r_d C^3\phi}\mu_\psi$$

$$A_{6,3} = -\frac{C\psi S\phi}{r_d C^2\phi}\mu_\theta + \frac{C\psi}{r_d C^2\phi}\mu_\psi$$

$$A_{6,4} = \frac{VS\psi S\phi}{r_d C^2\phi}\mu_\theta - \frac{VS\psi}{r_d C^2\phi}\mu_\psi$$

$$A_{7,2} = -\frac{C\psi S\phi}{r_d C^2\phi}\mu_\theta + \frac{C\psi}{r_d C^2\phi}\mu_\psi$$

$$A_{7,3} = S^*C_D\rho_d\mu_V - S^*C_L\rho_d(C\beta + \frac{2C_1}{V^2S^2\beta})\frac{C_1\mu_\psi}{V^3S\beta}$$

$$- 2C_2 - 6C_3V$$

$$A_{7,4} = \frac{S\psi}{r_d C\phi}\mu_\theta - \frac{C\psi}{r_d}\mu_\phi - \frac{S\psi S\phi}{r_d C\phi}\mu_\psi$$

$$A_{8,2} = \frac{VS\psi S\phi}{r_d C^2\phi}\mu_\theta - \frac{VS\psi}{r_d C^2\phi}\mu_\psi$$

$$A_{8,3} = \frac{S\psi}{r_d C\phi}\mu_\theta - \frac{C\psi}{r_d}\mu_\phi - \frac{S\psi S\phi}{r_d C\phi}\mu_\psi$$

$$\Lambda_{8,4} = \frac{VC\psi}{r_d C\phi} \mu_\theta + \frac{VS\psi}{r_d} \mu_\phi - \frac{VC\psi S\phi}{r_d C\phi} \mu_\psi$$

APPENDIX E

Boundary conditions for the constrained reentry problem are as follows:

The boundary condition at t_o is

$$h_o = [H_o] \tag{E.1}$$

Thus

$$\frac{\partial h_o}{\partial \lambda_o} = [\ \dot{r},\ \dot{\theta},\ \dot{\phi},\ \dot{V},\ \dot{\gamma},\ \dot{\psi}\ ]_{t_o} \tag{E.2}$$

and

$$\dot{h}_o = [0] \tag{E.3}$$

The boundary conditions at t_1 are

$$h_1 = \begin{bmatrix} r - r_d \\ \gamma \\ (\ C_1 - C_2V^2)(\lambda_\gamma^2 + \lambda_\psi^2)^{1/2} + V^2\lambda_\gamma \end{bmatrix}_{t_1} \tag{E.4}$$

Thus

$$\frac{\partial h_1}{\partial z_1} = \begin{bmatrix} 1\ , & 0\ , & 0\ , & 0\ , & 0\ , & 0\ , & 0\ , & 0\ , & 0\ , & 0\ , & 0\ , & 0 \\ 0\ , & 0\ , & 0 & 0\ , & 1\ , & 0\ , & 0\ , & 0\ , & 0\ , & 0\ , & 0\ , & 0 \\ 0\ , & 0\ , & 0\ , & b_V, & 0\ , & 0\ , & 0\ , & 0\ , & 0\ , & 0\ , & b_{\lambda_\gamma}, & b_{\lambda_\psi} \end{bmatrix}_{t_1} \tag{E.5}$$

where

$$\begin{aligned} b_V &= -2V[C_2(\lambda_\gamma^2 + \lambda_\psi^2)^{1/2} - \lambda_\gamma] \\ b_{\lambda_\gamma} &= (C_1 - C_2V^2)\frac{\lambda_\gamma}{(\lambda_\gamma^2 + \lambda_\psi^2)^{1/2}} + V^2 \\ b_{\lambda_\psi} &= (C_1 - C_2V^2)\frac{\lambda_\psi}{(\lambda_\gamma^2 + \lambda_\psi^2)^{1/2}} \end{aligned} \tag{E.6}$$

and

$$\dot{h}_1 = \begin{bmatrix} \dot{r} \\ \dot{\gamma} \\ b_V\dot{V} + b_{\lambda_\gamma}\dot{\lambda}_\gamma + b_{\lambda_\psi}\dot{\lambda}_\psi \end{bmatrix}_{t_1} \tag{E.7}$$

Boundary conditions at t_2 are

$$h_2 = [(C_1 - C_2V^2)(\lambda_\gamma^2 + \lambda_\psi^2)^{1/2} + V^2\lambda_\gamma]_{t_2} \tag{E.8}$$

and derivatives of this function are shown above by Eqs. (E.5), (E.6), and (E.7).

Boundary conditions at t_f are

$$h_f = \begin{bmatrix} \lambda_r \\ \theta - \theta_{fs} \\ \phi - \phi_{fs} \\ V - V_{fs} \\ \lambda_\gamma \\ \lambda_\psi \end{bmatrix}_{t_f} \tag{E.9}$$

$$\frac{\partial h_f}{\partial z_f} = \begin{bmatrix} 0 , 0 , 0 , 0 , 0 , 0 , 1 , 0 , 0 , 0 , 0 , 0 \\ 0 , 1 , 0 , 0 , 0 , 0 , 0 , 0 , 0 , 0 , 0 , 0 \\ 0 , 0 , 1 , 0 , 0 , 0 , 0 , 0 , 0 , 0 , 0 , 0 \\ 0 , 0 , 0 , 1 , 0 , 0 , 0 , 0 , 0 , 0 , 0 , 0 \\ 0 , 0 , 0 , 0 , 0 , 0 , 0 , 0 , 0 , 0 , 1 , 0 \\ 0 , 0 , 0 , 0 , 0 , 0 , 0 , 0 , 0 , 0 , 0 , 1 \end{bmatrix} \tag{E.10}$$

$$\dot{h}_f = \begin{bmatrix} \dot{\lambda}_r \\ \dot{\theta} \\ \dot{\phi} \\ \dot{V} \\ \dot{\lambda}_\gamma \\ \dot{\lambda}_\psi \end{bmatrix}_{t_f} \tag{E.11}$$

APPENDIX F

The multiplier equations for the regularized reentry equations are shown below:

$$\lambda_r' = \frac{\bar{V}C^2\gamma C\psi}{r^2 C\phi}\lambda_\theta + \frac{\bar{V}C^2\gamma S\psi}{r^2}\lambda_\phi$$

$$- (\frac{4\mu}{r^3}\bar{V}C\gamma S\gamma - (\rho_r S^* C_D \bar{V}^2 C\gamma)\lambda_{\bar{V}}$$

$$- (\frac{2\mu C^2\gamma}{r^3} - \frac{\mu C^2\gamma}{r^2} + \frac{1}{2}\rho_r S^* C_L \bar{V}C\gamma C\beta)\lambda_\gamma$$

$$- (\frac{\bar{V}C^2\gamma C\psi S\phi}{r^2 C\phi} - \frac{1}{2}\rho_r S^* C_L \bar{V}S\beta)\lambda_\psi - \bar{Q}_r$$

$$\lambda_\theta' = 0$$

$$\lambda_\phi' = - \frac{\bar{V}C^2\gamma C\psi S\phi}{rC^2\phi}\lambda_\theta + \frac{\bar{V}C^2\gamma C\psi}{rC^2\phi}\lambda_\psi$$

$$\lambda_{\bar{V}}' = - C\gamma S\gamma\lambda_r - \frac{C^2\gamma C\psi}{rC\phi}\lambda_\theta - \frac{C^2\gamma S\psi}{r}\lambda_\phi$$

$$+ (\frac{2\mu}{r^2}C\gamma S\gamma + 2\rho S^* C_D \bar{V}C\gamma)\lambda_{\bar{V}}$$

$$- (\frac{C^2\gamma}{r} + \frac{1}{2}\rho S^* C_L C\gamma C\beta)\lambda_\gamma$$

$$+ (\frac{C^2\gamma C\psi S\phi}{rC\phi} + \frac{1}{2}\rho S^* C_L S\beta)\lambda_\psi - \bar{Q}_{\bar{V}}$$

$$\lambda_\gamma' = \bar{V}(S^2\gamma - C^2\gamma)\lambda_r + \frac{2\bar{V}C\gamma S\gamma C\psi}{rC\phi}\lambda_\theta$$

$$+ \frac{2\bar{V}C\gamma S\gamma S\psi}{r}\lambda_\phi$$

$$- [\frac{2\mu}{r^2}\bar{V}(S^2\gamma - C^2\gamma) + \rho S^*C_D\bar{V}^2 S\gamma]\lambda_{\bar{V}}$$

$$- (\frac{2\mu}{r^2}C\gamma S\gamma - \frac{2\bar{V}C\gamma S\gamma}{r} - \frac{1}{2}\rho S^*C_L\bar{V}S\gamma C\beta)\lambda_\gamma$$

$$- \frac{2\bar{V}C\gamma S\gamma C\psi S\phi}{rC\phi}\lambda_\psi - \bar{Q}_\gamma$$

$$\lambda_\psi' = \frac{\bar{V}C^2\gamma S\psi}{rC\phi}\lambda_\theta - \frac{\bar{V}C^2\gamma C\psi}{r}\lambda_\phi - \frac{\bar{V}C^2\gamma S\psi S\phi}{rC\phi}\lambda_\psi$$

where

$$\bar{Q} = [1/2(C_L^2 + C_D^2)^{1/2} S^*\rho\bar{V}^{3/2} + \lambda_o\rho^{1/2}\bar{V}^2]C\gamma$$

$$\bar{Q}_r = [1/2(C_L^2 + C_D^2)^{1/2} S^*\rho_r\bar{V}^{3/2} + 1/2\,\frac{\lambda_o\rho_r}{\rho^{1/2}}\bar{V}^2]C\gamma$$

$$\bar{Q}_{\bar{V}} = [3/4(C_L^2 + C_D^2)^{1/2} S^*\rho\bar{V}^{1/2} + 2\lambda_o\rho^{1/2}\bar{V}]C\gamma$$

$$\bar{Q}_\gamma = -[1/2(C_L^2 + C_D^2)^{1/2} S^*\rho\bar{V}^{3/2} + \lambda_o\rho^{1/2}\bar{V}^2]S\gamma$$

BIBLIOGRAPHY

1. Levinsky, E. S., "Application of Inequality Constraints to Variational Problems of Lifting Re-Entry," *Journal of the Aerospace Sciences*, April 1962, pp. 400-409.

2. Bryson, A. E., Denham, W. F., Carroll, F. J., and Mikami, K., "Determination of Lift or Drag Programs to Minimize Re-Entry Heating," *Journal of the Aerospace Sciences*, April 1962, p. 420-430.

3. Leondes, C. F., and Niemann, R. A., "Optimization of Aerospace Re-Entry Vehicle Trajectories through Independent Control of Lift and Drag," *Journal of Spacecraft and Rockets*, Vol. 3, No. 5, May 1966, pp. 618-623.

4. Wagner, W. E., and Jazwinski, A. H., "Three-Dimensional Re-Entry Optimization with Inequality Constraints," AIAA Astrodynamics Conference, August 19-21, 1963.

5. Bryson, A. E., Denham, W. F. and Dreyfus, S. E., "Optimal Programming Problems with Inequality Constraints I: Necessary Conditions for Extremal Solutions," *AIAA Journal*, November 1963, pp. 2544-2550.

6. Denham, W. F.,and Bryson, A. E., "Optimal Programming Problems with Inequality Constraints II: Solution by Steepest-Ascent," *AIAA Journal*, January 1964, p. 25-34.

7. McCarthy, J. F., Jr. and Hanley, G. M., "Manned Earth Entry at Hyperbolic Velocities," *Journal of Spacecraft and Rockets*, September 1968, p. 1009.

8. Paiewonsky, B., "On Optimal Control with Bounded State Variables," ARAP Report No. 60, July 1964.

9. Berkovitz, L. D., "On Control Problems with Bounded State Variables," *Journal of Mathematical Analysis and Applications* *5* (1962), pp. 488-498.

10. Busemann, A., Vinh, N. X., and Kelley, G. F., "Optimum Maneuvers of Hypervelocity Vehicles," NASA CR-1078, June 1968.

11. Chapman, D. R., "An Approximate Analytical Method for Studying Entry into Planetary Atmospheres," NASA TR R-11, 1959.

12. Valentine, F. A., "The Problem of Lagrange with Differential Inequalities as Added Side Conditions," *Contributions to the Calculus of Variations 1933-1937*, The University of Chicago Press (1937).

13. Lastman, G. J., "Optimization of Nonlinear Systems with Inequality Constraints," Ph.D. Dissertation, The University of Texas, 1966.

14. Lastman, G. J., and Tapley, B. D., "Optimization of Nonlinear Systems with Inequality Constraints Explicitly Containing the Control," (To be published).

15. Payne, J. A., "Computational Methods in Optimal Control Problems Ph.D., Dissertation, University of California at Los Angeles, 1965.

16. Pontryagin, L. S., Boltyanskii, V. G., Gamkrelidze, E. F., and Mishchenko, E. F., The Mathematical Theory of Optimal Processes, Wiley (1962).

17. Dreyfus, S. E., "Variational Problems with Inequality Constraints," Journal of Mathematical Analysis and Applications 4 (1962), pp. 297-308.

18. Young, J. W., and Smith, R. E., Jr., "Trajectory Optimization for an Apollo-Type Vehicle under Entry Conditions Encountered during Lunar Returns," NASA TR R-258, May 1967.

19. Paine, G., "The Application of the Method of Quasilinearization to the Computation of Optimal Control," Report No. 67-49, Department of Engineering, University of California at Los Angeles, August 1967.

20. Muzyka, A. and Blanton, H. E., "Optimum Earth Re-Entry Corridors," NASA CR-394, March 1966.

21. Jacobson, D. H., and Lele, M. M., "A Transformation Technique for Optimal Control Problems with a State Variable Inequality Constraint," Technical Report No. 574, Division of Engineering and Applied Physics, Harvard University, 1968.

22. McGregor, C. O., "Numerical Optimization of Atmospheric Reentry Trajectories by the Sweep Method," Ph.D. Dissertation, University of Texas, 1969.

23. Speyer, J. L. and Bryson, A. E., Jr., "Optimal Programming Problems with a Bounded State Space," AIAA Journal, August 1968, pp. 1488-1491.

24. Speyer, J. L., Mehra, R. K., and Bryson, A. E., Jr., "The Separate Computation of Arcs for Optimal Flight Paths with State Variable Inequality Constraints," Division of Engineering and Applied Physics, Harvard University Technical Report No. 526, May 1967.

25. McGill, R., "Optimal Control, Inequality State Constraints, and the Generalized Newton-Raphson Algorithm," S.I.A.M. Journal on Control 3 (1965), pp. 291-298.

26. Breakwell, J. V., Speyer, J. L., and Bryson, A. E., "Optimization and Control of Nonlinear Systems Using the Second Variation," S.I.A.M. Journal on Control 1 (1963), pp. 193-223.

27. Goodman, T. R., and Lance, G. N., "The Numerical Integration of Two-Point Boundary Value Problems," Mathematical Tables and Other Aids to Computation, Vol. 10, No. 54, 1956.

28. Dreyfus, S. E., Dynamic Programming and the Calculus of Variations, Academic Press (1965).

29. Bryson, A. E., and Ho, Y. C., Applied Optimal Control, Blaisdell (1969).

30. Sage, A. P., Optimum Systems Control, Prentice-Hall (1968).

31. Tapley, B. D., and Lewallen, J. M., "Comparison of Several Numerical Optimization Methods," Journal of Optimization Theory and Applications, Vol. 1, No. 1, (1967).

32. Jurovics, S. A., and McIntyre, J. E., "The Adjoint Method and Its Application to Trajectory Optimization," ARS Journal, Vol. 32, No. 9, 1962.

33. Fowler, W. T. and Lastman, G. J., "Fortran Subroutines for the Numerical Integration of First Order Ordinary Differential Equations," Engineering Mechanics Research Laboratory RM 1024, University of Texas, March 1967.

34. Berkovitz, L. D., and Dreyfus, S. E., "The Equivalence of Some Necessary Conditions for Optimal Control in Problems with Bounded State Variables," Journal of Mathematical Analysis and Applications 10 (1965), pp. 275-283.

35. Denham, W. F., "On Numerical Optimization with State Variable Inequality Constraints," A.I.A.A. Journal 4 (1966), pp. 550-552.

36. Kelley, H. J., "Method of Gradients," Optimization Techniques, G. Leitmann, ed., Academic Press, New York 1962, Chap. 6, p. 230.

37. Kelley, H. J., Falco, M., and Ball, D. J., "Air Vehicle Trajectory Optimization," presented at the Symposium on Multivariable System Theory, Fall Meeting of S.I.A.M., Cambridge, Massachusetts, 1962.

38. Dreyfus, S. E., "The Numerical Solution of Variational Problems," Journal of Mathematical Analysis and Applications 5 (1962), pp. 30-45.

39. Jacobson, D. H., Gershwin, S. B., and Lele, M. M., "Computation of Optimal Singular Controls," Division of Engineering and Applied Physics, Harvard University Technical Report No. 580, January 1969.

40. Hamilton, W. E., and Koivo, A. J., "On Computational Solutions of State Constrained Optimization Problems," Presented at the Joint Automatic Control Conference, Bolder, Colorado, August 1969.

41. Lastman, G. J., and Tapley, B. D., "Optimization of Nonlinear Systems Subject to State-Variable Inequality Constraints," (To be Published).

42. Speyer, J. L., "Optimization and Control of Nonlinear Systems with Inflight Constraints," Ph.D. Dissertation, Harvard University, 1968.

43. Fox, L., Numerical Solution of Ordinary and Partial Differential Equations, Pergamon Press, 1962.

44. Henrici, P., Discrete Variable Methods in Ordinary Differential Equations, John Wiley and Sons, Inc., 1964.

45. McDermott, Make, "An Automated Procedure for Numerical Optimization," Ph.D. Dissertation, University of Texas, June 1969.

46. Babuska, I., Prager, M., and Vitasek, E., Numerical Processes in Differential Equations, Interscience Publishers, 1966.

47. Jacobson, D. H., Lele, M. M. and Speyer J. L., "New Necessary Conditions of Optimality for Control Problems with State-Variable Inequality Constraints," (To be Published).

48. "Spacecraft Operational Trajectory for Apollo Mission F, Volume I - Operational Mission Profile Launched May 17, 1969," MSC Internal Note No. 69-FM-65, March 26, 1969.

49. Kelley, H. J., Kopp, R. E., and Moyer, H. G., "A Trajectory Optimization Technique based upon the Theory of the Second Variation," A.I.A.A. Astrodynamics Conference, Yale University, 1963.

50. Tapley, B. D., Szebehely, V., and Lewallen, J. M., "Trajectory Optimization Using Regularized Variables," A.A.S./A.I.A.A. Astrodynamics Specialist Conference, Jackson, Wyoming, September 1968.

51. Tapley, B. D., Fowler, W. T., and Williamson, W. E., "The Computation of Optimal Apollo-Type Reentry Trajectories," presented at JACC, Boulder, Colorado, August, 1969.

52. Hanrahan, J. S., and Bushnell, D., Space Biology, Basic Books, Inc. New York, 1960.

VITA

Walton E. Williamson, Jr. was born in Corpus Christi, Texas, on May 21, 1944, the son of Walton and Dorothy Williamson, Sr. He attended public school in Lubbock, Texas and graduated from Monterey High School in June 1962. From September 1962 to August 1963 he attended Texas Tech University at Lubbock, Texas. In September 1963, he entered Stanford University at Palo Alto, California. In June 1965 he married the former Judy Ruth Wimbish of Ft. Worth. He received his Bachelor of Science degree in Mechanical Engineering in June 1966 at Stanford University. In September 1966, he entered the graduate school of The University of Texas at Austin under a Ford Foundation Fellowship. He received his Masters Degree there in August 1967. Since that time he has been employed as a part time research assistant by the Aerospace Engineering Department of The University of Texas at Austin.

Permanent Address: 3405-54th
Lubbock, Texas

This dissertation was typed by Mrs. Patti Everett.